理學博士學位論文

*Bacillus subtilis*에서 세포 신장에 관여하는 polyamine과 methylglyoxal의 관계

Relationship between polyamine and methylglyoxal in the cell elongation of *Bacillus subtilis*

2015年 **8**月

서울大學校 大學院

生命科學部

宋 成 炫

Bacillus subtilis 에서 세포 신장에 관여하는 polyamine과 methylglyoxal의 관계

指導敎授 姜 思 旭

이 論文을 理學博士學位論文으로 提出함

2014年 **12**月

서울大學校 大學院
生命科學部
宋 成 炫

宋成炫의 理學博士學位論文을 認准함

2015年 **7**月

委 員 長 _____

副委員長 _____

委 員 _____

委 員 _____

委 員 _____

Relationship between polyamine and methylglyoxal in the cell elongation of *Bacillus subtilis*

by

Sung-Hyun Song

Advisor:

Professor Sa-Ouk Kang, Ph. D.

A Thesis Submitted in Partial Fulfillment
of the Requirements for
the Degree of Doctor of Philosophy

August, 2015

School of Biological Science
Graduate School
Seoul National University

ABSTRACT

Methylglyoxal is the metabolic intermediate and acts as a growth- or division inhibitor in cells. This α-ketoaldehyde, which have been recognized as the advanced glycation end product precursors such as glyoxal, methylglyoxal and deoxyglucosone, have been suggested to be regulated by endogenous or exogenous polyamines. Polyamines, which are abundant compounds in cells from bacteria to mammals, generally participate in various cell physiology such as the cell growth, division and differentiation.

Herein, the methylglyoxal was observed to react with several types of polyamines *in vitro* resulting from the electron paramagnetic resonance spectroscopy. To investigate the physiological function and relationship of both methylglyoxal and polyamines in *Bacillus subtilis*, polyamine biosynthesizing-genes such as *speA*, *speB*, and *yaaO* encoding the arginine decarboxylase, agmatinase, and lysine decarboxylase, were disrupted or overexpressed respectively. The growth rate was slightly retarded in all of the polyamine-deficient strains compared to wild-type cells. Additionally, the significant growth defect was observed in the $speB^{OE}$ and $yaaO^{OE}$ strains not in the case of the $speA^{OE}$ strain. The intracellular methylglyoxal content increased 2.5- to 3-fold in the $speB^{OE}$ and $yaaO^{OE}$ strains compared to the reference strain. In

addition, the *mgsA* gene expression, which is supposed to encode methylglyoxal synthase based on the genome database of *B. subtilils*, increased in the $speB^{OE}$ and $yaaO^{OE}$ strains. Based on these observations of the changes in the cell physiology in these cells, we microscopically examined whether the effect of the increased methylglyoxal or polyamine content might affect the cellular morphology. Over 60% of the elongated cells were observed in the $speB^{OE}$ and $yaaO^{OE}$ strains contrast to the reference strain. The expression of actin-like *mreB*, which codes a protein involved in the cell elongation predominantly in prokaryotes, increased in the $speB^{OE}$ and $yaaO^{OE}$ strains. These results indicated that methylglyoxal accumulation by the *mgsA* gene expression in the $speB^{OE}$ and $yaaO^{OE}$ strains caused the growth inhibition and altered the cell morphology by triggering *mreB* expression.

To reveal the relationship between cellular methylglyoxal and cell shape formation under other experimental conditions, *Bacillus* methylglyoxal synthase was purified using the *Escherichia coli* recombinant protein fused with the pET3a vector system. The K_m and k_{cat} values for *Bacillus* methylglyoxal synthase activity were revealed to be 3.17 mM and 0.009 (s^{-1}) respectively, when using dihydroxyacetone phosphate as a major substrate. The optimal temperature and pH for the *Bacillus* methylglyoxal synthase activity were observed 40°C and 5.5, respectively and furthermore native molecular mass

was calculated as a dimeric form. *Bacillus* methylglyoxal synthase activity decreased in an exogenous phosphate compounds concentration-dependent manner. These results indicated that *Bacillus* methylglyoxal synthase encoded by the *mgsA* gene catalyze dihydroxyacetone phosphate into methylglyoxal and showed a different biochemical properties compared to other bacterial proteins.

Interestingly, the $mgsA^{OE}$ cells showed a drastic increase in the cellular methylglyoxal content ranging from 2.5- to 3.5-fold higher compared to a reference strain. The cell growth and viability were also significantly inhibited in the $mgsA^{OE}$ strain. Likewise in the $speB^{OE}$ *or* $yaaO^{OE}$ strains, the cell length in the $mgsA^{OE}$ strain was observed ranging from 2.5- to 3-fold longer than the reference strain. Additionally, the *mreB* gene expression increased similar to the $speB^{OE}$ or $yaaO^{OE}$ strains in similar to the $mgsA^{OE}$ strain.

Taken together, these results suggested that cellular methylglyoxal and polyamines are involved in the cell elongation as important factors reciprocally during the *B. subtilis* cell growth.

Key words: Methylglyoxal, Methylglyoxal synthase, Polyamines, Cell elongation, *Bacillus subtilis*

CONTENTS

ABSTRACT i
CONTENTS iv
List of Tables ix
List of Figures x
List of Abbreviations xii

I. INTRODUCTION 1

1. Methylglyoxal 2

1.1. Chemical property of methylglyoxal 2

1.2. Effects of methylglyoxal in organisms 2

1.2.1. Inhibition of cell growth by methylglyoxal 2

1.2.2. Formation of advanced glycation end-products (AGEs) 4

1.2.3. Generation of the reactive oxygen species 5

1.3. Methylglyoxal metabolism 6

1.3.1. Non-enzymatic conversion of methylglyoxal 6

1.3.2. Enzymatic synthesis of methylglyoxal 6

1.3.3. Methylglyoxal detoxification in organisms 7

2. Polyamines 10

2.1. Polyamine overview 10

2.2. The enzymatic synthesis of polyamines 12
2.3. The functions of polyamine in bacteria 15
2.3.1. Interaction of polyamine and nucleic acid 15
2.3.2. Free radical scavengers by polyamine 15
2.3.3. Acid resistance by polyamine- 16
2.3.4. Interaction cell wall and polyamines 16
2.3.5. Siderophore and virulence with polyamines 17
2.3.6. Role of polyamine to biofilm formation 17
3. *Bacillus subtilis* 18
4. Cell size regulation in *Bacillus* 20
4.1. Overview 20
4.2. Molecular regulation of cell size in *Bacillus* 21
5. Aims of this study 25

II. MATERIALS AND METHODS 27
1. Materials 28
2. Methods 28
2.1. Bacterial strains and culture conditions 28
2.2. Media 31
2.3. General DNA manipulation 31

2.3.1. Polymerase Chain Reaction (PCR) and DNA sequencing 31

2.3.2. Cloniong.....33

2.3.3. Transformation.....33

2.3.3.1. *E. coli* 33

2.3.3.2. *Bacillus subtilis*.....33

2.3.4. Constructs for mutants 37

2.4. RNA analysis 37

2.4.1. Preparation of RNA from *B. subtilis* --.....37

2.4.2. Northern blot analysis.....38

2.5. Protein analysis 38

2.5.1. Preparation of the cell crude 38

2.5.2. Western blot analysis 39

2.6. Purification of methylglyoxal synthase (MGS) and determination of biochemical properties 40

2.6.1. Overproduction and purification of MGS.....39

2.6.2. Determination of enzyme kinetics 40

2.6.3. Determination of molecular mass 41

2.7. Additional methods.....41

2.7.1. Determination of methylglyoxal concentration 41

2.7.2. Determination of polyamine concentration 42

2.7.3. Microscopy analysis 42

2.7.4. EPR analysis.....43

III. RESULTS.....44

3.1. Free radicals generation by reaction of MG 45

3.2. Gene related with synthesis of polyamine in *B. subtilis* 46

3.3. Polyamine mutants and growth inhibition 46

3.4. Growth inhibition caused by MG accumulation.....53

3.5. Induction of the *mgsA* gene in polyamine overexpressed mutants.....56

3.6. Morphological change by MG accumulation in polyamine overexpressed mutants 58

3.7. MG accumulation modulates of cell division or elongation in polyamine mutants 58

3.8. Characterization of *Bacillus* MGS 64

3.8.1. Sequence analysis of *Bacillus* MGS 64

3.8.2 Purification of *Bacillus* MGS.....66

3.8.3. Enzyme activity of *Bacillus* MGS 68

3.8.4. Biochemical properties of *Bacillus* MGS 68

3.8.5. Native molecular mass of *Bacillus* MGS.....68

3.9. The functional roles of methylglyoxal synthase in *B. subtilis* 72

3.9.1. Construct for the deletion of the *mgsA* gene.....72

3.9.2. Construct for the overexpression of the *mgsA* gene.....72

3.9.3. MG production inhibits cell growth and viability.....75
3.10. Effect on cell morphology by MG overproduction.....81
3.10.1. Cell morphology change by MG overproduction.....81
3.10.2. MG overproduction leads to the cell elongation by the activation of MreB.....81
IV. DISCUSSION.....86
V. REFERENCES.....95
국문초록.....121

List of Tables

Table 1. *B. subtilis* and *E. coli* strains used in this study 29

Table 2. Plasmids used in this study 32

Table 3. Primers used in this study 34

Table 4. Comparison of the synthesis of polyamine proteins 47

List of Figures

Scheme 1. Chemical structure of methylglyoxal 3
Scheme 2. Metabolic pathways of methylglyoxal 9
Scheme 3. Chemical structure of polyamine 11
Scheme 4. Metabolic pathways of polyamine synthesis in *E. coli* 14
Scheme 5. Life cycle of Bacillus subtilis..... 19
Scheme 6. Model of cell division (FtsZ) and elongation (MreB)..... 22
Fig. 1. Disruption and overexpression of polyamine enzymes in *B. subtilis*... 50
Fig. 2A. Growth inhibition in the polyamine defective mutants 51
Fig. 2B. Growth inhibition in the polyamine-overexpressing mutants..... 52
Fig. 3. Intracellular concentration of polyamine in the polyamine mutants 54
Fig. 4. Intracellular concentration of methylglyoxal in the polyamine mutants 55
Fig. 5. Expression level of *mgsA* in the polyamine-overexpressing mutants .. 57
Fig. 6. Cell morphology of the polyamine defective mutants..... 59
Fig. 7. Cell size distribution in the polyamine defective mutants..... 60
Fig. 8. Cell morphology of the polyamine-overexpressing mutants..... 61
Fig. 9. Cell size distribution in the polyamine-overexpressing mutants..... 62
Fig. 10. Expression level of *mreB* in the polyamine-overexpressing mutants. 63
Fig. 11. The location of *mgsA* gene and amino acid sequence alignment with other bacterial MGSs 65
Fig. 12. Purification of *Bacillus* MGS 67
Fig. 13. Lineweaver-Burk plot for *Bacillus* MGS 69
Fig. 14. Biochemical properties of *Bacillus* MGS on temperature and pH 70

Fig. 15. Inhibitory effect of *Bacillus* MGS by phosphate compounds 71
Fig. 16. Native molecular mass of *Bacillus* MGS 73
Fig. 17. Deletion the *mgsA* gene in *B. subtilis* 75
Fig. 18. Scheme of the overexpression the *mgsA* gene by insertion of RBS from *sodA* 76
Fig. 19. Overexpression mutant of the *mgsA* in *B. subtilis* 77
Fig. 20. Intracellular concentration of MG in the *ΔmgsA* and $mgsA^{OE}$ mutants 78
Fig. 21. Inhibition of growth in $mgsA^{OE}$ strain 79
Fig. 22. Defect viability in $mgsA^{OE}$ strain 80
Fig. 23. Cell morphology of the *ΔmgsA* and $mgsA^{OE}$ mutants..... 82
Fig. 24. Cell size distribution in the *ΔmgsA* and $mgsA^{OE}$ mutants 83
Fig. 25. Expression level of *mreB* in the *ΔmgsA* and $mgsA^{OE}$ mutants..... 85
Fig. 26. The model of cell elongation by methylglyoxal and polyamine 94

List of Abbreviations

AGEs	Advanced Glycation End-products
AGM	agmatine
BCIP	5-bromo-4-chloro-3-indoyl phosphate
bp	base pair
CAD	cadaverine
cAMP	cyclic adenosine monophosphate
DHAP	dihydroxyacetone phosphate
EDTA	ethylene diamine tetraacetic acid
EPR	electron paramagnetic resonance
G3P	glyceraldehyde-3-phosphate
HPLC	high performance liquid chromatography
IPTG	isopropyl-β-D-thiogalactopyranoside
MG	methylglyoxal
MGS	methylglyxoal synthase
NBT	nitro blue tetrazolium
OD	optical densityd
ORF	open reading frame
PAGE	polyacrylamide gel electrophoresis
PCR	polymerase chain reaction
PMSF	phenylmethylsulphonyl fluoride
PUT	putrescine
SDS	sodium dodecyl sulfate
SPD	spermidine

SPM	spermine
UV	ultraviolet

I. INTRODUCTION

1. Methylglyoxal

1.1. Chemical property of methylglyoxal

Methylglyoxal (MG) is yellow volatile liquid oil with pungent odor that polymerizes readily and is formed as an intermediate in the metabolism or fermentation of carbohydrates and lactic acid spontaneously (Cooper, 1984) (Scheme 1).

Methylglyoxal, as the meaning of the medical subject headings (MeSH), (CH_3-CO-CH=O or $C_3H_4O_2$, molar mass 72.0627) has several nomenclatures because of its various aspects of chemical properties, generally so called pyruvaldehyde, pyruvic aldehyde, 2-ketoproprion aldehyde, α-oxoaldehyde, α-ketoaldehyde, acetylformaldehyde or 2-oxo-propanal which is used in IUPAC name, is the aldehyde form of D-pyruvic acid (Cooper, 1984).

Methylglyoxal contains two carbonyl moieties, therefore it is a dicarbonyl compound. Methylglyoxal has an aldehyde and a ketone. Methylglyoxal is also called a ketal because it has important two functional groups, an aldehydic and ketonic carbonyl group (Inoue and Kimura, 1995).

1.2. Effects of methylglyoxal on organisms

1.2.1. Inhibition of cell growth by methylglyoxal

Szent-Györgyi suggested that MG or glyoxal derivatives act as a growth-inhibiting factor, called retine, whereas glyoxalase promotes cell growth, called promine (Szent-Györgyi*, et al.*, 1967). Because the modification of DNA by MG induced single-strand breaks, DNA-protein cross-links and cytotoxicity in cultured cells (Marinari*, et al.*, 1984). For example, the modification of guanyl residues in DNA or RNA by the reaction with MG is thought to contribute to

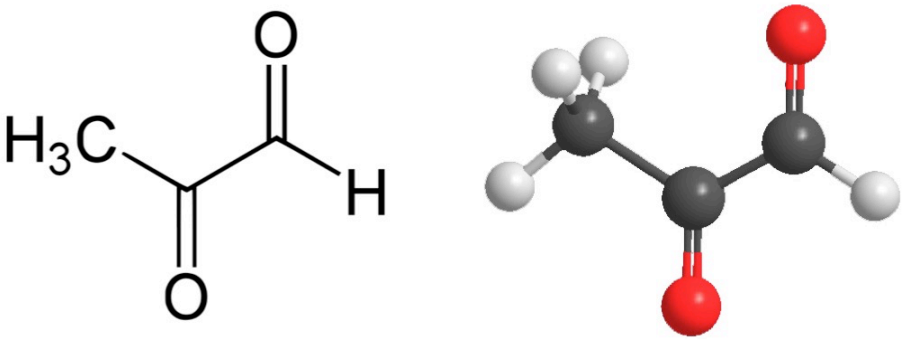

Scheme 1. Chemical structure of methylglyoxal

the anti-proliferative activity of MG (Apple and Greenberg, 1967; Jerzykowski*, et al.*, 1970; Conroy*, et al.*, 1979), which inhibited the DNA synthesis (Reiffen and Schneider, 1984) and the initiation of translation (White and Rees, 1982).

Additionally, the exogenous treated MG showed inhibition of tumor cell growth by blocking of the glycolysis and the mitochondrial respiration when treated MG (Ray*, et al.*, 1991). Furthermore, MG induced growth arrest in the G1 phase of the cell cycle and toxicity in human leukemia 60 cells *in vitro* and incubation of human leukemia cells with MG led to the rapid accumulation of adducts of MG with DNA (Kang*, et al.*, 1996).

1.2.2. Formation of the advanced glycation end-products (AGEs)

The aldehyde or ketone can react with amino groups of proteins and also with phospholipid and nucleic acids by a non-enzymatic reaction such as Schiff base formation or Amadori reaction. This reaction occurs very slowly until reaching the equilibrium when it is reversible reaction. During the early glycation process, the glycation adduct can be formed. Then, the glycation adduct can undergo further rearrangement such as eventually dehydration, condensation, fragmentation, oxidation and cyclization reactions, which is giving a rise to compounds bound irreversibly, the so-called Advanced glycation end-products (AGEs) (Grillo and Colombatto, 2008). In addition, MG modified plasma proteins bind to AGE-receptors and undergo the endocytosis and degradation (Westwood*, et al.*, 1994; Thornalley, 1996).

Also, MG causes the diabetes and its complications by the formation of AGEs (Vander Jagt, 2008). Due to malfunction of glucose uptake in a high cellular glucose level, hyperglycemia can occur (Dominiczak, 2003; Brownlee, 2005). The levels of NADH and FADH increased in hyperglycemic cells

accompanying with the proton gradient beyond a threshold at complex III, which prevents stopping the electron transport chain. Moreover, poly [ADP-ribose] polymerase 1 (PARP-1) was activated by the ROS in mitochondrial cell during the damage of DNA by MG. These metabolites activate the multiple pathogenic mechanisms, one of which includes increase production of AGEs. More AGEs are formed in a high concentration of sugar in blood and have been initially connected with diabetes and its complications or hypertension (Chang and Wu, 2006; Vander Jagt, 2008). Later it has been also shown that AGEs are involved also in aging and in neurodegenerative diseases, such as Alzheimer's disease in the human body (Angeloni*, et al.*, 2014).

1.2.3. Generation of the reactive oxygen species

The reactive oxygen species (ROS) are chemically reactive molecules containing oxygen. The generation of the superoxide anion has been investigated during the glycation reaction of amino acids by MG under aerobic conditions (Yim*, et al.*, 1995). The superoxide anion initiates the lipid peroxidation (Gutteridge and Halliwell, 1990) and it may be a potential factor to the lipid peroxidation in animal cells when treated with MG (Choudhary*, et al.*, 1997). In addition, MG generated a high concentration of hydrogen peroxide in human platelets (Leoncini and Poggi, 1996). However, ROS were not essentially involved in the toxicity related with MG because the lost of cell viability already started before the release of the ROS in the hepatocytes (Kalapos*, et al.*, 1994). Also, ROS from MG was accompanied with a decrease of the rate of cell division in the cultured cortical neurons from rat fetus (Breborowicz*, et al.*, 2004).

1.3.Methylglyoxal metabolism

1.3.1. Non-enzymatic conversion of methylglyoxal

In many organisms, MG is formed as a byproduct through several metabolic pathways (Inoue and Kimura, 1995). The major MG formation pathway is the glycolysis by catalyzing dihydroxyacetone phosphate (DHAP) or glyceraldehyde-3-phosphate (G3P) by the elimination of phosphate (Phillips and Thornalley, 1993). Additionally, the oxidation of aminoacetone, which is an intermediate of threonine catabolism, generates amounts of MG in the presence of Cu^{2+} ion (Hiraku*, et al.*, 1999; Dutra*, et al.*, 2001). In addition, MG produces from the lipid peroxidation (Poli*, et al.*, 1985).

1.3.2. Enzymatic synthesis of methylglyoxal

In contrast with non-enzymatically, MG is synthesized from three kinds of enzymatic regulation; methylglyoxal synthase (MGS) mainly found in prokaryotes, cytochrome p450 IIE1 isozyme(s), and amine oxidase (Kalapos, 1999). MGS catalyzes the conversion of DHAP to phosphate and the intermediate ene-diol-form, which subsequently tautomerizes to form MG (Rose and Nowick, 2002). Because it is inhibited by inorganic phosphate (Pi), it has been suggested that MGS play a role in the control of glycolysis depending on the availability of intracellular Pi (Hopper and Cooper, 1971). Characterization of MGS has been explained some bacteria such as *Pseudomonas saccharophila* (Cooper, 1974), *Proteus vulgaris* (Tsai and Gracy, 1976), *Clostridium acetobutylicum* (Huang*, et al.*, 1999), and *Thermus* sp. strain GH5 (Pazhang*, et al.*, 2010). The most extensive investigations on this enzyme have been performed in *E. coli* including physiological, biochemical studies and the genetic engineering study for the production of 1,2-propanol (Hopper and

Cooper, 1972; Saadat and Harrison, 1998; Totemeyer, *et al.*, 1998; Saadat and Harrison, 1999; Marks, *et al.*, 2004; Jain and Yan, 2011). However, there is no study of MGS in gram-positive bacteria except for *C. acetobutylicum* (Huang, *et al.*, 1999) in spite of the existence the *mgsA* gene in *Bacillus subtilis* (Kunst, *et al.*, 1997) and also the activity of *Bacillus* MGS was not detected in previous study (Hopper and Cooper, 1971).

In addition other enzymes for the synthesis of MG, one is isozyme(s) of Cytochrome P450 involved in acetone metabolism(Coleman, 1980). The conversion of acetone into MG needs two consecutive steps via acetol as intermediate by consuming $NADPH+H^+$(Casazza, *et al.*, 1984). It can be induced by several agents (acetone, ethanol, pyrazole, imidazole, etc.) or under different physiological conditions. The other is monoamine oxidase involved in the conversion aminoacetone to MG. This aminoacetone is from the oxidized L-threonine by NAD-dependent threonine dehydrogenase produces 2-amoinoacetacetate, and this compound is spontaneously decarboxylated to become aminoacetone. Formation of MG from aminoacetone was reported in bacteria (Elliott, 1960) and mammals (Ray and Ray, 1987).

1.3.3. Methylglyoxal detoxification in organisms

High concentration of MG can induce cell death, so that the detoxification of MG is essential system for cell growth and viability. There are several pathways for the detoxification of MG. Most well known, the glyoxalase system catalyzes the conversion of MG to D-lactate with S-D-lactoylglutathione as an intermediate (Thornalley, 1995). It consists of glyoxalase I (GLO I) and II (GLO II). GLO I (S-lactoylglutathione methylglyoxal-lyase) catalyze the one-substrate isomeration of hemimercaptal

into S-D-lactoylglutathione using a reduced glutathione (GSH) (Mannervik and Ridderstrom, 1993). GLO II (S-2-hydroxyacylglutathione hydrolase) separates S-D-lactoylglutathione into D-lactate and GSH (Vander Jagt, 1993). Incase glyoxalase III (GLO III) catalyzes the conversion of MG directly to D-lactate without GSH. GLO III catalyzing the conversion of MG into D-lactate has been reported in *E. coil* (Misra*, et al.*, 1995). GLO III shuffled inhibition and reactivation by thiol-blocking or containing agents because the involvement of the thiol group for catalysis in this enzyme (Misra*, et al.*, 1995). Interestingly, the activity of GLO III is not elevated in *E. coli* when GLO I disrupted and the expression of GLO III was dependent on the growth condition (MacLean*, et al.*, 1998; Subedi*, et al.*, 2011). In addition to glyoxalase system, aldose reductase takes part in the MG metabolism found in yeast and other microorganisms (Gomes*, et al.*, 2005; Ko*, et al.*, 2005; Xu*, et al.*, 2006). This enzyme mediated the reduction of MG to acetol and D-lactaldehyde using NADPH as a cofactor. Aldose reductase null mutant showed MG accumulation (Xu*, et al.*, 2006)and they inhibit MG-mediated AGE formation (Gomes*, et al.*, 2005) and its null mutant shows the accumulation of MG. However, in *B. subtilis*, the detoxification system is not well studied unlike *E. coli*. Recently, such enzymes involving in MG conversion into D-lactate or acetol were identified that one pathway is using bacillithiol (BSH) as cofactor instead of GSH like GLO system or the other pathways are independent on BSH in *B. subtilis* (Chandrangsu*, et al.*, 2014). But, each enzyme needs to be characterized to be confirming its activity *in vitro*. Overall metabolic pathways of MG in organism are diagramed (Scheme 2).

Additionally, polyamine might be considered as blocking agents against advanced glycation-end product (AGE) precursors such as deoxyglucosone,

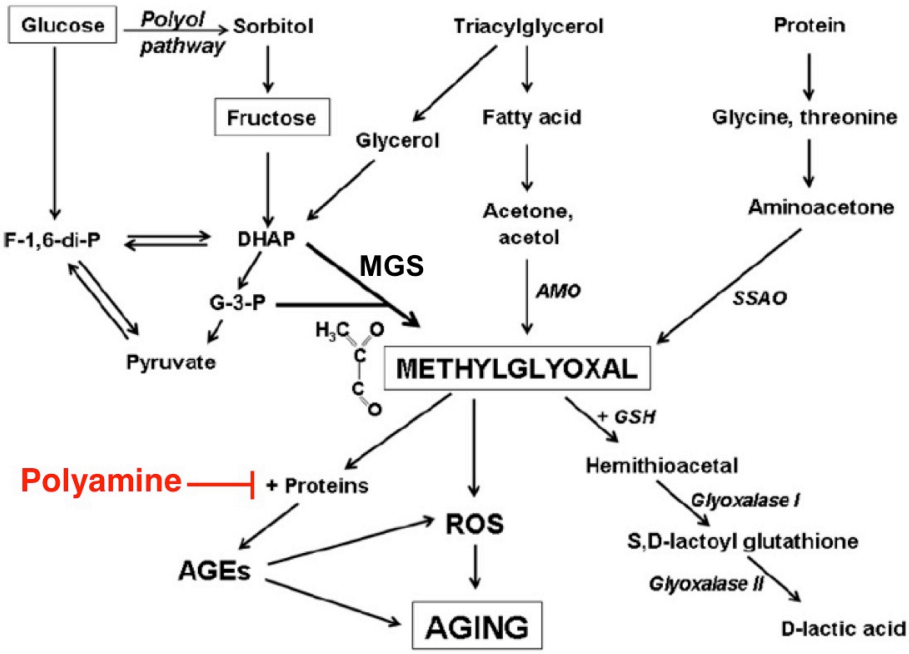

Scheme 2. Metabolic pathways of methylglyoxal

glyoxal or MG (Gugliucci and Menini, 2003; Méndez and Leal, 2004).

2. Polyamines

2.1. Polyamine overview

Polyamines are aliphatic polycations that are present in all biological organisms and have been implicated in wide functions of biological reactions, including synthesis of DNA, RNA, and protein. Because of the difference with cations such as Mg^{2+} and Ca^{2+}, the positive charges on polyamines are found at regularly spaced intervals along flexible hydrocarbon chains. Because of their unique charge-structure confirmation, polyamines can serve as electrostatic bridge between negative phosphate charges on nucleic acids and other negatively charged polymers. The structure and chemical synthesis of spermine found out in 1926 (Dudley*, et al.*, 1926). Well-known polyamines as diamine putrescine (PUT), triamine spermidine (SPD), tetraamine spermine (SPM), cadaverine (CAD) are existed (Agostinelli, 2010). Structures of polyamine are represented with agmatine (AGM), which is decarboxylated arginine (Scheme 3).

In mammalian cells, the natural polyamines-PUT, SPD, SPM are found in millimolar concentration (Pegg and McCann, 1982). But, in bacteria, the concentration of SPD (1-3 mM) is higher than that of PUT (0.1~0.2 mM), although PUT (10-30 mM) is the predominant polyamine than SPD concentration in *E. coli* (Cohen, 1997). But, SPM is not well detected in bacterial cells. CAD is the least prevalent of all naturally occurring bacterial polyamine, except for *E. coli*. However, *E. coli* can synthesize CAD from lysine under low pH condition during anaerobic growth (Watson*, et al.*, 1992)

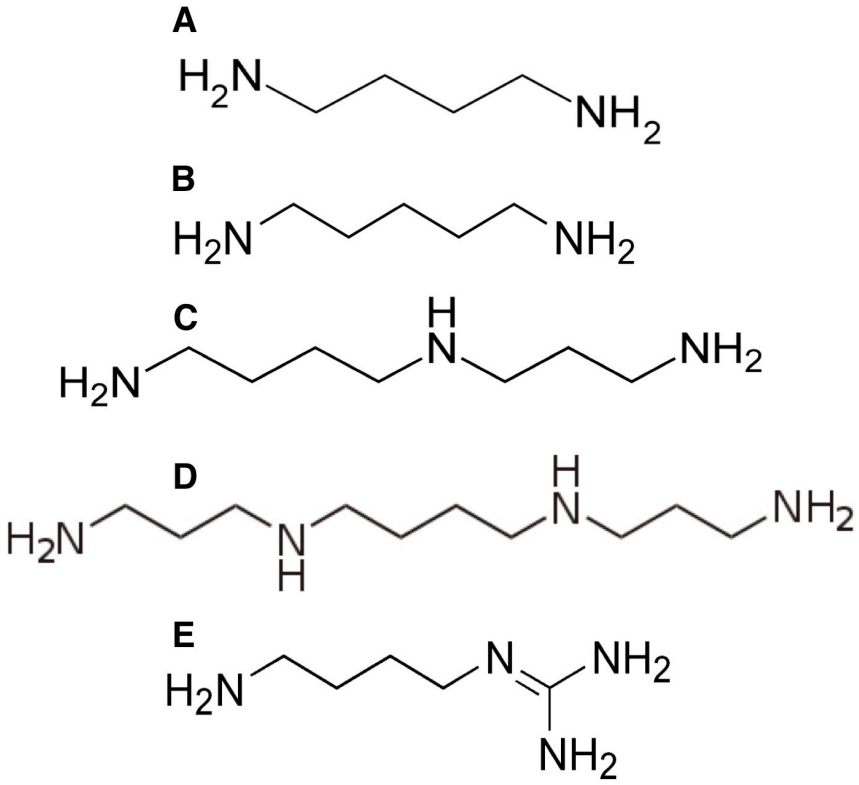

Scheme 3. Chemical structure of polyamines (A) putrescine (PUT), (B) cadaverine (CAD), (C) spermidine (SPD), (D) spermine (SPM), and (E) agmatine (AGM).

or in the absence of PUT biosynthesis (Cohen, 1997).

Although it is clear that the polyamines are essential for normal growth and have important physiological roles. These molecules are known to be the tight regulation. Because polyamine affects so many cell processes, intracellular pools maintained through the control of anabolism/catabolism and import/export enzymes (Alhonen-Hongisto*, et al.*, 1980). Regulation of polyamine metabolism has been considered as a therapeutic strategy to treat diseases (Marton and Pegg, 1995).

2.2. The enzymatic synthesis of polyamines

Most living organisms are capable of synthesizing polyamines through the decarboxylation of amino acid such as arginine, methionine, and lysine (Morgan, 1999). The biosynthetic pathways of polyamines are conserved from bacterial to animals and plants with some variations (Tabor and Tabor, 1984). In mammalian cells and in fungi the initial and at this stage rete-limit in step is the decarboxylation of ornithine to form PUT catalyzed by ornithine decarboxylase (ODC) (Morris and Fillingame, 1974). The source of the starting material; is not entirely clear and ornithine is also a product of the urea cycle.

However, many microorganisms and higher plants have a second constitutive pathway via agmatine (AGM) from arginine formed by arginine decarboxylase (ADC) instead of ODC (Moore and Boyle, 1991). AGM is hydrolyzed by agmatinase to form PUT with the elimination of the side chain of amine(Satishchandran and Boyle, 1984). In a step common to most organisms, SPD is formed from PUT by addition of an aminopropyl group from decarboxylated S-adenosylmethionine. Addition of a second aminopropyl group to SPM, catalyzed by a different aminopropyltransferase, SPD synthase, forms

SPM in higher organisms not including plants or microorganisms. The synthesis of SPD and SPM is dependent in the availability of the aminopropyl donor; hence, *S*-adenosylmethionine decarboxylase (SAMDC) is rate limiting in polyamine biosynthesis (Wallace*, et al.*, 2003). However, ODC has been considered than SAMDC (Davis*, et al.*, 1992; McCann and Pegg, 1992).

CAD is also one of diamine like PUT, is synthesized from the decarboxylation of lysine by lysine decarboxylase. Even though CAD or its aminopropyl derivative is not existed in *E. coli* grown in purified media, these amines are present when growth takes place in crude media or if the biosynthesis of PUT is blocked by mutations (Hafner*, et al.*, 1979; Goldemberg, 1980). Lysine decarboxylase has been purified to homogeneity form containing lysine at pH 5.5 media under semianaeronbic conditions (Sabo*, et al.*, 1974; Sabo and Fischer, 1974). Two genes have been described that are involved in lysine decarboxylase activity, *carR* and *cadA* in *E. coli* (Tabor*, et al.*, 1980). In addition, the *ldcC* gene encoded another lysine decarboxylase as constitutively expressed enzyme than *cadA* in *E. coli* (Yamamoto*, et al.*, 1997). Overall polyamine biosynthesis pathways are well elucidated in *E. coli* (Scheme 4).

Despite the intracellular importance of polyamines in all living organisms, the research about polyamines in *B. subtilis* is not well established. SPD is the major polyamine of *Bacillus* sp. (Setlow, 1974). Through the genome sequencing project of *B. subtilis* (Kunst*, et al.*, 1997), the some genes related with polyamine synthesis was characterized (Sekowska*, et al.*, 1998). In recently, arginine decarboxylase required the formation of biofilm development in *B. subtilis* (Burrell*, et al.*, 2010), but the other genes related with polyamine synthesis is required the experimental evidence.

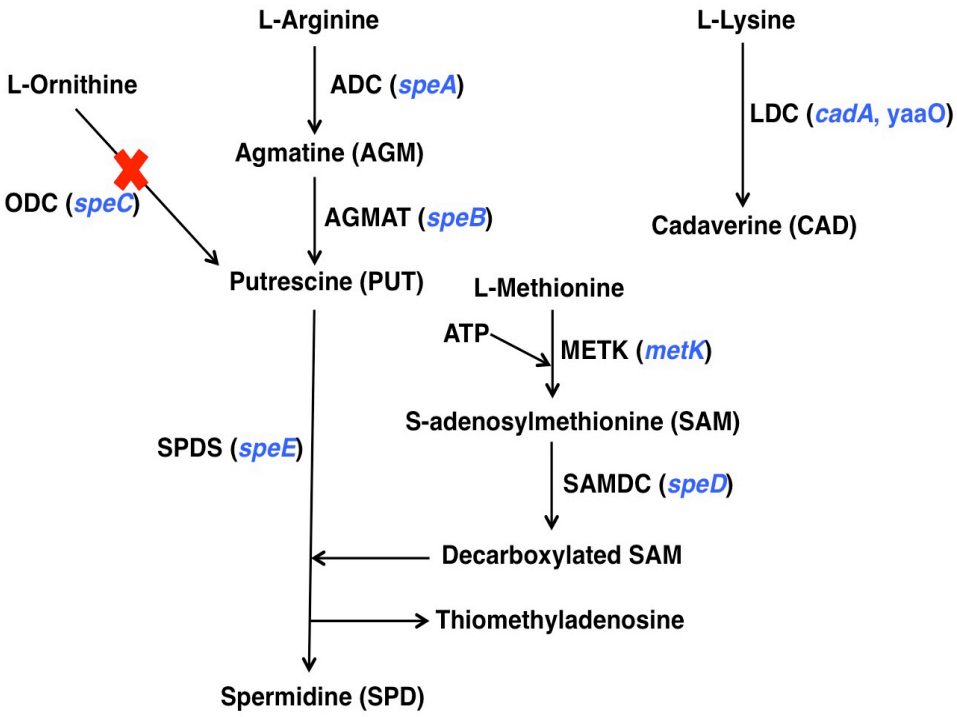

Scheme 4. Metabolic pathway of polyamine synthesis in *E. coli*

ADC, arginine decarboxylase; AGMAT, agmatinase; ODC, ornithine decarboxylase (not encoded in *B. subtilis* represents X); SAMDC, S-adenosylmethionine decarboxylase; METK, methionine adenosyltransferase; SSPDS, spermidine synthase; LDC, lysine decarboxylase (as *yaaO* in *B. subtilis*). Blue characters represent the gene name (Shah and Swiatlo, 2008).

2.3. The functions of polyamine in bacteria

2.3.1. Interaction of polyamine and nucleic acid

Polyamines can be considered of as an organic cation that can act as a counterion to nucleic acids (Wallace*, et al.*, 2003). Almost 90% of SPD bounds with RNA, 5.1% to DNA and only 3.8% free form. But in case of PUT, 9.3% with RNA, 48% with DNA, and 39% remains free PUT in *E. coli* (Miyamoto*, et al.*, 1993). Polyamines have also been shown to play a role in DNA condensation by stabilizing bends in DNA. This ability to bind and stabilize bent DNA is important since many DNA binding proteins, including transcription factors, recognize or induce bends in DNA upon binding (Pastre*, et al.*, 2006).

2.3.2. Free radical scavengers by polyamine

Oxidative stress induced damage to cell when the result of the loss of the protective effects of polyamine. It shows severe growth defect in *E. coli* (Jung*, et al.*, 2003). There are two mechanisms protecting cells. First, polyamine upregulated the *oxyR* and *katG* genes, which is are involved in the cellular response to oxidative stress (Tkachenko*, et al.*, 2001). Second, polyamines may interact directly with free radical species and inactivate them. In vitro experiments with SPM have shown that it can react with a hydroxyl radical to form a dialdehyde; this product has a significantly reduced effect and when modified by reactive oxygen species, will be released from DNA and taken into a cellular detoxification system (Ha*, et al.*, 1998). And, SPD, PUT and CAD protected cells from oxidative stress in *E. coli* (Chattopadhyay*, et al.*, 2003). Thus, polyamines protect the cell from oxidative stress by regulation of such

genes or chemically interaction.

2.3.3. Acid resistance by polyamine

The acid-inducible arginine decarboxylase (*adiA*), ornithine decarboxylase (*speF*) and lysine decarboxylase (*cadA*) are all polyamine biosynthetic enzymes that are part of the low pH response in *E. coli* (Foster, 2004). In low pH condition, these genes are able to raise the internal cellular pH by as much as two units. In case of CAD decarboxylase functions as a secondary less effective system in acid response (Foster, 2004). By addition of CAD, OmpC, which is outer membrane channel that allows free diffusion of small hydrophilic molecules across the outer membrane in *E. coli* (Samartzidou*, et al.*, 2003). This indicates that CAD or other polyamines, may contribute to additional acid tolerance mechanisms.

2.3.4. Interaction cell wall and polyamines

Cationically charged polyamines have been shown to interact with cell envelopes. In one set of experiments approximately 8% and 13% of the total polyamine content of *Salmonella typhimurium* and *E. coli*, bound to noncovalently with the outer membrane of these bacteria. Polyamines have also been shown to stabilize bacterial spheroplasets and protplastes form osmotic shock (Koski and Vaara, 1991) and improve the survival rate of freeze thawed *E. coli* cells (Souzu, 1986). Covalent interactions between polyamines and peptidoglycan have also been found. The evidence thus far has come almost exclusively in the form of anaerobic Gram-negative bacteria that have polyamines covalently linked to the peptidoglycan layer in *Selenomonas ruminantiurm* (Takatsuka and Kamio, 2004). In *S. ruminantirum*, CAD is

covalently linked to the peptidoglycan layer. The addition of CAD prevented DL-α-difluoromethyllysine (DFML) activity, which is an inhibitor of lysine decarboxylase causing the cell lysis (Kamio*, et al.*, 1986; Kamio, 1987).

2.3.5. Siderophore and virulence with polyamines

The production of iron scavenging organic molecules called siderophores is known to be important for virulence of many pathogenic bacteria. The ability to chelate iron in the low–iron environment of a mammalian host is required for bacterial survival and pathogenesis (Litwin and Calderwood, 1993). There is a class of bacterial siderophores that are built on polyamine backbone. Alcaligin, one of siderophore causing whooping cough by *Bordetella pertussis*, could not be produced by mutation of ODC (Brickman and Armstrong, 1996). In addition, the mutation of polyamine transport genes such as *potD* in *Streptococcus pneumonia* significantly attenuated virulence in a murine animal model of both septicemia and pneumonia (Ware*, et al.*, 2006).

2.3.6. Role of polyamine to biofilm formation

Polyamines have been implicated in the control of biofilm formation in several human pathogens such as *Yersinia pestis* (Patel*, et al.*, 2006). The deletion mutants related with polyamine synthesis genes revealed decreased biofilm formation accompanying with the reduced intracellular PUT level. Addition of PUT restored biofilm production in a dose-dependent manner and the restoration of the *speA* gene was sufficient for biofilm formation. The effects of polyamine in biofilm formation have also been demonstrated in *Vibrio cholera* (Karatan*, et al.*, 2005) and *B. subtilis* (Burrell*, et al.*, 2010). In *V. cholera*, deletion of a putative PotD homologue, *nspS*, disrupts biofilm

formation and it is proposed that NspS is a polyamine sensor for accepting extracellular signals. Like wise *Y. pestis*, the polyamine biosynthesis gene in *B. subtilis* controls the biofilm formation directly.

3. *Bacillus subtilis*

The Gram-positive bacterium *B. subtilis* is simple and the most extensively tools for genetically or developmental biology. Life cycle of *B. subtilis* is divided to three kinds: vegetative growing cell, sporulation for forming endospore, and germination and outgrowth (Scheme 5).

Sporulation is very important process to evolve to increase their fitness by limiting competition from other microbes and enlarging the range of carbon/nitrogen sources that can be utilized. Sporulation in *B. subtilis* provides a powerful system for explaining mechanisms of temporal and spatial gene regulation during development. More than 100 genes are expressed during sporulation in *B. subtilis*. Endospore formation in *B. subtilis* requires the integration of both external and internal stimuli including starvation, cell density, and cell cycle signals.

In respect of nutrient limitation, the intracellular concentration of GTP is very important factor. A rapidly decrease of intracellular concentration of GTP induces efficiently the sporulation even in the presence of excess nutrients. Also, the pheromone-like factors induce the sporulation on the cell density signals (Grossman and Losick, 1988). The sporulation initiation is organized into the complex regulation systems by the cascade of sigma factors. Of the regulation systems, Spo0A and σ^H are the starting point of sporulation initiation. Many various signals activate the phosphorylation of Spo0A and then an elevated level of Spo0A-P induces the sporulation by activating σ^A- and σ^H- RNAP

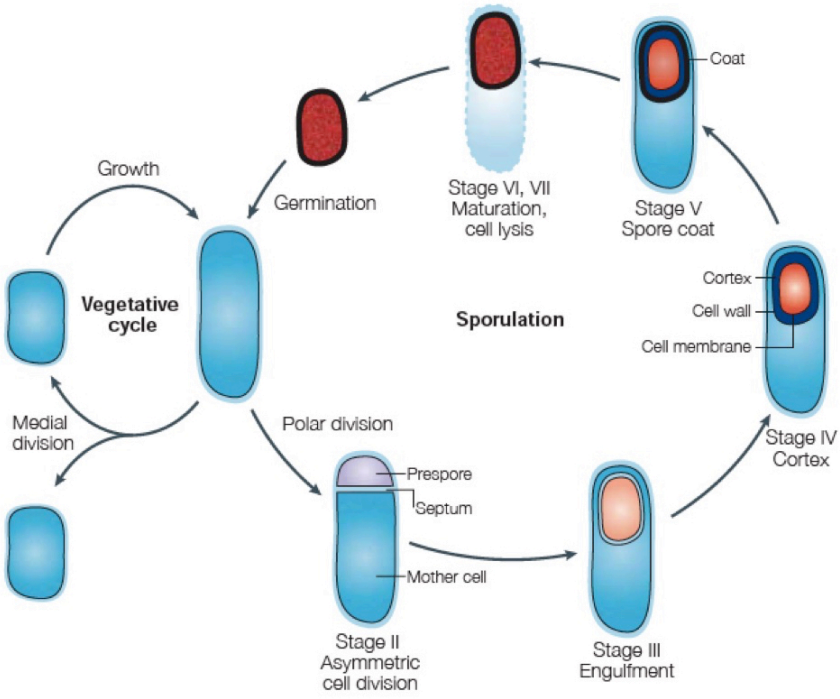

Scheme 5. Life cycle of *Bacillus subtilis* (Errington, 2003)

already present in the cell and increase the level of σ^H by repressing AbrB. The elevated σ^H induce polar septum formation not in the middle of cells (Levin and Losick, 1996). In addition, FtsZ is required in the process for the formation of asymmetric septum instead of the septum in the middle in vegetative growth (Beall and Lutkenhaus, 1991). After septum formation, the regulation of sigma factors appears to a different pattern between in the mother cell and forespore respectively. Signaling coordinates the distinct programs of gene expression in the in the mother cell and forespore.

4. Cell size regulation in *Bacillus*

4.1. Overview

When cells growth with division is important to ensure that cells are the appropriate size for the adaptation on various environmental circumstances and developmental fate. This universal phenomenon occurs from animal to single microorganism. Unlike mammalian and plant cells, bacterial cells show in a variety of shapes and the most common species are either spherical or rod-shaped. From the phylogenetic analysis, spherical cells are from rod-shaped cells because of a loss of specific genes (Siefert and Fox, 1998). Also, rod-shaped bacteria morphology was changed into spherical cells by interrupted with the certain genes (Doi*, et al.*, 1988). In other phenotypes, bacteria show various morphologies from rods and filaments to cocci, spirals and amoeboid-like forms with different cell size.

Maintaining cell size within constant range indicates cells have systems to transiently adjust the timing of division. So, many higher organisms have the cell cycle under the tight regulation by cyclin proteins regulated by cyclin

dependent kinase in each cell cycle steps. In contrast to mammals, bacterial cell division have many patterns, including binary fission, budding, hyphal growth, daughter cell formation, and the formation of multicellular baeocytes (Chien*, et al.*, 2012). Binary fission is the most common in *B. subtilis* or *E. coli*. During exponential growth, cells double in mass and then divided in the middle to generate equal sized daughter cells. And, this pattern requires cells to double in mas, initiate and terminate at least one round of chromosome replication, segregation of nucleoids, assemble the division machinery at mid-cell, and coordinate membrane insertion with cell wall synthesis to prepare a septum (Rothfield*, et al.*, 1999). The current view of cell division is the septum-specific and elongation-specific cell wall synthesizing machineries with large complex molecules, which are directed by the tubulin-like (FtsZ) and the actin-like (MreB) cytoskeleton, respectively. The overall comparison of cell division and cell elongation of current model in *B. subtilis* was simply elucidated in Scheme 6.

4.2. Molecular regulation of cell size in *Bacillus*

Bacterial shapes are related with the synthesis of peptidoglycan (PG) or cell wall. Thus, the study of bacterial morphogenesis has proceeded to PG of the cell envelope. For the synthesis of PG, there are two mechanisms to determine the cell shape, one is elongation and other is septation. In bacteria, the most *fts* genes are involved in the septation but other genes are needed for cell elongation.

For cell division, the Z ring, which is present in all bacteria, recruits proteins for the septum formation. The Z ring also recruits peptidoglycan hydrolases necessary for progression of septation and for the separation of the

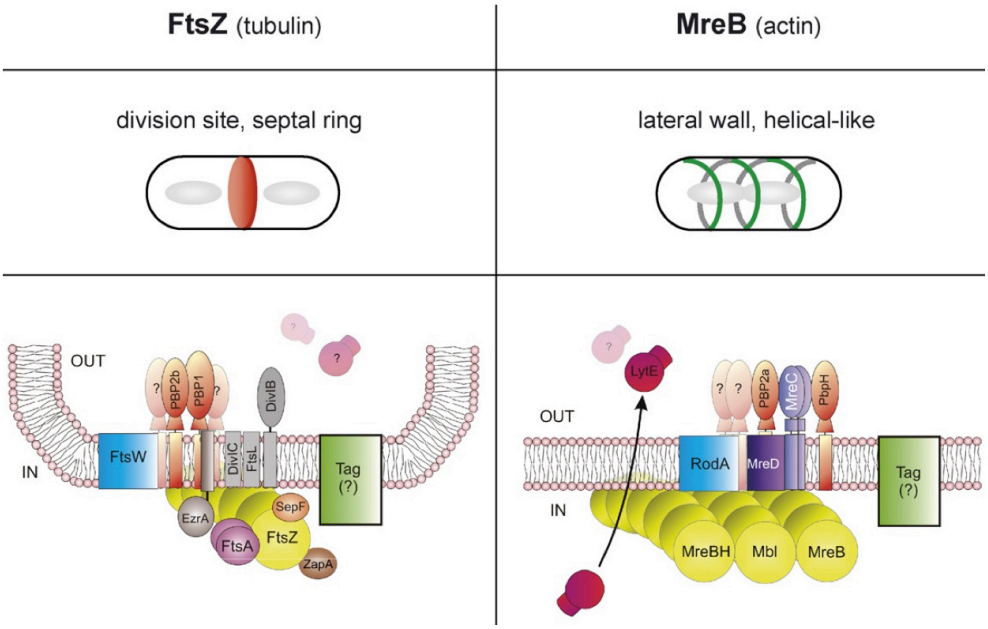

Scheme 6. Model of cell division (FtsZ*)* and elongation (MreB)

(Carballido-López and Formstone, 2007)

daughter cells after division (Priyadarshini, *et al.*, 2007). Regulation of Z ring formation plays a role in cell size determination. In rich media bacteria grow faster and divide at a larger size than in minimal media but the mechanisms that coordinate cell size with growth rate are needed more information of its mechanism. FtsZ, a homologue of tubulin, is important to form the septum in the middle cell for cell division by the dynamic movement of MinCDE proteins in *E. coli* (Lutkenhaus, 2007). The Z ring is constantly turned over *in vivo*, both before and during the constriction, through FtsZ exchange between the ring and the intracellular FtsZ pool (Stricker, *et al.*, 2002; Anderson, *et al.*, 2004). This dynamic behavior depends on the ability of FtsZ to bind and hydrolase GTP (de Boer, *et al.*, 1992; Mukherjee, *et al.*, 1993; Stricker, *et al.*, 2002). Many proteins controlled the Z ring formation that directly bind FtsZ and modulate its assembly properties in *B. subtilis*. For example, as positive regulator, FtsA (Feucht, *et al.*, 2001), SepF (Hamoen, *et al.*, 2006; Ishikawa, *et al.*, 2006) were reported. In inhibitor of FtsZ, MinC (Gregory, *et al.*, 2008), Noc (Wu and Errington, 2004), EzrA (Levin, *et al.*, 1999), ClpX and UgyP (Weart, *et al.*, 2005; Weart, *et al.*, 2007) were reported (Scheme 6).

FtsZ was known to be a tubulin homologue and to play an essential role in the formation of septum during cell division, but septum is common to all bacteria regardless of their shape (Beall and Lutkenhaus, 1991; Lowe and Amos, 1998). Thus, an additional FtsZ-independent system is required in the rod shape bacteria. The first breakthrough came with the discovery that proteins of the MreB family are actin homologues that assemble into helical filaments and have an essential role in coordinating cylinder elongation (Jones, *et al.*, 2001). The second discovery came when both insertion and degradation of the sidewall peptidoglycan of *B. subtilis* were shown to occur in helical-like configurations,

which appears to be directed by the underlying actin-like filaments (Carballido-López*, et al.*, 2006). Three actin isoforms are present in *B. subtilis*. MreB, Mbl and MreBH, which colocalize in a single helical structure, all mutants show specific cell shape defects. Mbl is considered to effect linear axis control by directing peptidoglycan insertion over the lateral wall synthesis (Jones*, et al.*, 2001; Daniel and Errington, 2003). MreB is an important determinant of cell width, and it is also thought to direct to correct assembly of a cell wall component (Jones*, et al.*, 2001). Finally, MreBH has been shown to have a distinct role in cell morphogenesis, probably the control of the autolytic activity over the lateral cell wall by directing the localization of the cell wall hydrolase LytE over the cell cylinder (Carballido-López*, et al.*, 2006). Although much progress has been made and the three MreB isoforms have been shown to play distinct role in *B. subtilis* morphogenesis, their mechanisms and effector proteins remain uncertain. Furthermore, MreC and MreD (encoded by the *mreBCD* operon) are considered to function in the same morphogenetic pathway as MreB.

In addition, the different types of the penicillin-binding proteins (PBPs) interact with the bacterial cell wall. The different PBPs bind to the various cell components to regulate cell division or cell elongation during cell growth. Among the three kinds of PBPs, class A and class B PBPs are involved in the cell shape by the interaction with specific cell components through the differential protein localization (Popham and Young, 2003). Recently, they also play a role in helical growth of the cylindrical cell wall and that they do this through interactions with elongation-specific high molecular weight PBPs such as PBP2a and PbpH (Leaver and Errington, 2005; van den Ent*, et al.*, 2006).

5. Aims of this study

As mentioned above, MG acts a cell division inhibitor and is known to be toxical to cells. In contrast with MG, polyamines involve in the interaction with nucleic acid for the stabilization, the synthesis of cell wall or peptidoglycan, and the protection from electrophiles such as glyoxal or MG. In addition, polyamines act as blocking agents of the AGEs, which caused by glyoxal or MG in diabetes patients (Gugliucci and Menini, 2003; Méndez and Leal, 2004).

Polyamine content can affect cellular protein synthesis at a translational level and sequentially cause to repress cell cycle and proliferation, leading to the morphological transition (Goldemberg and Algranati, 1977; Chattopadhyay*, et al.*, 2002; Takahashi and Kakehi, 2010). Polyamine concentration is controlled by the tight regulation. Polyamine antienzymes contribute the regulation of the synthesis of polyamines. This means that all cells intend to keep balance with any response. So, we intended to control the polyamine concentration by the production of electrophiles such as glyoxal or MG. We also expected that this phenomenon reaveals the cell morphology for the balancing in cells. In prokaryotes, tubulin homologue FtsZ and actin-like MreB were well known as global regulators of cell division or cell elongation, respectively (Carballido-López and Formstone, 2007; Souza, 2012; Celler*, et al.*, 2013). However, the morphological activators or inhibitors associated with these cytoskeletons have not been sufficiently investigated with polyamines or MG.

In our previous study, MG-accumulated cells significantly exhibited the inability of hyphal formation and virulence in *Candida* cells (Kwak*, et al.*, 2014). Herein, because *B. subtilis* has been studied for decades due to the ease

of genetic manipulation and one of the smallest known essential gene sets, it has become widely adopted as a model organism for laboratory studies (Commichau*, et al.*, 2013). We therefore intend to verify the morphological changes in the polyamine concentration cells by overproducing MG. We will also explain the growth-defective and elongated cells followed by stimulating MGS (encoded by *mgsA*) gene expression in *B. subtilis*. This work implicates that the increased polyamine content followed by MG induction triggers cell elongation factors such as MreB not FtsZ as cell division molecular. Through this we suggest that MG and polyamine is related with the cell elongation in *B. subtilis*.

II. MATERIALS AND METHODS

1. Materials

Enzymes used in DNA manipulations were purchased from Koscochem (Korea), Roche Molecular Biochemicals, or Promega Life Science. Nylon membrane, nitrocellulose membranes, and bacterial alkaline phosphatase were purchased from MBI fermentas. Q-sepharose resin, antibiotics and most of chemicals were purchased from Sigma-Aldrich. The Gene frame was purchased from Thermo and the low melting agarose for the immobilization of cells was from Lonza.

2. Methods

2.1. Bacterial strains and culture conditions

Bacillus subtilis and *Escherichia coli* strains used in this study are listed in Table 1. *B. subtilis* PS832 was grown in 2×YT medium or Spizizen's minimal media (SMM) for liquid culture. Cells were grown in 2×YT medium by inoculating with overnight cell and incubating with 200 rpm at 37°C. For growth in SMM, cells were grown in Luria-Bertani (LB, 1% Bacto-Trypton, 0.5% Bacto-Yeast extract, and 1% NaCl) or 2×YT medium from a single colony for overnight at 37°C and washed twice with SMM and inoculated starting with O.D (600 nm)=0.05 for 16 h at 37°C as used a seed culture. After grown in SMM seed, cells were transferred in main SMM with started O.D (600 nm)=0.05 at 37°C with 200 rpm.

E. coli DH5α was used for all initial transformation of plasmids. *E. coli* BL21(DE3)pLysS was used to overproduce proteins by using pET system. For transformation in *B. subtilis*, *E. coli* DH5α and *E. coli* JM105 were used. *E. coli* was grown in LB broth and agar plate containing 1.5% agar.

Table 1. *B. subtilis* and *E. coli* strains used in this study

Strains	**Genotype or description**	**Reference or sources**
PS832	Wild type (Trp^+ revertant of *B. subtilis* 168)	Peter Setlow
HB001	PS832 derivative (control strain) containing pRB374	(Ryu, *et al.*, 2006)
ΔmgsA	PS832 *mgsA:cat*	This study
$mgsA^{OE}$	PS832 containing pHS104	This study
ΔspeA	PS832 containing pHS105	This study
$speA^{OE}$	PS832 containing pHS106	This study
ΔspeB	PS832 containing pHS107	This study
$speB^{OE}$	PS832 containing pHS108	This study
ΔyaaO	PS832 *yaaO:cat*	This study
$yaaO^{OE}$	PS832 containing pHS109	This study

Strains	Genotype or description	Reference or sources
E. coli DH5α	*F-ΔlacU169(f80lacZDM15)endA1 rec1hsdR17 deoR supE44 thi-1 λ-gyrA96 elA1*	(Hanahan, 1983)
JM105	*supEendAsbcB15hsdR4rpsL thi*Δ(*lac-proAB*)	(Yanisch-Perron, *et al.*, 1985) ; Helmann, J.D.
BL21(DE3)pLysS	F⁻*ompT*r_B-m_B-(DE)/pLysS	(Studier, 1991)

2.2. Media

All media used in this study were made according to the method described in Molecular Biological Methods for *Bacillus* (Harwood and Cutting, 1990).

2×YT medium

2×YT medium consisted of 1.6% Bacto-Trypton, 1% Bacto-Yeast extract, and 0.5% NaCl.

Schaeffer's solid medium (DSM)

Schaeffer's solid medium consisted of 8% Difco-nutrient broth, 1% KCl, 1.2% $MgSO_4 \cdot 7H_2O$ (pH 7.0~7.2), 1 mM Na_2SO_4, 10 μM $MnCl_2$, 1 μM $FeSO_4$.

Spizizen's minimal media (SMM)

Spizizen's minimal media (SMM) consisted of 1.4% K_2HPO_4, 0.6% KH_2PO_4, 0.2% $(NH_4)_2SO_4$, 0.1% Na-citrate$\cdot 2H_2O$, and 0.02% $MgSO_4 \cdot 7H_2O$ with containing 0.5% glucose and trace elements solution.

2.3. General DNA manipulation

General DNA techniques for purification and manipulation of DNA in *B. subtilis* or *E. coli* were as described previously (Harwood and Cutting, 1990; Sambrook and Russell, 2001). All plasmids used in this study are listed in Table 2.

2.3.1. Polymerase Chain Reaction (PCR) and DNA sequencing

DNA fragments were amplified by Taq polymerase as described in

Table 2. Plasmids used in this study

Plasmids	Description	References or sources
pGEM-T easy	PCR cloning vector	Promega
pET15b	N-terminal 6 His-tag expression vector for overproduction	Novagen
pET3a	Overproduction vector without tag	Novagen
pRB374	Expression vector for *Bacillus*	Piggot,P.J.
pHP13	Expression vector for *Bacillus*	Piggot,P.J.
pMutin2	Gene disruption vector for *Bacillus*	Piggot,P.J.
pHS100	pET15b:*mgsA*	This study
pHS101	pET3a:*mgsA*	This study
pHS102	pHP13:*sodA*	This study
pHS103	pHP13:(RBS) *mgsA*	This study
pHS104	pRB374:(RBS) *mgsA*	This study
pHS105	pMutin2:*speA*	This study
pHS106	pRB374:*speA*	This study
pHS107	pMutin2:speB	This study
pHS108	pRB374:*speB*	This study
pHS109	pRB374:*yaaO*	This study

manufacturer (Koschemco). For the reactions, 50 pmol of each 5′ and 3′ primers, 200 ng of genomic DNA, and 0.5 U of Taq polymerase were mixed in a final volume of 50 μl with reaction buffer; 50 mM KCl, 1.2 mM $MgCl_2$, 10 mM Tris-HCl (pH 8.4), and 50 μM dNTPs. The mixture was subjected to 25 cycles of 30 sec denaturation at 95°C, 30 sec annealing at 50°C, and 30 sec extension at 72°C. The PCR product was purified by using Gene clean kit (MO BIO). For DNA sequencing was performed by automatically using ALF express DNA sequencer (Pharmacia).

2.3.2. Cloning

The primers for the overexpression of genes, overproduction of proteins, and disruption or deletion of gene are listed in Table 3. For DNA sequencing, pGEM-T easy vector was used. After each plasmids were digested with appropriate restrict enzyme, each fragments were introduced into secondary plasmid for the purpose.

2.3.3. Transformation

2.3.3.1. *E. coli*

Insertion of the desired DNA into *E. coli* was performed by $CaCl_2$ method as described previously (Sambrook and Russell, 2001).

2.3.3.2. *B. subtilis*

Insertion of DNA into *B. subtilis* was carried out as described (Kunst and Rapoport, 1995). Samples were spread onto LB agar plate with appropriate selective antibiotics and incubated at 37°C for overnight.

Table 3. Primers used in this study

Primers	Sequence	Sources
MGS_F	5′-GGATAACATATGAAAATTGCTTTG-3′	This study
MGS_R	5′-CTCGAGATCATCACTGTGGGCGCC-3′	This study
M1	5′-GAAGCTGATCTAGAAGAGCTCACA-3′	This study
M2	5′-CTTTAGTTGAAGAATAAAGGATCCCTAATCAATGATATTTTC-3′	This study
M3	5′-CAGTCGGTTTTCATATGTCACTAATGCTGACGTTCTTGCTTTTGG-3′	This study
M4	5′-CTATTGTACTCGAGATATCAATAAC-3′	This study
C1	5′-AATGGATCCTTTATTCTTCAACTAAAGCAC-3′	This study
C2	5′-GTTAGTGACATATGAAAACCGACTGTA-3′	This study
CP	5′-GTGAATTTAGTGTCTGCTTTCTTC-3′	This study
S1*	5′-AAGCTTCGTCATTTCAGTACATATACTAAGGAGGAATTCATATGGCT-3′	This study

Primers	Sequence	Sources
S2	5′-GGTTTGGGATCCTTGTGATTTCAAG-3′	This study
a1	5′-CGTTAAGCTTAGATTTGATTAATATTG-3′	This study
a2	5′-CAATATTAAAGGATCCACGAAGCC-3′	This study
A1	5′-GTCGACAAACTGATTTTAATACACAC-3′	This study
A2	5′-GGATCCCTTAAAGCGGCATGC-3′	This study
b1	5′-AAGCTTATTCAGGAAAAGTATTTATCG-3′	This study
b2	5′-GGATCCAGCACTTCAAATTTTGAG-3′	This study
B1	5′-GTCGACTGCGCTTTTTTACAG-3′	This study
B2	5′-GGATCCATGTTTGTAAAGACTG-3′	This study
y1	5′-AAGTGCACCGCAAATCAGGCTGAT-3′	This study

Primers	Sequence	Sources
y2	5′-CTTTAGTTGAAGAATAAAGGATCCGTGTTCATAAACAATCCTTTG-3′	This study
y3	5′-CAGTCGGTTTTCATATGTCACTAACGGTTTATTTATTACATTCGAAG-3′	This study
y4	5′-TATGAAAGTCCAGTTTTTCTAAATCG-3′	This study
Y1	5′-GGATCCCTTAAAGCGGCATGC-3′	This study
Y2	5′-GAATTCGCTCATGATTTCTCCTCT-3′	This study
CM	5′-CGCCATCAAAAATAATTCGCGTCTG-3′	This study

* S1 primer contains the ribosome binding site of the *sodA* gene (box) and *Nde*I sites (underlined).

2.3.4. Constructs for mutants

For the deletion construct of the *mgsA* (M1, M2, M3 and M4 primers) and *yaaO* (y1, y2, y3 and y4 primers) gene the long-flanking homologous (LFH) recombinant method with chloramphenicol resistant gene (C1 and C2 primers) was introduced (Wach, 1996). The *speA* (a1 and a2) and *speB* (b1 and b2) gene were disrupted by the insertion the desired fragments into pMutin2. To obtain *mgsA*-overexpressing mutant, cloning was performed by the insertion of the *sodA* gene (encoding superoxide dismutase) including its ribosome binding site (RBS) using S1 and S2 primers. This amplified fragment by PCR was introduced into pGEM T-easy vector (Promega). From the fragment digested by *Hin*dIII and *Bam*HI was ligated into pHP13 vector and yielded pHS102. The ORF of *mgsA* digested by *Nde*I and *Bam*HIof pHS101 was ligated into pHS102 instead of the *sodA* gene. To utilize the strong promoter of pRB374, the fragment of pHS103 digested by *Hin*dIII and *Bam*HI was inserted into pRB374 for resulting in pHS104 plasmid. For the overexpression of *speA* (A1 and A2 primers), *speB* (B1 and B2 primers), and *yaaO* (Y1 and Y2 primers) the desired fragments were ligated into pRB374.

2.4. RNA analysis

2.4.1. Preparation of RNA from *B. subtilis*

Total RNA isolation from *B. subtilis* was performed by using 'Modified Kirby Mix' (Van Dessel*, et al.*, 2004). RNA was isolated from *B. subtilis* grown in 2×YT. Cells were resuspended in Kirby mixture [2% lauroylsarcosine, 12% sodium 4-aminosalicylate, 12% phenol equilibrated with the buffer (pH 8.0)] provided by manufacturer. The resuspended cells were disrupted by sonication with a micro tip at 15% of the maximum amplitude for 15 sec and then the

equal volume of phenol:chloroform:isoamylalcohol (25:24:1) was added at mixture. After centrifugation at 12,000 rpm for 20 min, supernatant was precipitated with equal volume of isopropanol and washed with 70% ethanol. The pellet was treated with 1 U of RNA-free DNase for 15 min at 37°C. Following treatment with DNase, the RNA pellet was dissolved in DEPC-water. The concentration of RNA was quantified by Nanodrop (Thermo).

2.4.2. Northern blot analysis

Northern blot analysis was adopted from general method. The probe was amplified by PCR and labeled with [α-^{32}P]-dATP. For northern blot analysis, 20 μg of total RNA were separated on 1% agarose gel containing 0.22 M formaldehyde and transferred to Hybond-N+ membrane (Amersham Pharmacia Biotech, Buckinghamshire, UK) for overnight. The membrane preincubated at 65°C for 1 h and followed by incubated 2h with the isotope labeled DNA in Rapid buffer (GE Healthcare). And the membrane was washed with sodium saline citrate buffer (2x SSC) containing 0.1 % SDS. For developing, the membrane was covered with BAS film for overnight at RT. The signal was detected by BAS-2500 (Fujifilm).

2.5. Protein analysis

2.5.1. Preparation of the cell crude

Harvested cells were resuspended in lysis buffer [20 mM Tris-HCl (pH 8.0), 0.1 mM phenylmethylsulfonyl fluoride (PMSF), and 0.1 mM EDTA] containing lysozyme (0.1 mg/ml). The suspension was incubated at 37°C for 10 min and disrupted by sonication with ultrasonicator (Sonics and Materials Inc.). The suspension was centrifuged at 12,000 rpm for 20 min. the supernatant was

used as the total cell crude. The protein concentration was determined by using bradford assay kit (Bio-Rad Laboratories) with bovine serum albumin as standard.

2.5.2. Western blot analysis

A total 100 μg of crude extract was resolved on 16% Tricine SDS-PAGE. Following Tricine SDS-PAGE, the gel was electrotransferred to nitrocellulose transfer membrane Protran at 150 mA for 1h. Membrane was blocked in 10 mM Tris-buffered saline buffer (TBST) containing 0.15 M NaCl, 5 mM NaN_3, 0.05% Tween 20 for 30 min twice. The block membrane was incubated with antibody diluted in the same buffer for more than 12 h, and then washed with TBST for 30 min twice. Washed membrane was incubated with anti-mouse IgG antibody-alkaline phosphatase conjugate diluted to 1:10,000 in TBST for 90 min, and washed with TBST for 30 min twice. Washed membrane was rinsed with alkaline phosphatase buffer [100 mM Tris-HCl (pH 9.5), 100 mM NaCl, 10 mM $MgCl_2$]. For color development, the membrane was incubated in 20 ml of alkaline phosphatase buffer containing 8 mg/ml of BCIP and 16 mg/ml of NBT at 37°C.

2.6. Purification of methylglyoxal synthase (MGS) and determination of the biochemical properties

2.6.1 Overproduction and purification of MGS

For the overexpression of *mgsA* gene from *E. coli*, *mgsA* gene was amplified by PCR with MGS_F and MGS_R primers. Around 420 bp of the fragment was cloned into pGEM-T easy vector for DNA sequencing. After

*Nde*I/*Xho*I digestion, the fragment was cloned into pET15b vector (pHS100). For the overexpression without tag, the fragment digested by *Nde*I/*Bam*HI was ligated into pET3a.

For overproduction of MGS, *E. coli* BL21 cells were transformed with the gene product and grown on LB agar plate containing 50 μg/ml of ampicillin, 34 μg/ml of chlorampenicol at 37°C for 16 hrs. A fresh single colony was inoculated in liquid LAC medium and grown to A_{600} 0.4~0.5 at 37°C. And then cells were induced by adding 1 mM isopropylthio-β-D-galactoside (IPTG) and were harvested after further incubation at 37°C for 4hrs. Cells were harvested by centrifugation at 7000 rpm for 10 min, and the pellet was washed with 50 mM imidazole-HCl (pH 7.0) and stored at -80°C before use. The pellet was resuspended in 40 mL of 50 mM imidazole-HCl (pH 7.0) and 1 mM PMSF. After sonication for 20 min, crude lysate was centrifuged at 15000 rpm for 20 min at 4°C. The supernatant was heated in a water bath at 65 °C for 1 min and cooled in ice water. The supernatant was applied to a Fast flow Q-sepharose (Sigma) open column equilibrated with 50 mM imidazole-HCl (pH 7.0), and the column was washed with 1.5× the volume of the column with 50 mM imidazole-HCl (pH 7.0) buffer containing NaCl (0 to 300 mM) step by step. The protein was eluted from the column at 400 mM NaCl in 50 mM imidazaole-HCl (pH 7.0). The fractions were confirmed by 16% Tricine SDS-PAGE.

2.6.2. Determination of enzyme kinetics

Bacillus MGS activity was measured by a UV/VIS spectrophotometer (Shimadzu) at 550 nm. An absorbance of 16.4 represented the formation of 1 μmol of MG (Cooper, 1975). To determine enzyme kinetics, different

concentrations of DHAP were used as the blanks. Experimental data were analyzed by the Michaelis-Menten curve, and the K_m and V_{max} were determined using the Lineweaver–Burk plot.

2.6.3. Determination of molecular mass

Bacillus MGS and molecular mass standards (Sigma) were applied on a Superose 12 column (GE Healthcare) pre-equilibrated with 50 mM imidazole-HCl (pH 7.0) containing 400 mM NaCl. A standard curve was generated by plotting the logarithm of molecular mass of standard proteins against their K_{av}, where $K_{av} = (V_e-V_0)/(V_t-V_0)$: V_e, elution volume; V_0, void volume; V_t, total bed volume. K_{av} of methylglyoxal synthase determined by comparing with standard proteins: bovine serum albumin (66 kDa), carbonic anhydrase (29 kDa), cytochrome C (12.4 kDa), aprotinin (6.5 kDa).

2.7. Additional methods

2.7.1 Determination of methylglyoxal concentration

The intracellular concentration of MG was determined according to the method as described (Choi*, et al.*, 2008) with some modifications. The sample was disrupted by 0.5 M perchloric acid on ice for 20 min. The sample was centrifuged at 12000 rpm for 20 min to remove the pellet, and the supernatant was incubated with 1,2-diaminobenzene at 65°C for 3 h in the dark. The sample was passed through a C-18 solid phase extraction column and then eluted by methanol. Samples were concentrated and resuspended in the mobile phase to be applied on an Agilent 1200 series high performance liquid chromatography (HPLC) system with a C-18 analytic column (Zorbax Eclipse XDB C18, 4.6 × 150 mm, Agilent Technologies). The modified mobile phase was 67% HPLC

grade water, 3% acetonitrile, and 30% methanol for 60 min. The flow rate was 1 mL/min under a wavelength of 336 nm. 2-Methylquinoxaline was used as a standard.

2.7.2 Determination of polyamine concentration

Intracellular polyamines (AGM, PUT, SPD and CAD) levels were determined (Morgan, 1998) with some modification. Exponentially growing cells were harvest and resuspended cell twice in PBS. The supernatant added 100 μL of 50% TCA and mixed on a vortex shaker at 15 min. After mixing, the pellet was removed by centrifuged at 12000 rpm for5 min and 500 μL of cell extract, 100 μM PUT, SPD and 1, 3-diaminopropane as standard added 2 mL of 2M NaOH with 10 μL of 50% benzoyl chloride in methanol at RT for 40-60 min. The sample added 1 mL of chloroform, followed by vigorously vortexing for 1 min and centrifuged at 12000 rpm for 3 min briefly to separate the layer. The lower chloroform layer transferred new tube and one more chloroform extraction. The chloroform layers combined and added 1 mL of HPLC grade water. After sample vortexing, the mixture centrifuged at 12000 rpm for 3 min. The lower layer transferred new tube and was evaporation. The pellet was dissolved in the 100 μL of mobile phase buffer (60% HPLC grade methanol and 40% HPLC grade waters). The sample was separated on Waters ODS2-C18 column using Agilent 1200 series HPLC system. Dibenzoylated polyamine derivatives were detected at 229 nm.

2.7.3. Microscopy analysis

Cells were harvested at the exponential stage and washed twice with phosphate buffered saline (PBS). Cells were suspended in 100 μL of PBS.

Samples were observed by spotting 5 μL of cells onto a 1% low melting agarose pad in Gene Frame ® (Lonza, NUSIEVE® GTG and Thermo). Preparing the agarose pad was followed by the manufacture's manual. Microscopy was performed with an Axio observer Z1 (Zeiss). Analysis of cell length was performed using the AxioVision LE (Zeiss) program and calculated versus a standard scale.

2.7.4. EPR analysis

EPR spectra were recorded on a Bruker ESP 300S EPR spectrometer. An aqueous flat cell was used for the experiments. The reaction were started by injecting MG into samples initially containing 0.2 M PUT, 0.2 M SPD and 0.2 M MG in 0.5 M sodium bicarbonate buffer at pH 9.5. The buffers used for the reaction of polyamines with MG were treated with Chelex 100 resin (Bio-Rad) to remove traces of transition metal ions. The instrumental settings for spectral acquisition were, unless otherwise indicated, as follows: temperature, RT; microwavepower, 20 milliwatts; modulation amplitude, 1 G; conversion time, 10.24 ms; time constant, 82 ms; and sweep width, 100 G with 4096- point resolution.

III. RESULTS

3.1. Free radicals generation by MG

Previous reports showed that reaction between MG and lysine or alanine, containing amine group, formed free radicals that presumed to be involved in the advanced glycation of proteins (Yim*, et al.*, 1995; Lee*, et al.*, 1998). These findings provide the possibility that polyamines, which have two or more amine group, may be a good model system for the study about regulation of intracellular MG. Because polyamines are related with the protective mechanism of AGE precursors occurred by MG (Ulrich and Cerami, 2001; Gugliucci and Menini, 2003). To investigate the relationship between MG and polyamine, we first checked the reaction between MG and the precursors of polyamine *in vitro* by electron paramagnetic resonance (EPR) spectroscopy analysis. We hypothesized that the blocking of the polyamine genes causes to accumulate precursors, which reacts with MG in cells.

The radical signal of MG was not detected by itself. Free radical signals from the reaction of arginine, AGM, and PUT with MG showed very low frequencies at the same concentration or 2-folds higher of MG. But, the signal was detected weakly at the reactions of high concentration of MG with arginine, AGM, and PUT (0.2 M). However, the high signal was significantly high when the reaction of MG and lysine with the same concentration (0.2 M) mixed as shown in previous study (Shumaev*, et al.*, 2009). Likewise other reactions, increasing the concentration of MG with lysine showed also increased signals in EPR spectra (data not shown). This EPR analysis provided the possibility that MG react with the precursors needed for the synthesis of polyamine in cells. And, MG reacts with lysine easily *in vitro*, but it needs to be proved *in vivo*. Also, MG also binds with arginine, AGM or PUT weakly *in vitro*, so we manipulated the genes related with the synthesis of polyamine in *B. subtilis* to

find out the relationship between MG and polyamine.

3.2. Gene related with the synthesis of polyamine in *B. subtilis*

Through EPR analysis, we confirmed that polyamine and MG reacted each other *in vitro*. To investigate the relationship between polyamine and MG *in vivo*, we manipulate the synthesis of polyamine genes in *B. subtilis* and we compared these genes with *E. coli*, which is well-studied strain for polyamine biosynthesis (Tabor*, et al.*, 1980; Igarashi and Kashiwagi, 2006). As mentioned in introduction, *E. coli* have two pathways to produce PUT via ornithine decarboxylase (encoded by *speC*) or another alternative pathway via arginine decarboxylase (encoded by *speA*) and agmatinase (encoded by *speB*) (Scheme 4). But, ornithine decarboxylase is not existed in *B. subtilis*, it also mentioned in the previous study (Sekowska*, et al.*, 1998). But, each genes homology has the low sequence identity with *E. coli* proteins. And the gene of the *yaaO* found to be encoded as a putative lysine decarboxylase in *B. subtilis* (Table 4). Through this, the proteins of the synthesis of polyamine are expected different properties unlike *E. coli*. Even though the characterization of polyamine synthesis genes revealed in *B. subtilis* (Sekowska*, et al.*, 1998), the biosynthesis of polyamine has not been sufficient studied now.

3.3. Polyamine mutants and growth inhibition

To understand the functional roles of polyamine with MG, we manipulated the genes of polyamine except for *speD* (encoding spermidine synthase) and *speE* (S-adenosylmethionine decarboxylase) because these two genes are not late limit enzymes the synthesis of polyamine. To investigate the functions of polyamines with MG, we made deleted or overexpressed mutants.

Table 4. Comparison of the synthesis of polyamine proteins

Proteins	**Gene in *E. coli***	**Gene in *B. subtilis***	**Similarity (%)**
arginine decarboxylase (ADC)	*speA*	*speA*	16
agmatinase (AGMAT)	*speB*	*speB*	31
S-adenosylmethionine decarboxylase (SAMDC)	*speD*	*speD*	21
spermidine synthase (SPDS)	*speE*	*speE*	36
Lysine decarboxylase (LDC)	*cadA*	*yaaO*	20

For the deletion of the *yaaO* (encoding a putative lysine decarboxylase), LFH-PCR was performed as described previously (Wach, 1996). For the disruption of the *speA* (encoding arginine decarboxylase) and the *speB* (agmatinase) were introduced into pMutin2 by the single homologues recombination method (Vagner*, et al.*, 1998). The disruption or deletion mutants were confirmed by PCR with CM (disruption for *speA* and *speB*) and CP (deletion for *yaaO*). The products of PCR were shown at around 1400 bp for *speA*, 1100 bp for *speB*, and 700 bp for *yaaO* each. And, all overexpressed mutants were confirmed by northern blot analysis (Fig. 1.).

We expected that the growth inhibition occur in the disrupted polyamine strains because MG reacts with the amino acids as precursors of polyamine or PUT through the experiments of EPR analysis. To confirm, we measured the growth of mutants by UV-VIS spectroscopy at 600 nm. The growth inhibition was occurred slightly in the disrupted (*ΔspeA* and *ΔspeB*) and the deleted (*ΔyaaO*) mutants than PS832 used as wild type cells according to our expectation. In *ΔspeB* and *ΔyaaO* strains, the growth inhibition observed (Fig. 2A). Interestingly, the growth of $speB^{OE}$ and $yaaO^{OE}$ strains were inhibited remarkably. However, there was no difference between $speA^{OE}$ strain and vector control cells (HB001) (Fig 2B). In addition, the growth pattern was similarly observed in the minimal media (data not shown). These results partially support our hypothesis that MG accumulation by the blocking the synthesis of polyamine. However, the more explanation of growth inhibition are needed in the $speB^{OE}$ and $yaaO^{OE}$ strains.

Fig. 1. Disruption and overexpression of polyamine enzymes in *B. subtilis*.
(A) For arginine decarboxylase (*speA*) was disrupted and overexpressed. (B) agmatinase (*speB*) was disrupted and overexpressed. (C) Lysine decarboxylase (*yaaO*) was deleted and overexpressed. All disrupted or deleted mutants were confirmed by PCR using CP (*yaaO*) and CM (*speA* and *speB*) primers loading onto 0.8% agarose gel. All overexpressed mutants were confirmed by northern blot analysis using appropriates probes.

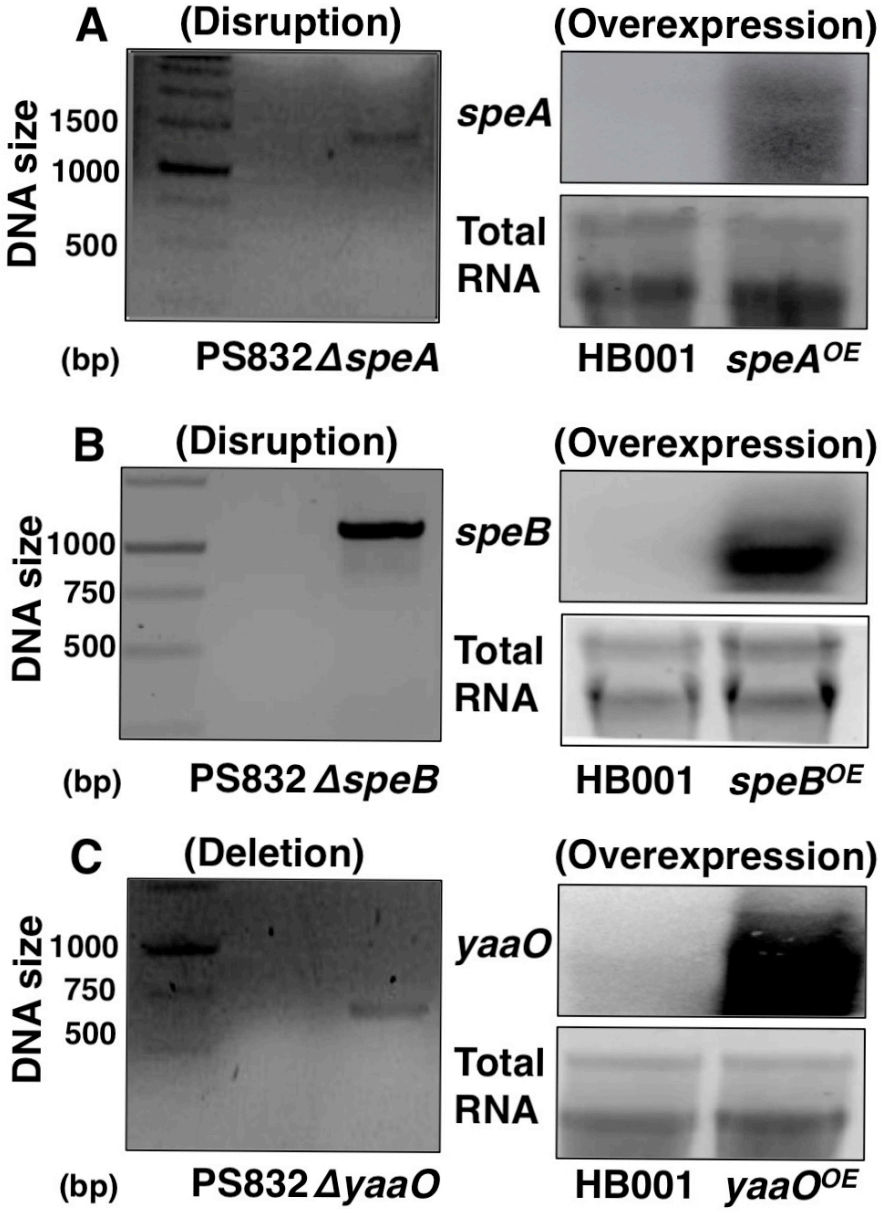
A
(Disruption)
(Overexpression)
DNA size
1500
1000
500
(bp)
PS832ΔspeA
speA
Total RNA
HB001
speA^OE
B
(Disruption)
(Overexpression)
DNA size
1000
750
500
(bp)
PS832 ΔspeB
speB
Total RNA
HB001
speB^OE
C
(Deletion)
(Overexpression)
DNA size
1000
750
500
(bp)
PS832 ΔyaaO
yaaO
Total RNA
HB001
yaaO^OE

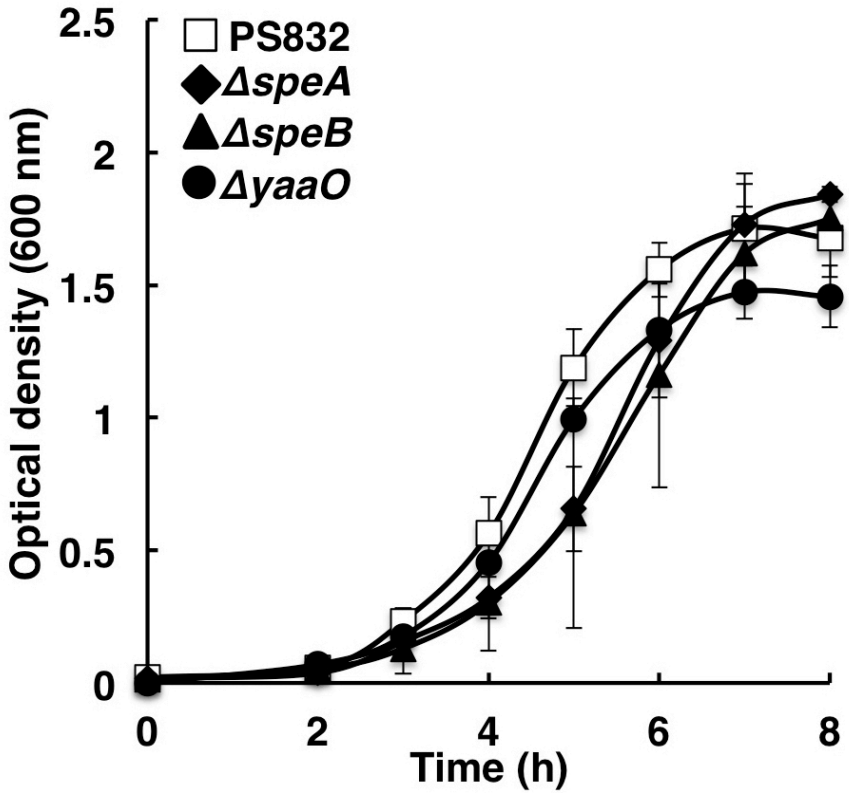

Fig. 2A. Growth inhibition in the polyamine defective mutants.

All strains were measured optical density at 600 nm in 2xYT media. PS832 as wild type cells (open square), *ΔspeA* (closed diamond), *ΔspeB* (closed triangle), and *ΔyaaO* (closed circle) strains are represented respectively.

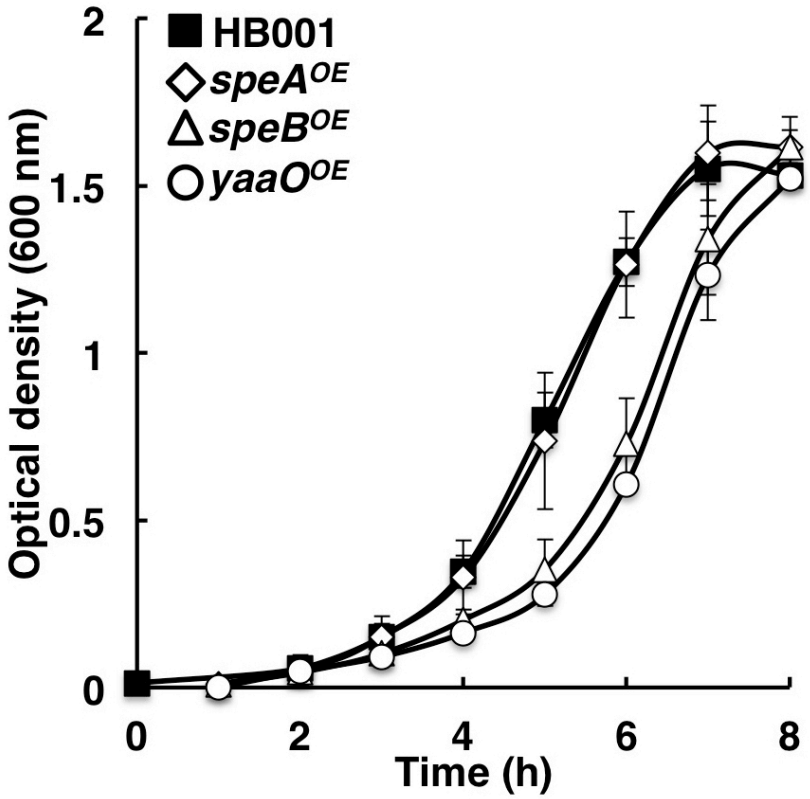

Fig. 2B. Growth inhibition in the polyamine-overexpressing mutants.

All strains were measured optical density at 600 nm in 2xYT media. HB001 as control cells (closed square), *speA*^{OE} (open diamond), *speB*^{OE} (open triangle), and *yaaO*^{OE} (open circle) strains are represented respectively.

3.4. Growth inhibition caused by MG accumulation

To investigate whether the concentration of polyamine affects the cell growth, we measured the intracellular concentration of polyamine derivatives by benzoyl chloride as described in Materials and methods.

AGM or PUT was detected 50- or 100- folds low concentration than CAD or SPD (data not shown). SPD is the major polyamine in *B. megaterium* as previous described (Setlow, 1974). In *B. subtilis* also, the major polyamine was detected SPD. In all disruption mutants, the intracellular SPD level decreased remarkably but CAD level was increased than PS832 except for *ΔyaaO* strain (Fig 3A). As our expectation, the intracellular SPD concentration increased in all overexpression strains than reference strain (HB001). But, we could not detect the difference between $speB^{OE}$ strain and HB001. The CAD level also increased in the $yaaO^{OE}$ strain significantly than other strains (Fig. 3B). The concentration of polyamine might affect the cell growth based on the result.

To investigate the further reason of cell growth inhibition, we measured the intracellular MG concentration during the exponential growth from each strain by detection of 2-methylqunoxaline derivatives as described in Materials and Methods. Since MG is well-known cell growth inhibitor (Szent-Györgyi*, et al.*, 1967) when cells were treated MG exogenously , it caused growth inhibition in *B. subtilis* (Nguyen*, et al.*, 2009). The *ΔspeA*, *ΔspeB* and *ΔyaaO* strains increased the intracellular concentration of MG 0.2~0.4 folds versus PS832 used as wild type (Fig. 4A). This result also supported the growth inhibition in *ΔspeA*, *ΔspeB* and *ΔyaaO* (Fig. 2A). Except for the $speA^{OE}$ strain, the intracellular MG concentration was significantly increased 1.5 folds in the $speB^{OE}$ and $yaaO^{OE}$ strains than the reference strain (HB001) (Fig. 4B). So, this result accompanied with the growth of $speB^{OE}$ and $yaaO^{OE}$ strains (Fig. 2B).

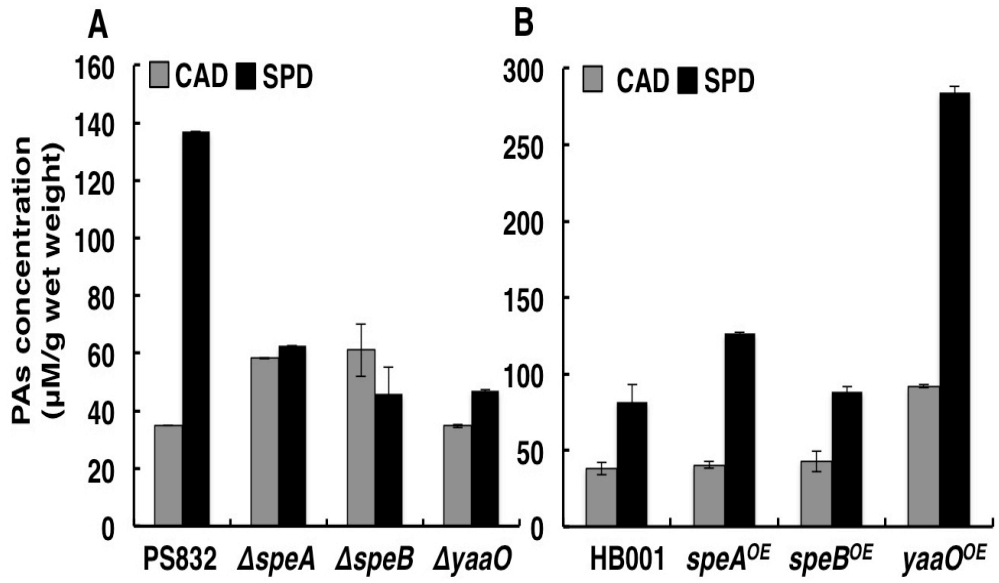

Fig. 3. Intracellular concentration of polyamine in the polyamine mutants.
(A) Defective and (B) overexpressed polyamine mutants were represented. Cadaverine (CAD, gray bar) and spermidine (SPD, black bar) are represented respectively. The values represent the average with standard deviation of three independent experiments.

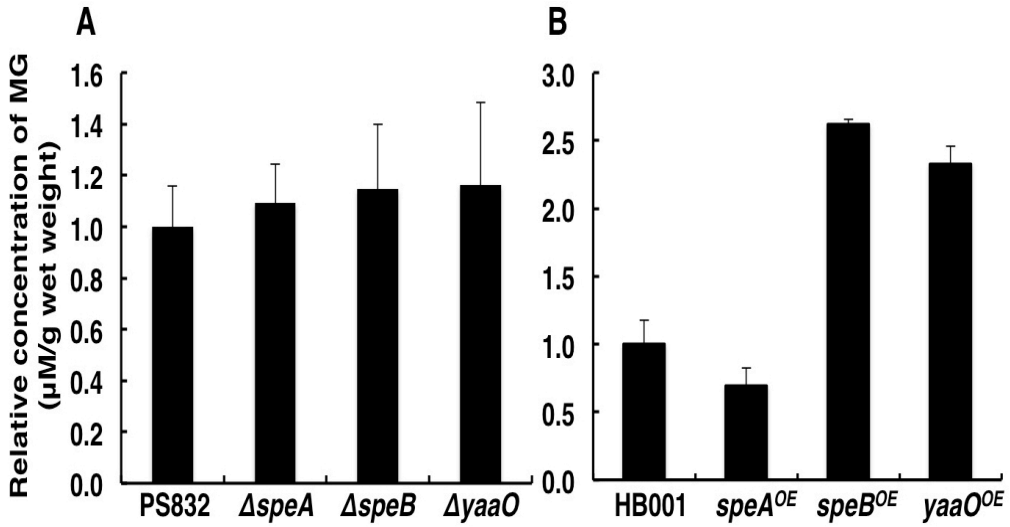

Fig. 4. Intracellulare concentration of methylglyoxal in the polyamine mutants.

(A) Defective and (B) overexpressed of polyamine mutants were represented. The values represent the average with standard deviation of three independent experiments.

From these results, we suggesteed that the MG accumulation caused by blocking the synthesis of polyamine or overexpressed polyamine genes accompanying by the inhibition of cell growth even through polyamine prevents from the oxidative stress (Chattopadhyay*, et al.*, 2003).

3.5. Induction of the *mgsA* gene in polyamine overexpressed mutants

To investigate whether the *mgsA* gene involved in the production of MG when the synthesis of polyamine genes blocked or overexpressed, we performed northern blot analysis using the labeled *mgsA* gene. In prokaryotic cells synthesis MG from methylglyoxal synthase (MGS, encoded by *mgsA*) in contrast with high organisms. *E. coli* MGS has been extensively studied for two decades (Hopper and Cooper, 1971; Saadat and Harrison, 1999). Even though, the *mgsA* gene was encodied as a putative methylglyoxal synthase (http://genolist.pasteur.fr/SubtiList/) (Kunst*, et al.*, 1997). Surprisingly, the expression of the *mgsA* gene was induced very strongly in $speB^{OE}$ and $yaaO^{OE}$ strains and slightly increased in the defective mutants of the synthesis of polyamine (Fig. 5.). This result explained the intracellular concentration of MG caused cell growth inhibition in the defective or overexpressed polyamine strains (Fig. 2 and 4). Taken together, there might be a correlation between polyamine synthesis and MG production. The MG accumulation occurred by the induction of *mgsA* gene in polyamine mutants, but the *mgsA* gene in *B. subtilis* still not confirmed of its protein activity, which catalyzed DHAP as substrate to MG.

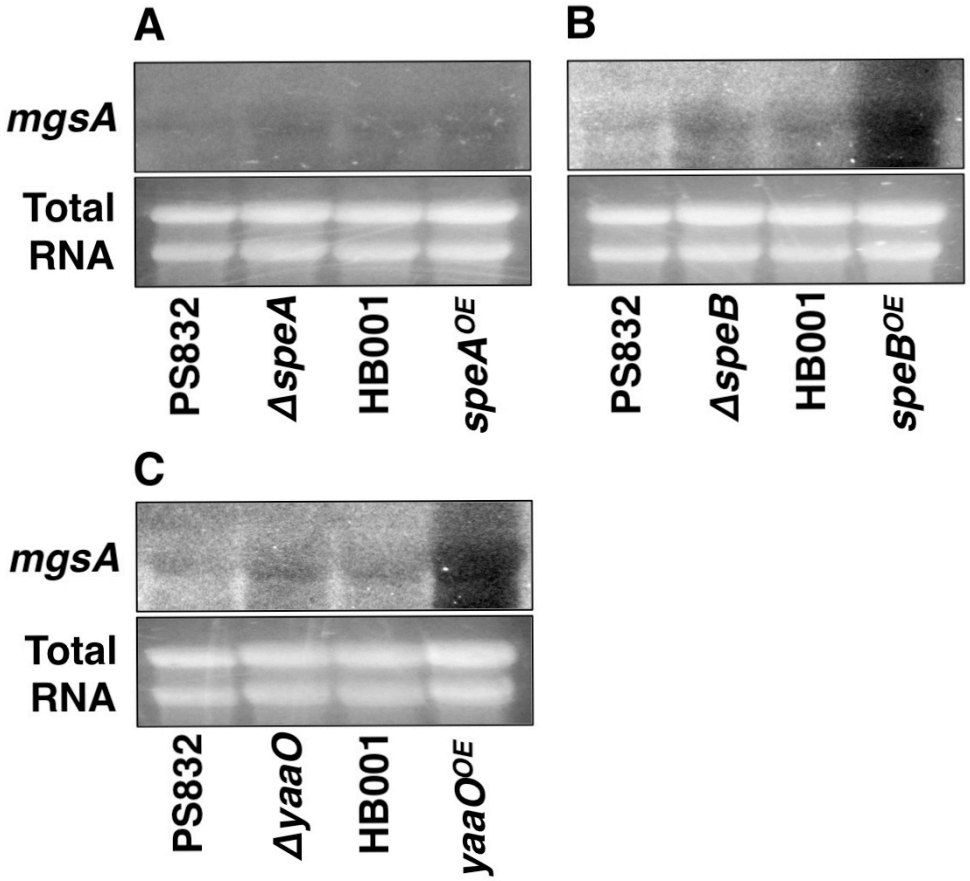

Fig. 5. Expression level of *mgsA* in the polyamine overexpressing mutants

All strains were harvested from exponential stage of growth in 2xYT media. Total RNA (20 μg) was loading onto 1% agarose gel and used loading control. The radio labeled *mgsA* gene was used as probe.

3.6. Morphological change by MG accumulation in polyamine overexpressed mutants

To investigate morphological change by MG accumulation in polyamine overexpressing strains, we observed the cell morphology by microscopy. In slightly increased intracellular MG concentration and induced of the *mgsA* gene in the defective polyamine strains displayed normal cell size of PS832 (3-4 or 4-5 μm) or a little small size of cell in *ΔyaaO* strain (2~3 μm). There was no specific difference between *ΔspeA* and *ΔspeB* with PS832. Cell size distribution was similar with PS832 except for *ΔyaaO* strain (Fig. 6 and 7). Interestingly, strongly induced the *mgsA* gene strains ($speB^{OE}$ and $yaaO^{OE}$) displayed significantly long rod-shaped cells, which found above 3-folds increased intracellular concentration of MG (Fig. 8 and 9). These two strains showed above 10 μm of cell size versus than the reference strain (HB001) and cell size distribution was toward long size of cells (Fig. 8 and 9). Though these results, the intracellular MG concentration affect on cell size accompanying cell morphological change.

3.7. MG accumulation modulates of cell division or elongation in polyamine mutants

Based on above findings, to investigate the expression of the cell division or elongation molecules, we performed northern blot analysis. Interestingly, significantly long rod-shaped cells, $speB^{OE}$ and $yaaO^{OE}$, the expression of *mreB* gene was strongly induced. But, in $speA^{OE}$ strain no noticeable change was found (Fig. 10.). Furthermore, the *rodA* or *divIVA*, which is another cell division molecule, the expression patterns was not

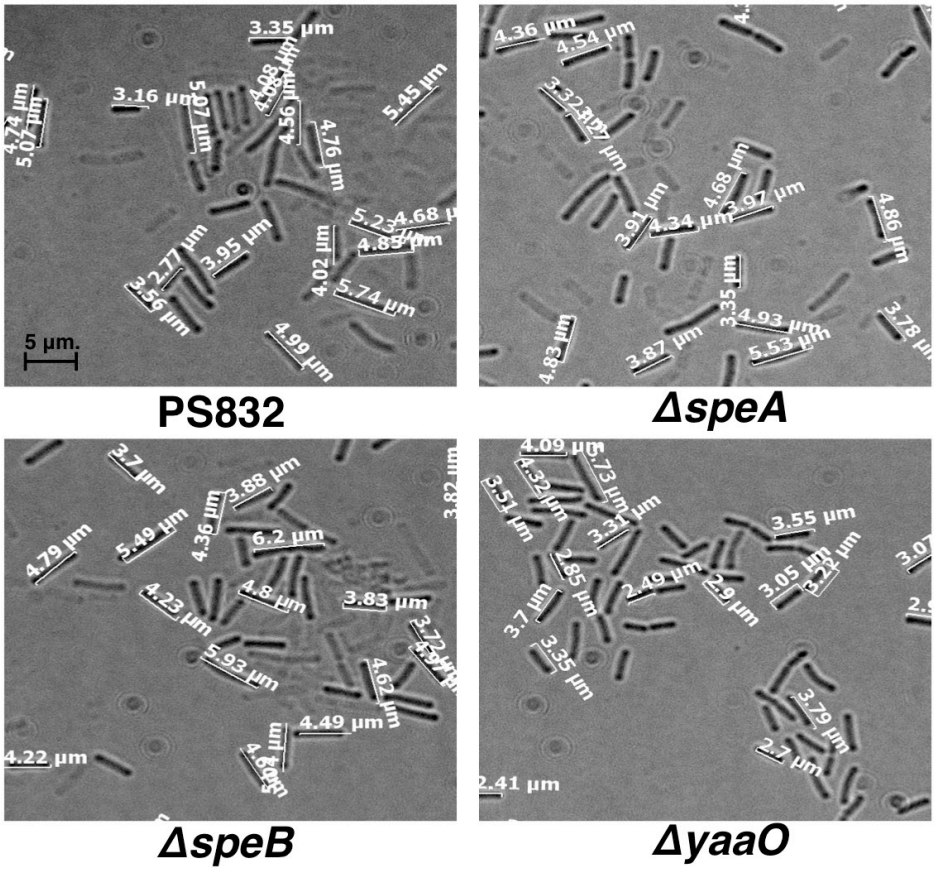

Fig. 6. Cell morphology of the polyamine defective mutants.

Samples were harvested at the middle exponential stage in 2xYT media and washed twice with PBS. Five microliters of resuspension samples was spotted on 1% low melting agarose pad. Samples were observed by Axio observer Z1 (inverted) with immersion oil. Black bar indicates a scale of 5 µm.

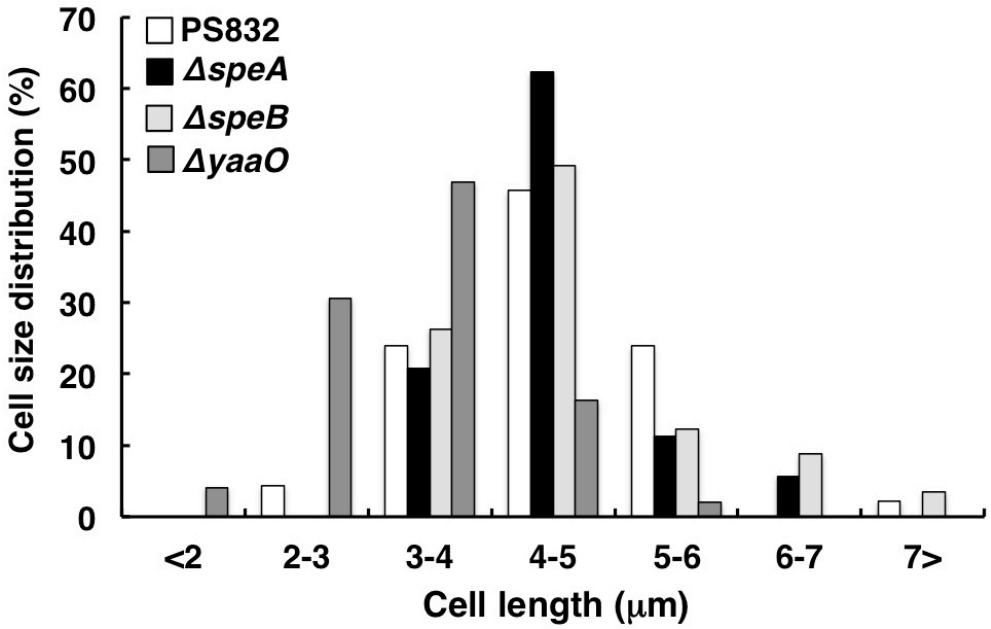

Fig. 7. Cell size distribution in the polyamine defective mutants.

At least 50 cells were measured the cell length by Axiovision (Zesis) versus automated scale bar. PS832 (wild type, white), *ΔspeA* (black), *ΔspeB* (light gray), and *ΔyaaO* (dark gray) were represented.

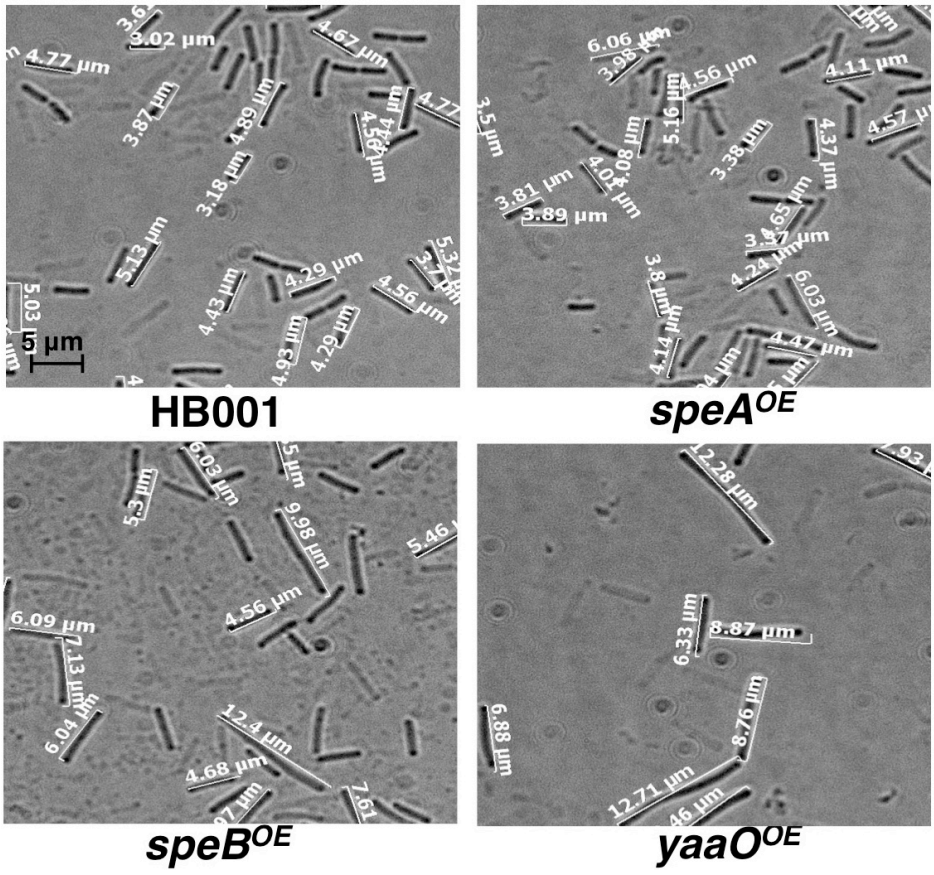

Fig. 8. Cell morphology of the polyamine overexpressiong mutants.

Samples were harvested at the middle exponential stage in 2xYT media and washed twice with PBS. Five microliters of resuspension samples was spotted on 1% low melting agarose pad. Samples were observed by Axio observer Z1 (inverted) with immersion oil. Black bar indicates a scale of 5 µm.

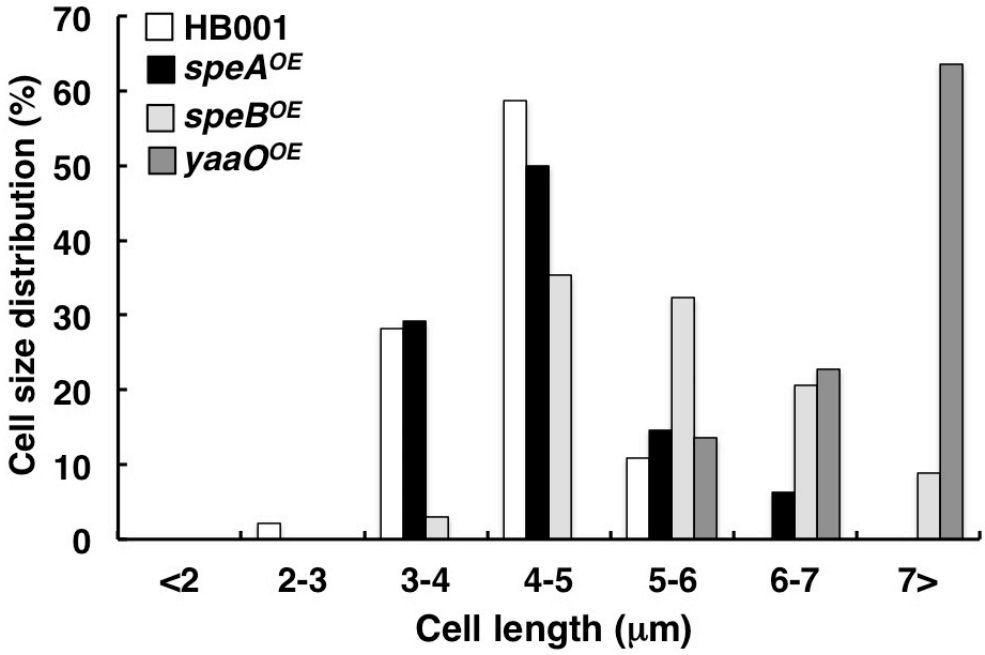

Fig. 9. Cell size distribution in the polyamine overexpressiong mutants.

At least 50 cells were measured the cell length by Axiovision (Zesis) versus automated scale bar. HB001 (vector control, white), *speA*^{OE} (black), *speB*^{OE} (light gray), and *yaaO*^{OE} (dark gray) were represented.

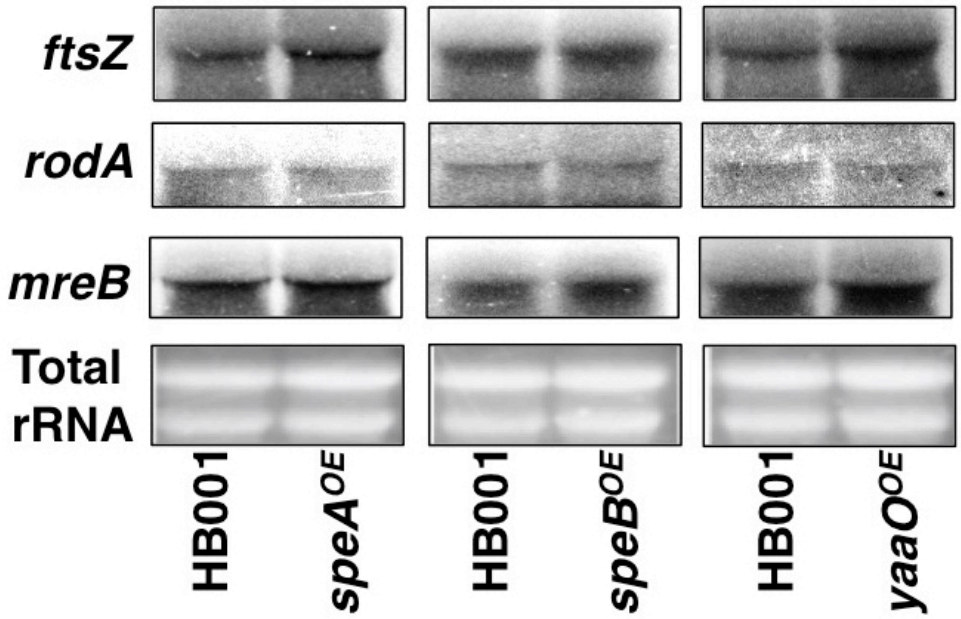

Fig. 10. Expression level of *mreB* in the polyamine overexpressing mutants. Total RNA (20 μg) was used as loading control. Northern blots were performed using fragments of the indicated genes as hybridization specific probes. *mreB*, actin-like protein; *ftsZ*, septum formation gene; *rodA*, elongation factor were indicated respectively.

different in all strains (*divIVA*, data not shown). And also, the expression of the genes used as probes was no difference with PS832 and the deleted mutant (data not shown). Thus, MG accumulation induces the expression of MreB in the overexpressing-polyamine mutants.

3.8. Characterization of *Bacillus* MGS

Through above results, MG accumulation was induced by the expression of the *mgsA* gene in the overexpressed polyamine mutants. The induction of the *mgsA* gene leads to cell elongation by the activation of *mreB*, actin-like protein in *B. subtilis*. However, there is no MG formation activity in *B. subtilis* in previous study (Hopper and Cooper, 1971).

3.8.1. Sequence analysis of *Bacillus* MGS

B. subtilis genome sequencing was completed in 1997 (Kunst*, et al.*, 1997). But, there is no research for the synthesis of MG in *B. subtilis* even though the putative methylglyoxal synthase encoded by the *mgsA* gene. The *mgsA* gene was located in the middle operon related with the synthesis of bacillithol (Gaballa*, et al.*, 2010) (Fig. 11A). However, they didn't explain the relation ship between MG and bacillithiol. The roles of MG or MGS are not elu cidated in *B. subtilis*.

Bacillus MGS consisted of a 411-bp nucleotide, 137 amino acids, and had a subunit mass of 15.2 kDa. Comparison of MGS with other strains showed an identity of 44% with *C. acetobutylicum* (Huang*, et al.*, 1999), 53% with *Thermus* sp.strain GH5 (Pazhang*, et al.*, 2010), and 42% with *E. coli*(Saadat and Harrison, 1998; 1999) (Fig. 11B). Four-conserved aspartic acids (Asp9,

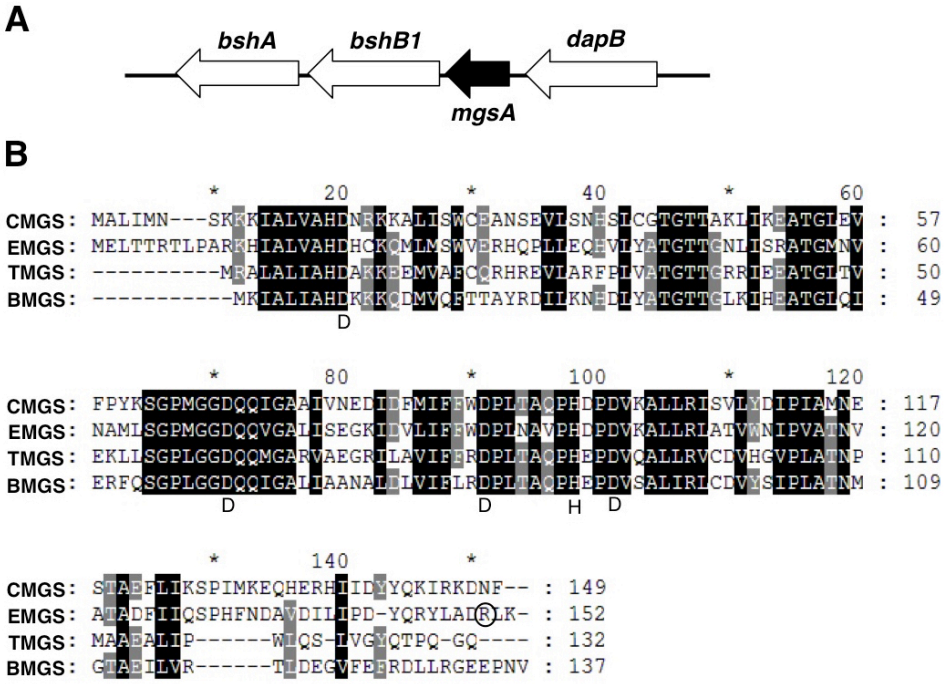

Fig. 11. The location of *mgsA* gene and amino acid sequence alignment with other bacterial MGSs (A) The *mgsA* region is indicated by block arrow with other genes. (B) Alignment of amino acid with other bacterial MGSs. CMGS represents MGS from *C. acetobutylicum,* EMGS from *E. coli*, TMGS from *Thermus* sp. strain GH5, and BMGS from *B. subtilis*, respectively. Identical residues are indicated with shaded letters. Large D characters and H character under each column indicate the conserved Asp acids and circle represents Arg150 in *E. coli* (Saadat and Harrison, 1998).

Asp60, Asp80 and Asp90) were founded in *B. subtilis*, corresponding to those found in *E. coli* (Saadat and Harrison, 1998; 1999). And also, His88 was existed corresponding with His98 in *E. coli*, which is related with the tautomerization reaction when the formation of MG by moving oxygen molecular and the conformational change (Marks*, et al.*, 2004). However, Arg150, which is a binding site for phosphate ions and forms a salt bridge with Asp20 in *E. coli*, was observed neither in *B. subtilis* nor in *Thermus* sp. strain GH5 (Saadat and Harrison, 1999; Pazhang*, et al.*, 2010) (Fig. 11B). Through this result, we sought to determine *Bacillus* MGS activity through *E. coli* overproduction system.

3.8.2. Purification of *Bacillus* MGS

For the purification of Bacillus MGS, we cloned the *mgsA* ORF by PCR as described in Materials and Methods. The fragment was ligated into pET15b for using His-tag purification. However, the recombinant MGS was not purified clearly after thrombin cleavage (data not shown). So, we re-ligated into pET3a with appropriate enzyme site for the purification of no tag. Firstly, cells (BMGS02 strain, hovering pHS101) was induced at 22°C for overnight under 1 mM IPTG with the same as BMGS01 strain (hovering pHS100). But, BMGS02 strain showed that cells were disrupted with becoming pulpy state and was impossible to harvest. So, we induced the recombinant protein under 1 mM IPTG at 37°C for 3~4 h.

By using the Q-sepharose column, the recombinant MGS was purified after heat shock to remove the big size proteins in the crude extract. Overall 90% of the recombinant protein was purified (Fig. 12.). To confirm the activity of Bacillus MGS, the recombinant was purified from *E. coli*.

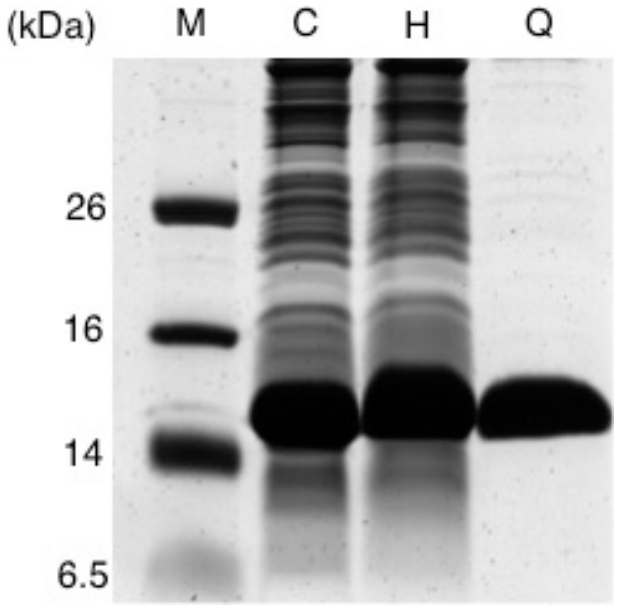

Fig. 12. Purification of *Bacillus* MGS Samples were electrophoresed on a 16% Tricine SDS-PAGE gel. The resulting gel was subjected to staining with Brilliant Blue R. Lane M, molecular weight markers; lane C, crude extract from ; lane H, heat treatment 65°C for 1 min; lane Q, MGS from the elution fraction of Q-sepharose fast flow column in 50 mM imidazole-HCl (pH 7.0) containing 400 mM NaCl.

3.8.3. Enzyme activity of *Bacillus* MGS

To determine the kinetic parameter, we first decided the concentration of the recombinant protein. Maximal MG formation was detected at the concentration of 1 μM of the protein (data not shown). To determine the parameters of enzyme kinetics, the samples were mixed under different DHAP concentrations. From the Lineweaver–Burk plot, the K_m value was 3.17 mM and the K_{cat} value was 0.009 (s^{-1}) (Fig. 13.). Additionally, *Bacillus* MGS activity corresponding to G3P as another substrate was not detected (data not shown). *Bacillus* MGS uses DHAP as a substrate than G3P.

3.8.4. Biochemical properties of *Bacillus* MGS

Other biochemical properties were investigated. Optimal temperature and pH showed at 40°C and 5.5, respectively (Fig. 14A and B). Phosphate compounds are known as inhibitors of MGS (Hopper and Cooper, 1972). To determine this inhibitory effect, several concentrations of phosphate compounds were used as inhibitors of *Bacillus* MGS with a constant concentration of DHAP (0.75 mM). Increasing the concentration of phosphate compounds decreased the activity of *Bacillus* MGS. However, the activity of *Bacillus* MGS increased slightly with the fructose-1,6-bisphosphate by increasing its concentration. And Bacillus MGS activity didn't drop below 50% at the 5 mM ATP treatment (Fig.15.). Thus, *Bacillus* MGS influenced by phosphate compounds like other bacterial MGSs except for fructose-1,6-bisphosphate.

3.8.5. Native molecular mass of *Bacillus* MGS

To confirm the oligomeric state, purified *Bacillus* MGS was applied on a Superose 12 10/300 GL gel permeation chromatography with low molecular

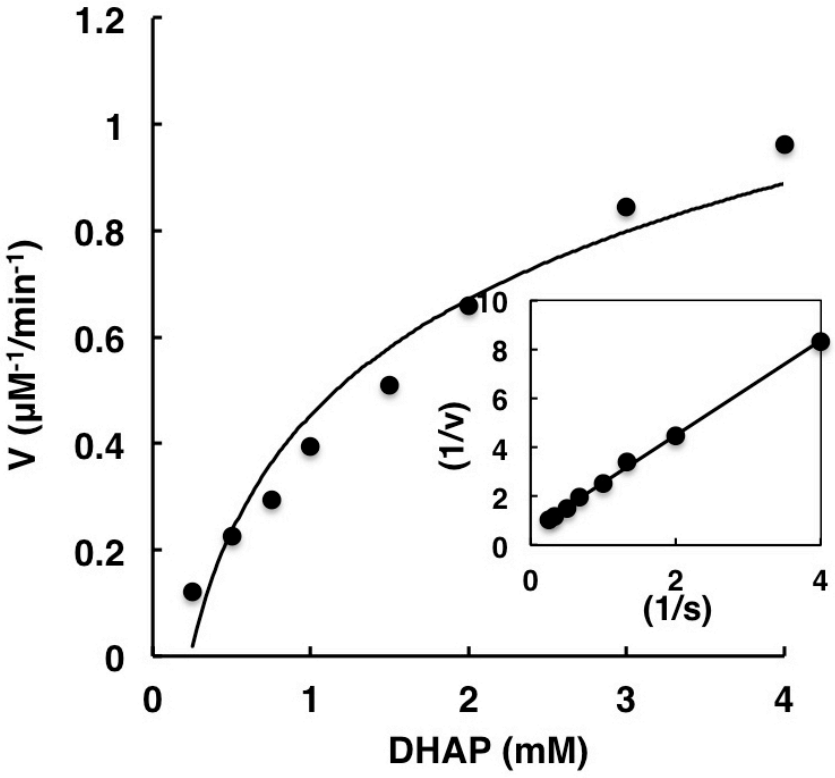

Fig. 13. Lineweaver-Burk plot for *Bacillus* MGS

Activity of samples (total 100 μl) was measured by UV-VIS spectrophotometer containing 50 mM imidazole-HCl (pH 6.0) for 5 min at 30°C detected by colorimetically (Cooper, 1975). The Lineweaver-Burk plot of the Michaelis-Mentens equation is shown.

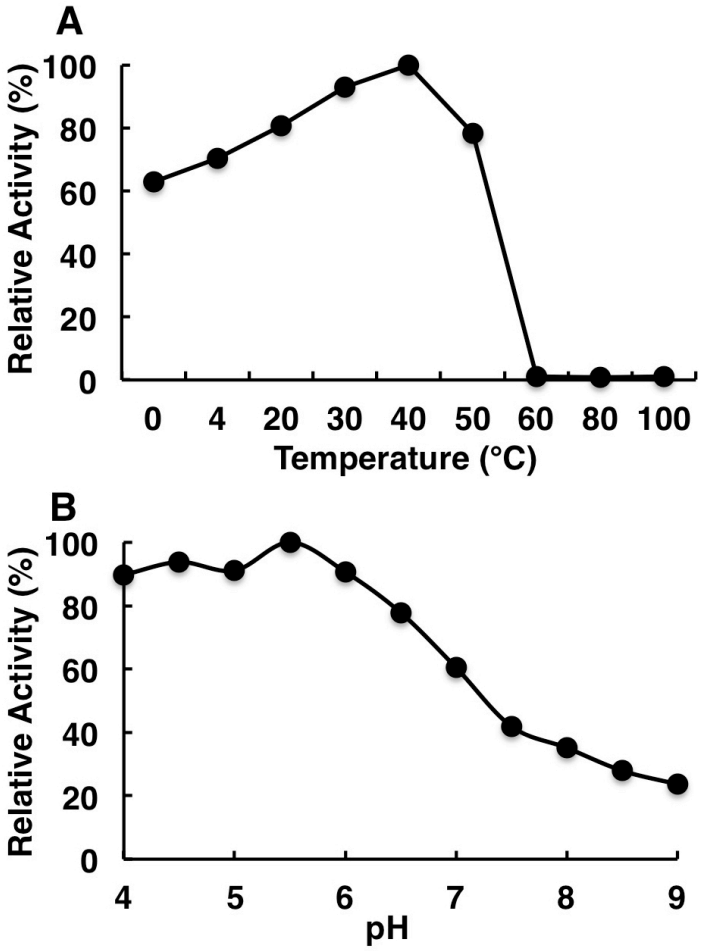

Fig. 14. Biochemical properties of *Bacillus* MGS on temperature and pH. (A) *Bacillus* MGS was incubated at desired temperatures for 10 min and then cooled on ice. After cooling, the protein was mixed with DHAP for activity. (B) *Bacillus* MGS was incubated in 50 mM imidazole-HCl between pH 4 and 9 range at increments of 0.5. All experiments were calculated as relative activity (%) versus the highest value.

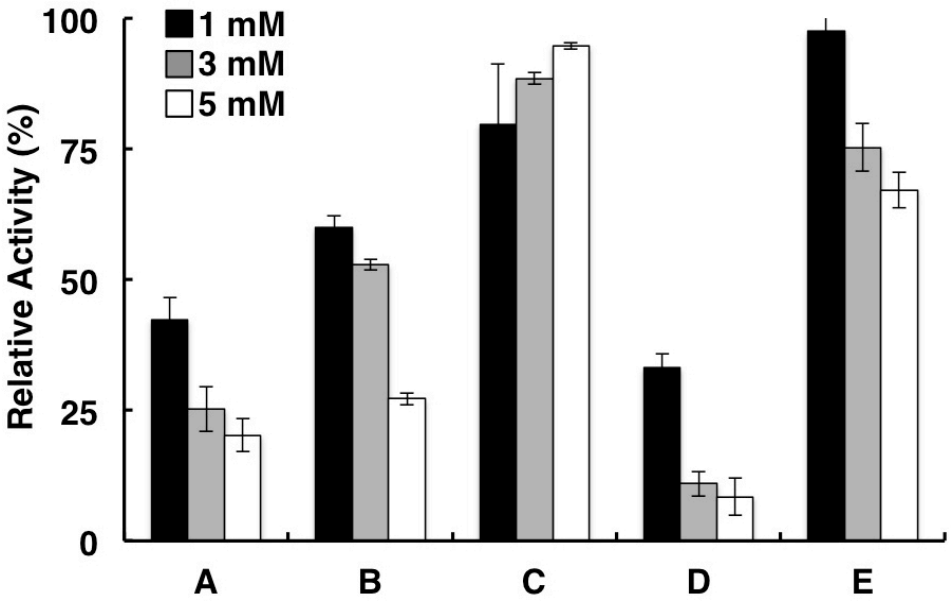

Fig. 15. Inhibitory effect of *Bacillus* MGS by phosphate compounds.

Bacillus MGS was incubated with the phosphate compound and DHAP (0.75 mM). The columns represent 1 mM (black bar), 3 mM (gray bar) and 5 mM (white bar) as the concentrations of phosphate compounds. A, Orthophosphate; B, Pyrophosphate; C, fructose-1,6-bisphosphate; D, phosphoenolpyruvate; E, ATP are indicated. All samples were calculated as relative activity (%) versus no treatment of phosphate compounds (DHAP control).

mass standards preequilibrateed with 50 mM imidazole-HCl (pH 7.0) and 400 mM NaCl. A standard curve was generated by the plotting the logarithm of molecular mass of standard proteins against their K_{av}, where $K_{av}=(V_e-V_0)/(V_t-V_0)$: V_e, elution volume; V_0, void volume; V_t, total bed volume. K_{av} of *Bacillus* MGS determined by using the same column and was compared to the profile of proteins standards; BSA, 66 (kDa); Carbonic Anhydrase 29 (kDa); Cytochrome C, 12.5 (kDa); Aprotinin, 6.5 (kDa). Predicted molecular mass of *Bacillus* MGS was 37.15 kDa indicating that *Bacillus* MGS exhibited as a dimmer in solution (Fig. 16.).

3.9. The functional roles of methylglyoxal synthase in *B. subtilis*

3.9.1. Construct for the deletion of the *mgsA* gene

From the above results, we confirmed the formation of MG by *Bacillus* MGS using DHAP as an *in vitro* substrate. Next, to investigate the functional roles of MG in cells, we manipulated the *mgsA* gene, which synthesizes MG. First, the deletion mutant of the *mgsA* gene was obtained by LFH-PCR as described previously (Wach, 1996). The scheme was presented and the mutant was confirmed by PCR with M1 and CP primers as described in Table 3 (Fig. 17.).

3.9.2. Construct for the overexpression of the *mgsA* gene

To overproduce MG in cells, we constructed the overexpression mutant of the *mgaA* gene. First, we cloned the ORF *mgsA* gene with its ribosme binding site (RBS) and ligated into pRB374. However, many nucleotides in this fragment had been changed and this mutant did not show the overexpression pattern upon western blot analysis (data not shown). So, we considered a new

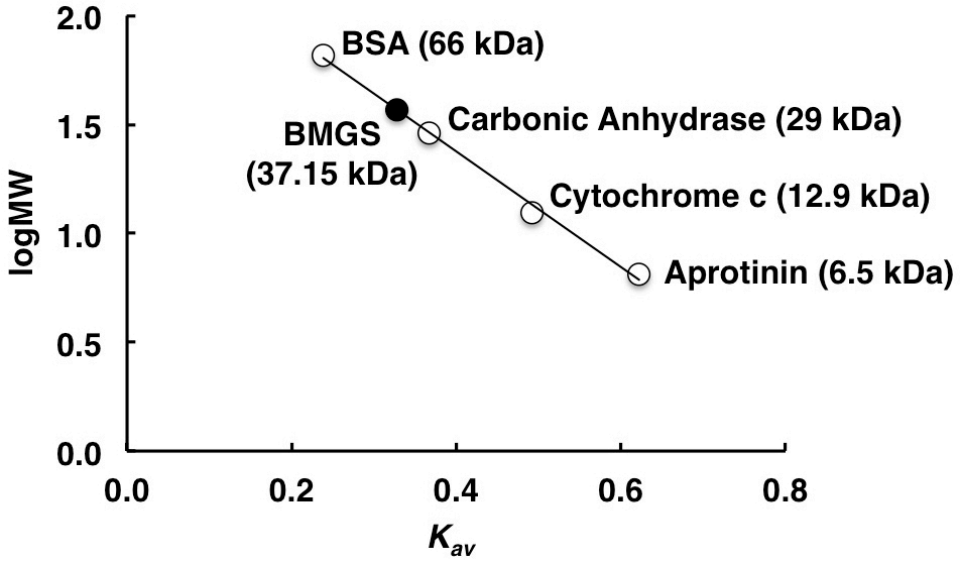

Fig. 16. Native molecular mass of *Bacillus* MGS.

Bacillus MGS was loaded on Superose 12 column (30/100 GL) with standard marker proteins. BSA, 66 (kDa); Carbonic Anhydrase 29 (kDa); Cytochrome c, 12.5 (kDa); Aprotinin, 6.5 (kDa) (open circles), and *Bacillus* MGS (BMGS, closed circle) were represented.

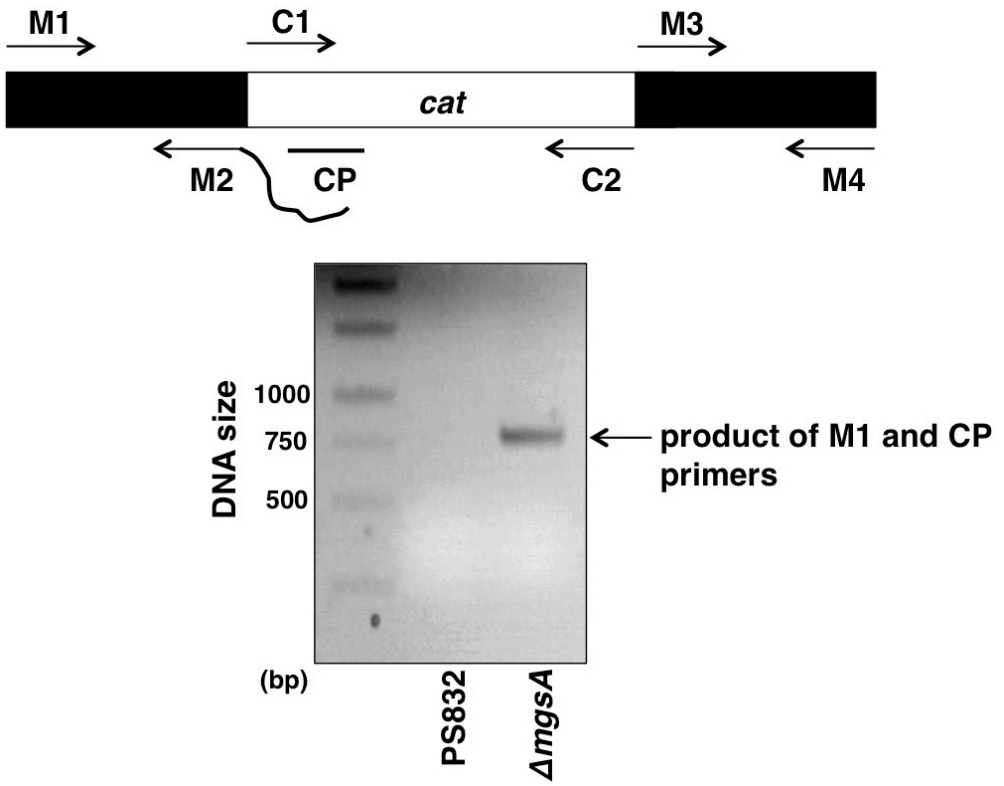

Fig. 17. Deletion the *mgsA* gene in *B. subtilis*.

Long-flanking homologous recombination scheme is shown. After this construct was transformed to PS832, colonies were selected from chloramphenicol plate. M, DNA ladder; PS832 and *ΔmgsA* were loaded on 0.8% agarose gel. Black arrow indicates the amplified fragment by PCR with M1 and CP primers.

vector system inserting the RBS for the overexpression of the *mgsA* gene. The RBS site of the *sodA* (encoded superoxide dismutase) was introduced. Several subcloning steps were performed to obtain the MG overproduction MG mutant. It was confirmed by western and northern blot analysis (Fig. 18 and 19.). The recombinant of the RBS is appropriate with the *mgsA* ORF to express *Bacillus* MGS.

3.9.3. MG production inhibits cell growth and viability

Based on the result of *Bacillus* MGS activity *in vitro*, we preliminarily investigated the physiological roles of the *mgsA* gene in *B. subtilis* through the gene disrupted- or overexpressing-cells (Fig. 17 and 19.). First, we measured the intracellular MG concentration to confirm the MG production from the overexpressed *mgsA* gene in *B. subtilis*. MG production was increased above 3 folds in the $mgsA^{OE}$ strain than the refencence strain (HB001) but the concentration of MG reduced in the *ΔmgsA* strain by half amount compared to than wild-type cells (PS832) (Fig. 20.). Thus, the recombinant of RBS is working for the production of MG highly in the $mgsA^{OE}$ strain.

As suggested by the model of effects of both keto-aldehydes directly affecting cell division (Szent-Györgyi*, et al.*, 1967) and exogenous MG inhibiting the *Bacillus* cell growth inhibition (Nguyen, *et al.*, 2009), we measured the cell growth and cell viability to observe the effect of the production of MG *in vivo*. The $mgsA^{OE}$ strain displayed the defect in the cell growth concomitantly followed by the decreased cell growth (Fig. 21 and 22.). However, the slightly decreased MG concentration in the *ΔmgsA* strain did not coincide with the partially reduced cell viability or growth rate compared to

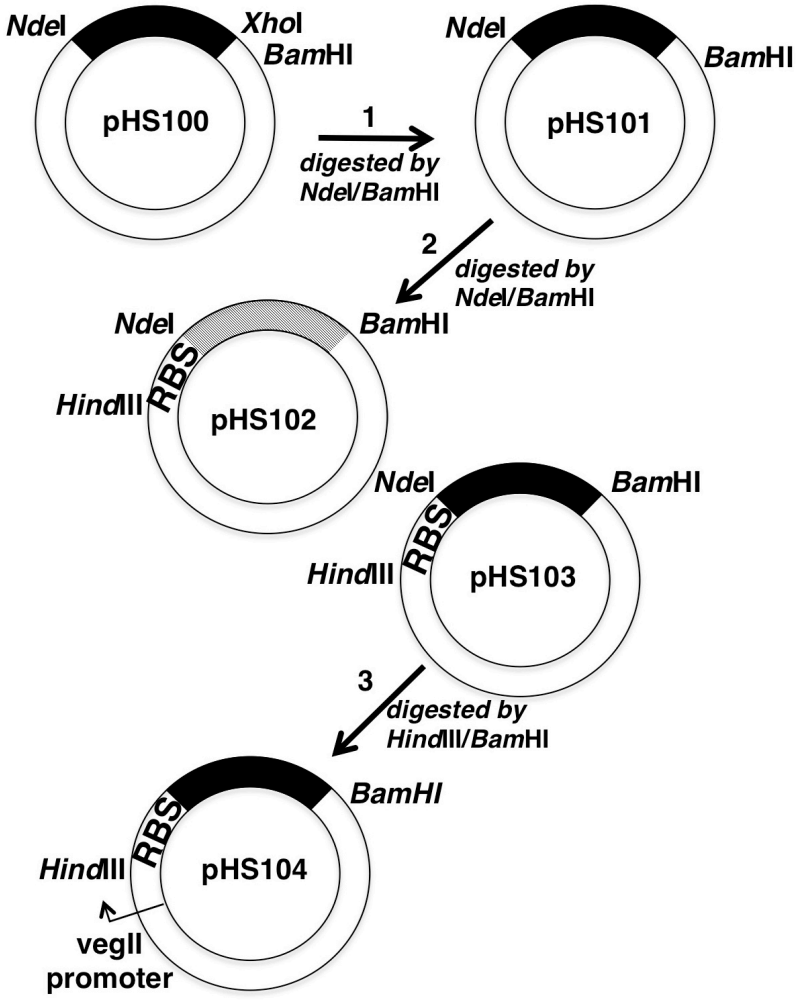

Fig. 18. Scheme of the overexpression of the *mgsA* gene by insertion of RBS from *sodA*

From pHS100 to pHS104 except pHS102, a black box indicates the *mgsA* gene. In pHS102 vector, a slant box indicates the *sodA* gene. The RBS indicates the ribosome binding site of the *sodA* gene. Each step was confirmed by 0.8% agarose gel and the final vector (pHS104) was transformed to PS832.

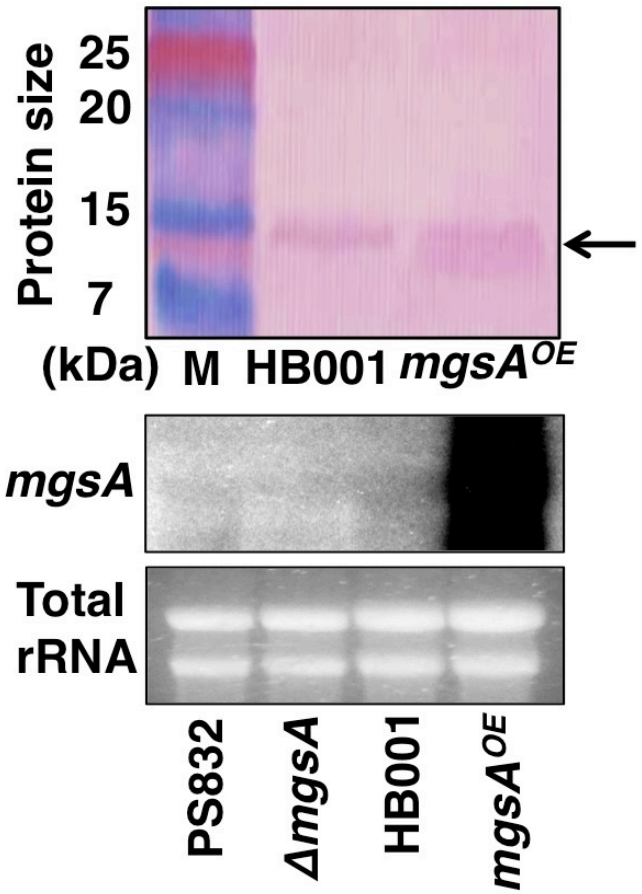

Fig. 19. Overexpression mutant of the *mgsA* in *B. subtilis*.

After transformation, a selected mutant on the neomycin plate was performed by western blot analysis with HB001 (up). M, protein marker; HB001 and $mgsA^{OE}$ strain were loaded on 16% Tricine SDS-PAGE and transferred. Black arrow indicates the anti-methylglyoxal synthase. Northern blot was also represented. The *mgsA* gene used as probe (down).

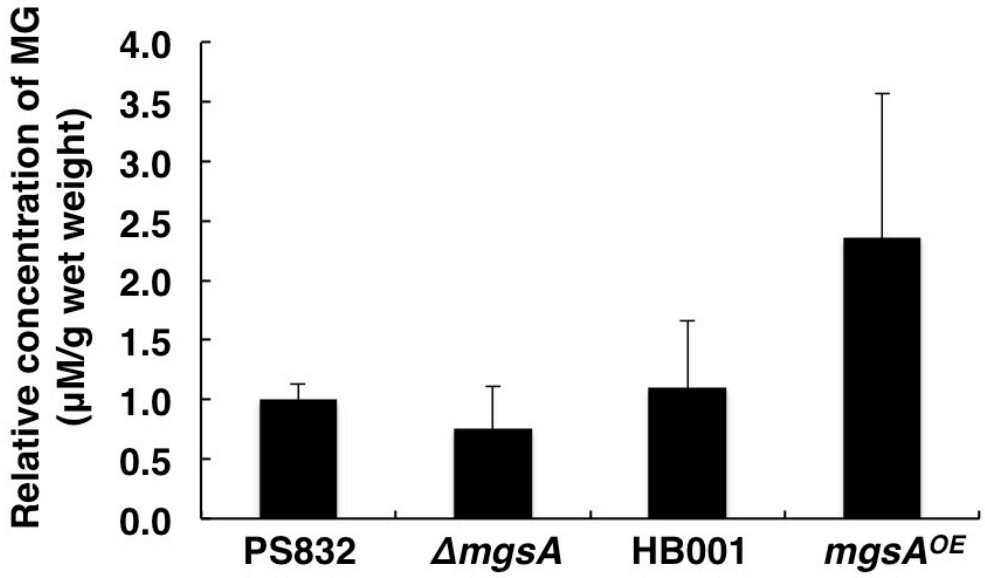

Fig. 20. Intracellular concentration of MG in the *ΔmgsA* and *mgsA*^{OE} mutants.

Intracellular MG concentration as its derivative was measured by HPLC at 336 nm. All samples were harvested at the middle exponential period in SMM media at 37°C. The average and standard deviation calculated from three independent experiments are shown. Relative concentration was calculated versus PS832.

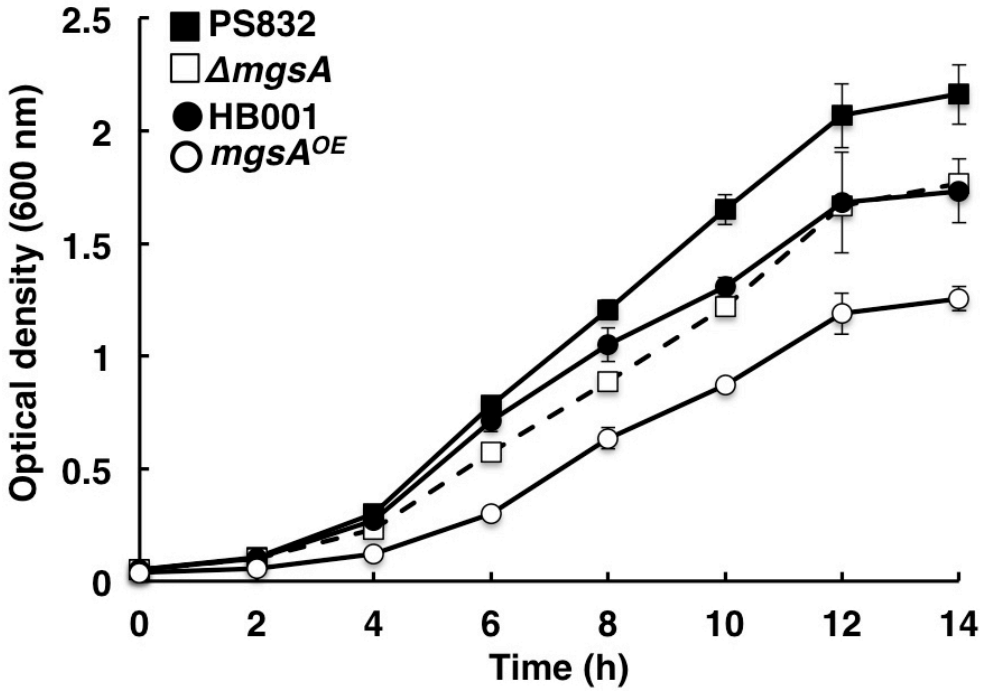

Fig. 21. Inhibition of growth in *mgsA*^{OE} strain.

Growth curve was measured at 600 nm every 2 hours growing at 37°C with 200 rpm in SMM media. PS832 (closed square), *ΔmgsA* (open square), HB001 (closed circle) and *mgsA*^{OE} (open circle) are indicated respectively.

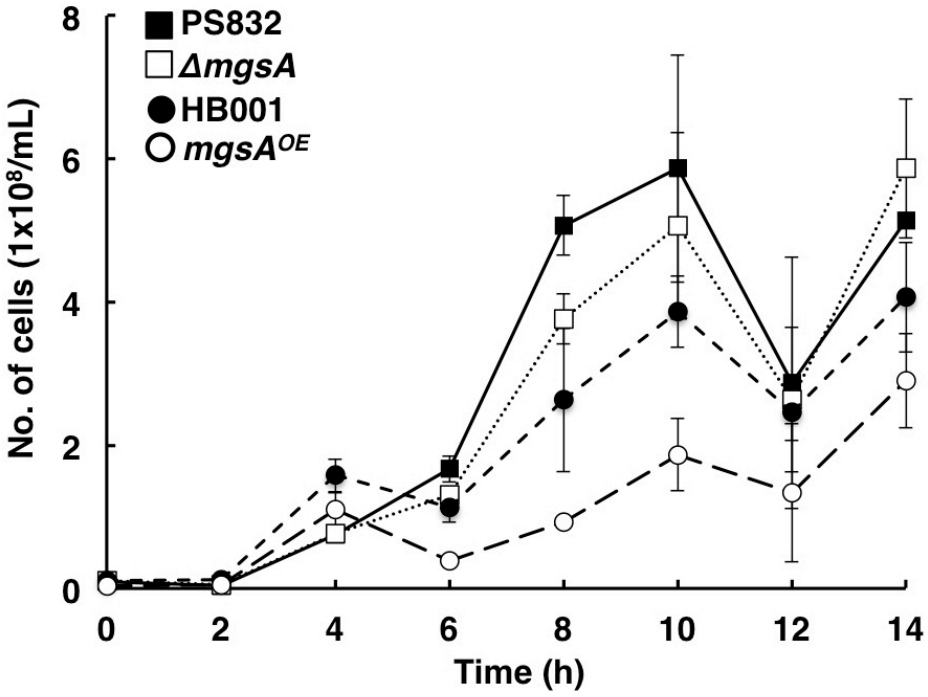

Fig. 22. Defect viability in *mgsA*^{OE} strain.

Every two hours including t=0, all strains were diluted in SMM (no glucose and trace metal solution) appropriately. One hundred microliters of the diluted solution was spread on LB agar plate and incubated for 16 h at 37°C. PS832 (closed square), *ΔmgsA* (open square), HB001 (closed circle) and *MGS*^{OE} (open circle) are indicated respectively.

wild-type cells (PS832), though its mechanism was obscure. Nevertheless, we validated the cell growth defect in the MG-accumulated *mgsA*^{OE} strain indicating that the increased intracellular MG by the *mgsA* overexpression inhibited the cell growth and viability in this study similar to the effect of exogenous MG as reported previously (Nguyen*, et al.*, 2009).

3.10. Effect on cell elongation by MG overproduction

3.10.1. Cell morphology change by MG overproduction

From above results, MG accumulated cells such as the *mgsA*^{OE} strain caused growth inhibition and defective cell viability similar to polyamine-overproducing cells (Fig. 2B, 4, and 20-22). To investigate the cell morphology like the polyamine overexpressed mutants, we microscopically examined. Interestingly, the *mgsA*^{OE} strain showed extremely elongated rod-shaped morphology likewise in the *speB*^{OE} or *yaaO*^{OE} compared to HB001, in contrast, shorter cell-length was found in the *ΔmgsA* strain (Fig. 23.). For more detail investigation, we measured the cell length in all strains respectively. In PS832 and HB001 was shown 3~4 μm average cell length. But, MG accumulated such as the *mgsA*^{OE} strain was distributed the longer cell length than wild type or the reference strain. In contrast, shorter rod-shaped cells were found in in the *ΔmgsA* strain (Fig. 24.). Thus, the MG accumulation by the overexpression of the mgsA gene in B. subtilis affected cell length likewise in the overexpressed polyamine mutants.

3.10.2 MG overproduction leads to the cell elongation by the activation of MreB

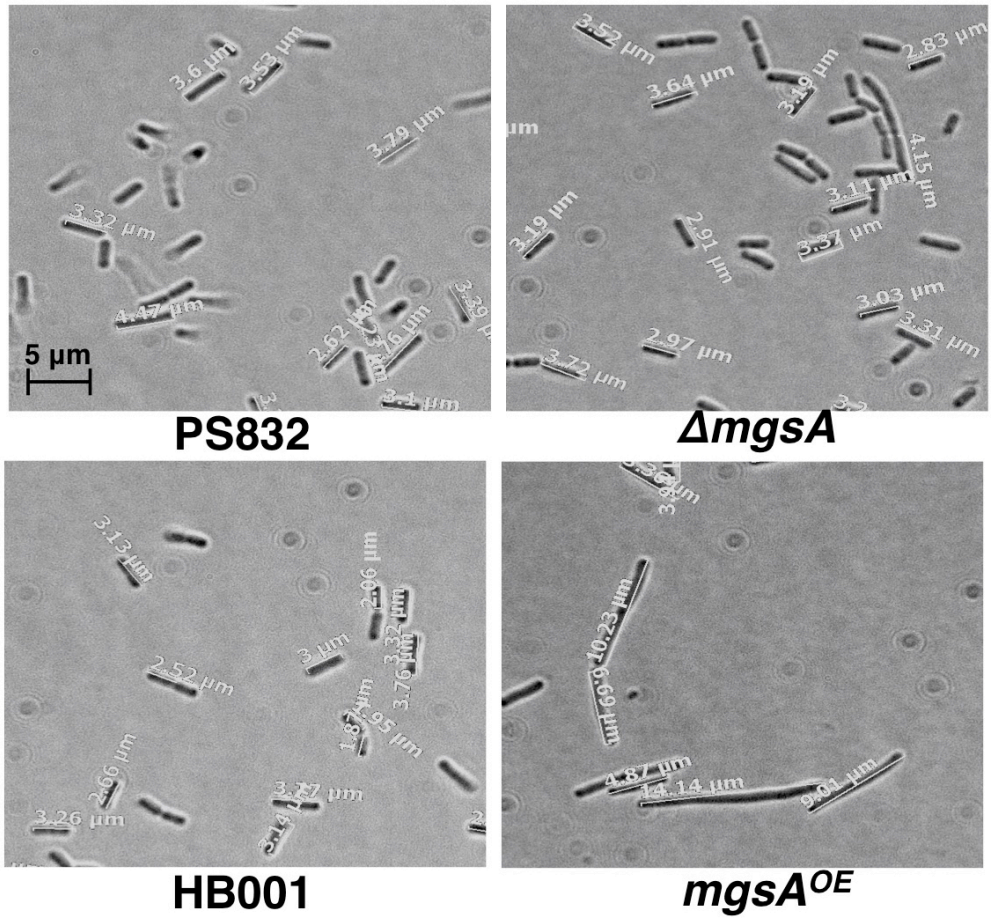

Fig. 23. Cell morphology of the *ΔmgsA* and *mgsA*^{OE} mutants.

Samples were harvested at the middle exponential stage in 2xYT media and washed twice with PBS. Five microliters of resuspension samples was spotted on 1% low melting agarose pad. Samples were observed by Axio observer Z1 (inverted) with the immersion oil. Black bar indicates a scale of 5 µm.

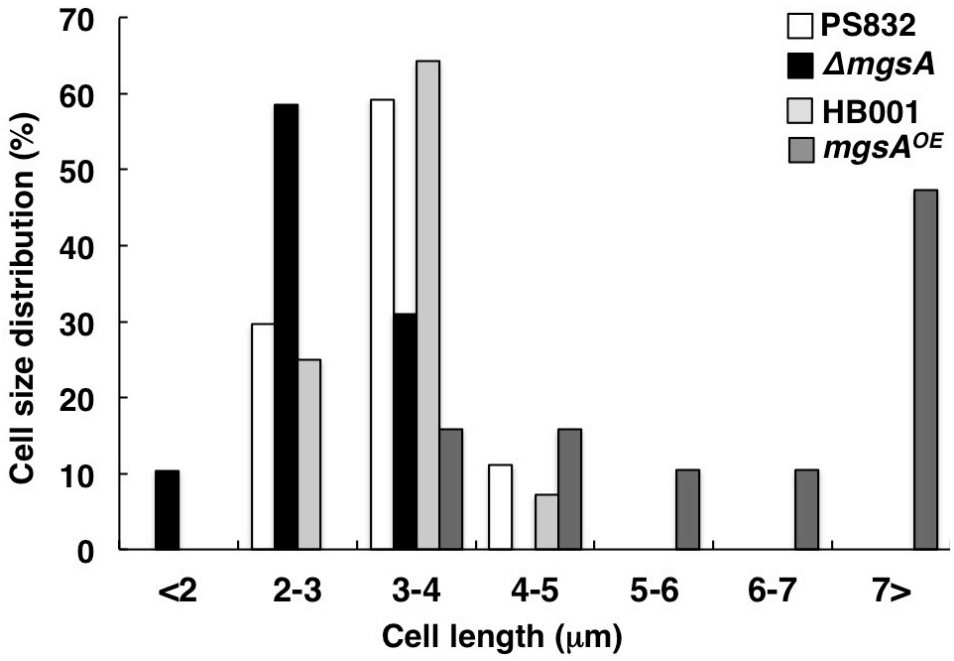

Fig. 24. Cell size distribution in the *ΔmgsA* and *mgsA*^{OE} mutants.

At least 50 cells were measured the cell length by Axiovision (Zesis) versus automated scale bar. PS832 (wild type, white), *ΔmgsA* (black), HB001 (light gray), and *mgsA*^{OE} (dark gray) were represented.

To investigate the cause of the morphological switch to the elongated or shorten rod-shaped cells, we examined the transcriptional levels at exponential phase regarding cell division and elongation regulators including *mreB, ftsZ,rodA* and *divIVA,* which is mainly component of cell division or cell elongation likewise performed at the polyamine mutants. The *ftsZ* drastically increased in the *ΔmgsA* strains at the early exponential stage than PS832 and decreased the *mreB* expression in the same time. However, the expression of *mreB* activated in the $mgsA^{OE}$ strain likewise in the $speB^{OE}$ and $yaaO^{OE}$ strains at the early exponential stage. But, there is no difference other key molecules of *rodA* or *divIVA* expression in all strain during the exponential stage (Fig. 25.). Thus, MG production or accumulation influenced the cell elongation by the modulation of *mreB* in *B. subtilis*.

Taken together, MG accumulation by the overexpressed polyamine or methylglyoxal synthase gene ($speB^{OE}$, $yaaO^{OE}$, and $mgsA^{OE}$) leads to cell elongation by the activation of MreB, actin-like protein in *B. subtilis*.

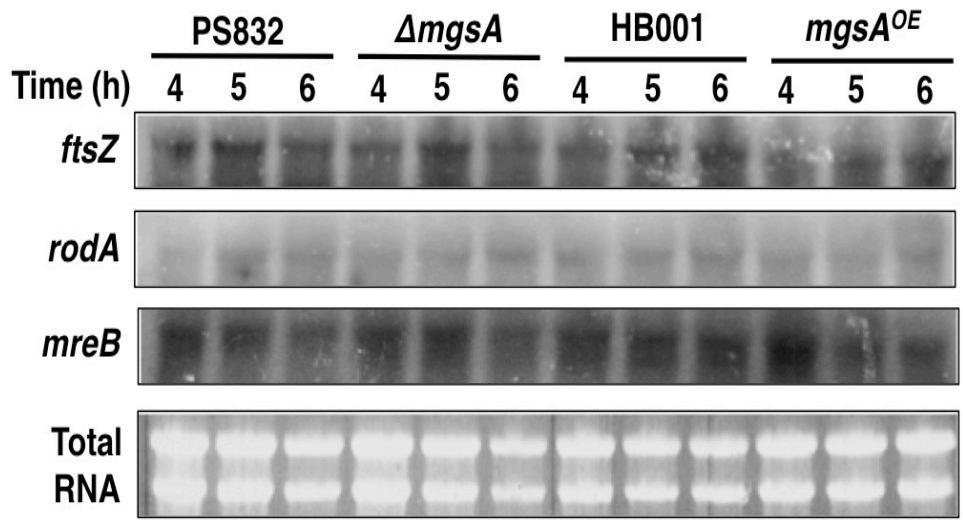

Fig. 25. Expression level of *mreB* in the *ΔmgsA* and *mgsA*^{OE} mutants.

Total RNA was isolated from the exponential stage of all strains. Total RNA (20 μg) was used as loading control. Northern blots were performed using fragments of the indicated genes as hybridization specific probes. *mreB*, actin-like protein; *ftsZ*, septum formation gene; *rodA*, elongation factor were indicated respectively.

IV. DISCUSSION

The polyamines as diamine putrescine (PUT), triamine spermidine (SPD) and tetraamine spermine (SPM) are low molecular mass aliphatic amines that are positively charged and ubiquitous in all living organism (Pegg and McCann, 1982). Although polyamines have prominent regulatory roles in growth and differentiation, precise molecular functions are not well established (Marton and Pegg, 1995). Several investigations have also shown by the electron paramagnetic resonance (EPR) spectroscopy that MG reacted amino group containing amino group (Yim*, et al.*, 1995; Lee*, et al.*, 1998). These findings provide the possibility that polyamines, which have two or more amine group, may be a good model system for the study about regulation of intracellular MG because polyamines are related with the protective mechanism of AGEs precursors occurred by MG (Ulrich and Cerami, 2001; Gugliucci and Menini, 2003). Through the EPR analysis, MG reacts with polyamine and its precursors such as arginine and lysine (data not shown). Moreover, a low concentration of MG reacts with lysine easily than arginine, AGM, PUT. This results support *in vitro* EPR analysis and previous study (Shumaev*, et al.*, 2009). However, this remains unsolved in *vivo* system still now. Therefore, we need to prove the signal from MG with lysine *in vivo* using the $mgsA^{OE}$ strain or measure the concentration of the radiolabeled lysine by consuming the reaction with MG in cells.

Moreover, MG was postulated that the intracellular polyamines could act as blocking agents against advanced glycation-end products (AGEs) precursors (Gugliucci and Menini, 2003). To establish the relationship between MG and polyamine in *B. subtilis*, we first investigated the genes for the synthesis of polyamines. The synthesis of polyamines is well studied in *E. coli* (Algranati and Goldemberg, 1977; Goldemberg and Algranati, 1977; Goldemberg, 1980;

Tabor, *et al.*, 1980; Chattopadhyay, *et al.*, 2003; Igarashi and Kashiwagi, 2006). There are some genes for the synthesis of polyamines in *B. subtilis*, which have the low similarity compared with *E. coli* (Table 4). To confirm polyamines act as blocking agent when its related genes deleted, we obtained mutants related with the synthesis of polyamine (Fig. 1.). Through the growth experiments, surprisingly the overexpressing polyamine mutants ($speB^{OE}$ and $yaaO^{OE}$) severely inhibited. Additionally, the growth in the deleted mutants displayed slightly slower than wild type (PS832) (Fig. 2.). To find out the factor that inhibits of growth, we measured the intracellular MG concentration since MG is reported as growth inhibitor (Szent-Györgyi, *et al.*, 1967). Interestingly, the overexpressing polyamine mutants ($speB^{OE}$ and $yaaO^{OE}$) showed very high concentration of MG than wild type (PS832) or vector control (HB001) (Fig. 5.). However, the intracellular SPD concentrations increased in the overexpressing mutants ($speB^{OE}$ and $yaaO^{OE}$) versus than vector control (HB001). The concentration of SPD or CAD decreased at each deleted mutants of polyamine (Fig. 3.). To investigate the cause MG accumulation, we performed northern blot analysis by using the *mgsA* probe. Interestingly, the *mgsA* gene expression was induced in the overexpressing polyamine mutants ($speB^{OE}$ and $yaaO^{OE}$) (Fig. 5.). This result also supported the growth inhibition of the polyamine overexpressing mutants ($speB^{OE}$ and $yaaO^{OE}$) (Fig. 2.).

Growth inhibition caused the cell morphology in the polyamine overexpressing mutants. The change of cell morphology in the polyamine overexpressing mutants ($speB^{OE}$ and $yaaO^{OE}$) except for $speA^{OE}$, exhibited long rod-shaped cells like as $mgsA^{OE}$ strain (Fig.8, 9, 23 and 24.). However, they showed the different pattern of the expression of *ftsZ* or *mreB* (Fig. 10.) unlike $mgsA^{OE}$ strain (Fig. 25.). In case of the polyamine overexpressing mutant

(*speB*^{OE} and *yaaO*^{OE}), the *ftsZ* and *mreB* expression increased, but no difference in the *speA*^{OE} and other deleted mutant (data not shown).

From above results, MG synthesized by the *mgsA* gene in the polyamine overexpressing mutant even though the *mgsA* gene annotated as a putative methylglyoxal synthase. However, there has not been studied about MG-producing enzyme in *B. subtilis* despite an annotation as a putative methylglyoxal synthase in genome sequence. However, *Bacillus* MGS activity was not detected in previous study (Hopper and Cooper, 1971). They used the crude extract of *B. subtilis* and reacted with glutathione as a cofactor. Therefore, we intended to purify the recombinant MGS from *E. coli* to confirm its activity of *mgsA*.

The sequence alignment of *Bacillus* MGS with other bacterial proteins showed a higher similarity with the gram-negative *Thermus* sp. strain GH5 than the gram-positive *C. acetobutylicum* (Fig. 11B) (Huang*, et al.*, 1999; Pazhang*, et al.*, 2010). Moreover, *Bacillus* MGS also had four-conserved Asp residues (Asp9, Asp60, Asp80, and Asp90), corresponding to those in *E. coli* MGS (Saadat and Harrison, 1998). In *E. coli*, Asp 71 and Asp101 are involved in the catalytic active site as determined by mutant proteins in all four conserved Asp residues and structural analysis (Saadat and Harrison, 1998; 1999). By similarity, the active site of *Bacillus* MGS was estimated to be at Asp60, but this needs to be confirmed by studying mutant protein.

In previous study, *Bacillus* MGS activity was not found in the crude extract (Hopper and Cooper, 1971). However, *Bacillus* MGS activity was confirmed through the recombinant protein, which was overproduced in *E. coli* in this study. To determine the activity of *Bacillus* MGS, we purified it by applying a Q-sepharose column (Fig. 12.). The K_m value of *Bacillus* MGS was

10-folds lower than previously reported values corresponding to DHAP (Fig. 13.) (Saadat and Harrison, 1998; Huang*, et al.*, 1999; Pazhang*, et al.*, 2010). We have tried to find the reason that *Bacillus* MGS exhibited low activity. Some biochemical properties explained. Firstly, *Bacillus* MGS had maximal activity at low pH than other bacterial proteins had. In case of *E. coli*, the maximal activity showed at pH 7.5 (Hopper and Cooper, 1972), but in *Bacillus* MGS activity decreased drastically after pH 6.5 (Fig. 14B). *Bacillus* MGS might be considered unstable form at the neutral pH. Secondly, the native form of other bacterial MGSs were shown to be tetramer (Huang*, et al.*, 1999) or hexamer (Saadat and Harrison, 1999; Pazhang*, et al.*, 2010) while *Bacillus* MGS was a dimeric form (Fig. 16.). Despite the differences as described above, *Bacillus* MGS activity was inhibited by phosphate compounds except for fructose-1,6-bisphosphate (Fig. 15.). Further investigations in terms of the biochemical and structural analysis of *Bacillus* MGS are required.

To reveal the physiological roles of the *mgsA* gene and its byproduct in *B. subtilis,* the deletion and overexpression of *mgsA* gene were constructed for further experiments (Fig. 17 and 19.). Evidently, we expected that the *mgsA* overexpression in the cell would influence cell growth. As shown in the results above, the cell growth was remarkably inhibited in the $mgsA^{OE}$ strain (Fig. 21.). In *E. coli*, the cell growth of the *mgsA*-overexpressing strain was similar with wild type in complex medium (Totemeyer*, et al.*, 1998). Though, the $mgsA^{OE}$ strain also showed growth inhibition in complex media (data not shown). Due to 3-folds higher concentration of MG than vector control strain, in the $mgsA^{OE}$ strain growth was inhibited (Fig. 20.). However, unlike our expectations, the growth and viability of the *ΔmgsA* strain were also inhibited compared with wild type (Fig. 21 and 22.) in spite of a low concentration of MG in the *ΔmgsA*

strain (Fig. 20.). In the case of *E. coli*, cell viability was maintained in the deletion mutant of the *mgsA* gene but was lost in the presence of cAMP (Totemeyer*, et al.*, 1998). Further investigation was needed to find out whether cAMP has an effect on the cell viability of the *ΔmgsA* strain. It was also suggested MG plays another role in *B. subtilis*. In addition, the remaining MG in the *ΔmgsA* strain suggests that the presence of other pathways involve in the synthesis of MG.

As mention above, when the intracellular MG increased by the *mgsA* overexpression, cell length in the $mgsA^{OE}$ strain exhibited long rod-shaped cells beyond 10 μm (Fig. 23 and 24.). In contrast, in the *ΔmgsA* strain, which was low concentration of MG, displayed below 3 μm (Fig. 23 and 24.). Through this observation, we established a relationship between intracellular MG concentration and cell length. The formation of septum is considered to be important factor for preceding the cell division in the middle of the cell (Beall and Lutkenhaus, 1991). However, our results displayed that increasing expression of *ftsZ* in the *ΔmgsA* strain (Fig. 25.). In contrast, *mreB*, which is an actin-like protein in *B. subtilis* (Jones, et al., 2001), was increased in the $mgsA^{OE}$ strain (Fig. 25.). Hence, we expected that MG concentration and cell elongation have an uncovered relationship.

Furthermore, there are two more actin-like proteins (Mbl and MreBH) that are involved in cell elongation in *B. subtilis*. Three actin-like proteins localize together in a single helical structure (Carballido-López, 2006). It was necessary to investigate the effect of these genes when the *mgsA* gene was overexpressed in *Bacillus* cells to confirm the morphology. However, there were no changes in the expression of *rodA* and *divIVA* (Fig. 25 and data not shown), which is another cell elongation protein (Henriques*, et al.*, 1998) and another cell

division molecule (Thomaides, *et al.*, 2001), because all strains maintained a rod-shaped phenotype. By the damage of DNA causes an SOS response, cell growth is inhibited and then becomes a long rod-shaped cell via the expression of YneA in *B. subtilis*. Because YneA protein acts as cell division suppressor during the SOS response (Kawai, *et al.*, 2003). We have observed that the DNA of the $mgsA^{OE}$ strain became very dimmed and scattered pattern than wild type through DAPI staining (data not shown), which may suggest that DNA damage has occurred in the $mgsA^{OE}$ strain because of MG production. However, there is no direct evidence for such suggestion, and we need to further investigate whether MG affects the expression of YneA.

Along with the defects in cell growth and viability in the *mgsA*-overexpressing cells, we found that the sporulation rate increased in the $mgsA^{OE}$ strain compared with vector control strain. But, the sporulation rate was not changed in both the *ΔmgsA* strain and wild type (data not shown). Thus, we expected that MG might be involved in the sporulation processes, so we treated MG into the DSM media exogenously. Also, the sporulation rate was increased by the dependent of MG concentration (data not shown). But, because there is no experimental evidence entirely to support the effect of MG on sporulation, further investigation is necessary to explain *Bacillu*s sporulation affected by MG. Additionally, in aspect of the detoxification systems to remove MG, glyoxalase system is mainly working for MG elimination in cells (Sousa Silva, *et al.*, 2013). Recently, MG detoxification pathways were involved with bacillithiol or not in *B. subtilis* (Chandrangsu, *et al.*, 2014). We expect to the $mgsA^{OE}$ strain may contribute to the research for the detoxification system in *B. subtilis*.

Taken together, MG accumulation found in the overexpressing mutant of

polyamine and overexpressed the *mgsA* gene. It causes the inhibition of cell growth accompanying cell elongation by the activation of MreB. So, we conclude that polyamine and MG involve in the cell elongation in *B. subtilis* (Fig. 26.).

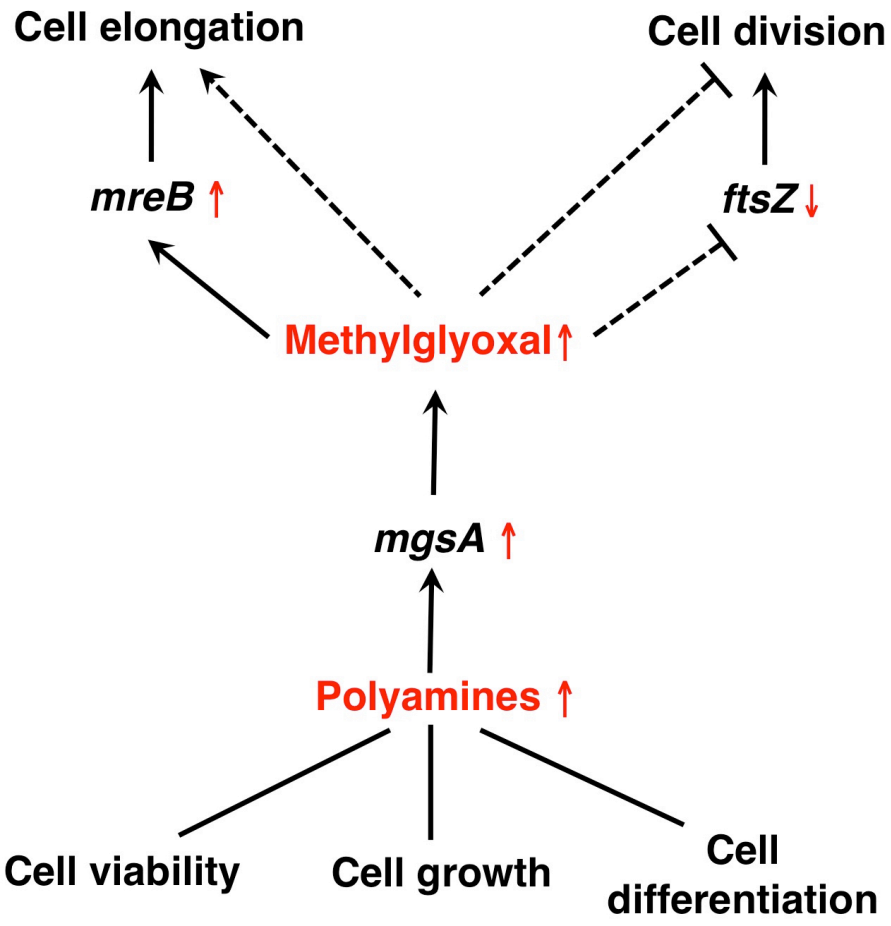

Fig. 26. The model of cell elongation by methylglyoxal and polyamine

V. REFERENCE

Agostinelli, E. (2010). Polyamines in biological systems. *Amino Acids* **38**, 351-352.

Algranati, I. D. and Goldemberg, S. H. (1977). Translation of natural mRNA in cell-free systems from a polyamine-requiring mutant of *Escherichia coli*. *Biochem Biophys Res Commun* **75**, 1045-1051.

Alhonen-Hongisto, L., Seppanen, P. and Janne, J. (1980). Intracellular putrescine and spermidine deprivation induces increased uptake of the natural polyamines and methylglyoxal bis(guanylhydrazone). *Biochem J* **192**, 941-945.

Anderson, D. E., Gueiros-Filho, F. J. and Erickson, H. P. (2004). Assembly dynamics of FtsZ rings in *Bacillus subtilis* and *Escherichia coli* and effects of FtsZ-regulating proteins. *J Bacteriol* **186**, 5775-5781.

Angeloni, C., Zambonin, L. and Hrelia, S. (2014). Role of methylglyoxal in Alzheimer's disease. *Biomed Res Int* **2014**, 238485.

Apple, M. A. and Greenberg, D. M. (1967). Inhibition of cancer growth in mice by a normal metabolite. *Life Sci* **6**, 2157-2160.

Beall, B. and Lutkenhaus, J. (1991). FtsZ in *Bacillus subtilis* is required for vegetative septation and for asymmetric septation during sporulation. *Genes Dev* **5**, 447-455.

Breborowicz, A., Witowski, J., Polubinska, A., Pyda, M. and Oreopoulos, D. (2004). L-2-oxothiazolidine-4-carboxylic acid reduces in vitro cytotoxicity of

glucose degradation products. *Nephrol Dial Transplant* **19**, 3005-3011.

Brickman, T. J. and Armstrong, S. K. (1996). The ornithine decarboxylase gene odc is required for alcaligin siderophore biosynthesis in *Bordetella* spp.: putrescine is a precursor of alcaligin. *J Bacteriol* **178**, 54-60.

Brownlee, M. (2005). The pathobiology of diabetic complications: a unifying mechanism. *Diabetes* **54**, 1615-1625.

Burrell, M., Hanfrey, C. C., Murray, E. J., Stanley-Wall, N. R. and Michael, A. J. (2010). Evolution and multiplicity of arginine decarboxylases in polyamine biosynthesis and essential role in *Bacillus subtilis* biofilm formation. *J Biol Chem* **285**, 39224-39238.

Carballido-López, R. (2006). The bacterial actin-like cytoskeleton. *Microbiol Mol Biol Rev* **70**, 888-909.

Carballido-López, R. and Formstone, A. (2007). Shape determination in *Bacillus subtilis*. *Curr Opin Microbiol* **10**, 611-616.

Carballido-López, R., Formstone, A., Li, Y., Ehrlich, S. D., Noirot, P. and Errington, J. (2006). Actin homolog MreBH governs cell morphogenesis by localization of the cell wall hydrolase LytE. *Dev Cell* **11**, 399-409.

Casazza, J. P., Felver, M. E. and Veech, R. L. (1984). The metabolism of acetone in rat. *J Biol Chem* **259**, 231-236.

Celler, K., Koning, R. I., Koster, A. J. and van Wezel, G. P. (2013).

Multidimensional view of the bacterial cytoskeleton. *J Bacteriol* **195**, 1627-1636.

Chandrangsu, P., Dusi, R., Hamilton, C. J. and Helmann, J. D. (2014). Methylglyoxal resistance in *Bacillus subtilis*: contributions of bacillithiol-dependent and independent pathways. *Mol Microbiol* **91**, 706-715.

Chang, T. and Wu, L. (2006). Methylglyoxal, oxidative stress, and hypertension. *Can J Physiol Pharmacol* **84**, 1229-1238.

Chattopadhyay, M. K., Tabor, C. W. and Tabor, H. (2002). Absolute requirement of spermidine for growth and cell cycle progression of fission yeast (*Schizosaccharomyces pombe*). *Proc Natl Acad Sci U S A* **99**, 10330-10334.

Chattopadhyay, M. K., Tabor, C. W. and Tabor, H. (2003). Polyamines protect *Escherichia coli* cells from the toxic effect of oxygen. *Proc Natl Acad Sci U S A* **100**, 2261-2265.

Chien, A. C., Hill, N. S. and Levin, P. A. (2012). Cell size control in bacteria. *Curr Biol* **22**, R340-349.

Choi, C.-H., Park, S.-J., Jeong, S.-Y., Yim, H.-S. and Kang, S.-O. (2008). Methylglyoxal accumulation by glutathione depletion leads to cell cycle arrest in *Dictyostelium*. *Mol Microbiol* **70**, 1293-1304.

Choudhary, D., Chandra, D. and Kale, R. K. (1997). Influence of methylglyoxal on antioxidant enzymes and oxidative damage. *Toxicol Lett* **93**,

141-152.

Cohen, S.S. (1997). A Guide to the Polyamines. New York, USA: Oxford University Press.

Coleman, D. L. (1980). Acetone metabolism in mice: increased activity in mice heterozygous for obesity genes. *Proc Natl Acad Sci U S A* **77**, 290-293.

Commichau, F. M., Pietack, N. and Stulke, J. (2013). Essential genes in *Bacillus subtilis*: a re-evaluation after ten years. *Mol Biosyst* **9**, 1068-1075.

Conroy, P. J., Von Burg, R., Passalacqua, W., Penney, D. P. and Sutherland, R. M. (1979). Misonidazole neurotoxicity in the mouse: evaluation of functional, pharmacokinetic, electrophysiologic and morphologic parameters. *Int J Radiat Oncol Biol Phys* **5**, 983-991.

Cooper, R. A. (1974). Methylglyoxal formation during glucose catabolism by *Pseudomonas saccharophila*. Identification of methylglyoxal synthase. *Eur J Biochem* **44**, 81-86.

Cooper, R. A. (1975). Methylglyoxal synthase. *Methods Enzymol* **41**, 502-508.

Cooper, R. A. (1984). Metabolism of methylglyoxal in microorganisms. *Annu Rev Microbiol* **38**, 49-68.

Daniel, R. A. and Errington, J. (2003). Control of cell morphogenesis in bacteria: two distinct ways to make a rod-shaped cell. *Cell* **113**, 767-776.

Davis, R. H., Morris, D. R. and Coffino, P. (1992). Sequestered end products

and enzyme regulation: the case of ornithine decarboxylase. *Microbiol Rev* **56**, 280-290.

de Boer, P., Crossley, R. and Rothfield, L. (1992). The essential bacterial cell-division protein FtsZ is a GTPase. *Nature* **359**, 254-256.

Doi, M., Wachi, M., Ishino, F., Tomioka, S., Ito, M., Sakagami, Y., Suzuki, A. and Matsuhashi, M. (1988). Determinations of the DNA sequence of the mreB gene and of the gene products of the mre region that function in formation of the rod shape of *Escherichia coli* cells. *J Bacteriol* **170**, 4619-4624.

Dominiczak, M. H. (2003). Obesity, glucose intolerance and diabetes and their links to cardiovascular disease. Implications for laboratory medicine. *Clin Chem Lab Med* **41**, 1266-1278.

Dudley, H. W., Rosenheim, O. and Starling, W. W. (1926). The Chemical Constitution of Spermine: Structure and Synthesis. *Biochem J* **20**, 1082-1094.

Dutra, F., Knudsen, F. S., Curi, D. and Bechara, E. J. (2001). Aerobic oxidation of aminoacetone, a threonine catabolite: iron catalysis and coupled iron release from ferritin. *Chem Res Toxicol* **14**, 1323-1329.

Elliott, W. H. (1960). Aminoacetone formation by *Staphylococcus aureus*. *Biochem J* **74**, 478-485.

Errington, J. (2003). Regulation of endospore formation in *Bacillus subtilis*. *Nat Rev Microbiol* **1**, 117-126.

Feucht, A., Lucet, I., Yudkin, M. D. and Errington, J. (2001). Cytological and biochemical characterization of the FtsA cell division protein of *Bacillus subtilis*. *Mol Microbiol* **40**, 115-125.

Foster, J. W. (2004). Escherichia coli acid resistance: tales of an amateur acidophile. *Nat Rev Microbiol* **2**, 898-907.

Gaballa, A., Newton, G. L., Antelmann, H., Parsonage, D., Upton, H., Rawat, M., Claiborne, A., Fahey, R. C. and Helmann, J. D. (2010). Biosynthesis and functions of bacillithiol, a major low-molecular-weight thiol in *Bacilli*. *Proc Natl Acad Sci U S A* **107**, 6482-6486.

Goldemberg, S. H. (1980). Lysine decarboxylase mutants of *Escherichia coli*: evidence for two enzyme forms. *J Bacteriol* **141**, 1428-1431.

Goldemberg, S. H. and Algranati, I. D. (1977). Polyamines and protein synthesis: studies in various polyamine-requiring mutants of *Escherichia coli*. *Mol Cell Biochem* **16**, 71-77.

Gomes, R. A., Sousa Silva, M., Vicente Miranda, H., Ferreira, A. E., Cordeiro, C. A. and Freire, A. P. (2005). Protein glycation in *Saccharomyces cerevisiae*. Argpyrimidine formation and methylglyoxal catabolism. *FEBS J* **272**, 4521-4531.

Gregory, J. A., Becker, E. C. and Pogliano, K. (2008). *Bacillus subtilis* MinC destabilizes FtsZ-rings at new cell poles and contributes to the timing of cell

division. *Genes Dev* **22**, 3475-3488.

Grillo, M. A. and Colombatto, S. (2008). Advanced glycation end-products (AGEs): involvement in aging and in neurodegenerative diseases. *Amino Acids* **35**, 29-36.

Grossman, A. D. and Losick, R. (1988). Extracellular control of spore formation in *Bacillus subtilis*. *Proc Natl Acad Sci U S A* **85**, 4369-4373.

Gugliucci, A. and Menini, T. (2003). The polyamines spermine and spermidine protect proteins from structural and functional damage by AGE precursors: a new role for old molecules? *Life Sci* **72**, 2603-2616.

Gutteridge, J. M. and Halliwell, B. (1990). The measurement and mechanism of lipid peroxidation in biological systems. *Trends Biochem Sci* **15**, 129-135.

Ha, H. C., Sirisoma, N. S., Kuppusamy, P., Zweier, J. L., Woster, P. M. and Casero, R. A., Jr. (1998). The natural polyamine spermine functions directly as a free radical scavenger. *Proc Natl Acad Sci U S A* **95**, 11140-11145.

Hafner, E. W., Tabor, C. W. and Tabor, H. (1979). Mutants of *Escherichia coli* that do not contain 1,4-diaminobutane (putrescine) or spermidine. *J Biol Chem* **254**, 12419-12426.

Hamoen, L. W., Meile, J. C., de Jong, W., Noirot, P. and Errington, J. (2006). SepF, a novel FtsZ-interacting protein required for a late step in cell division. *Mol Microbiol* **59**, 989-999.

Hanahan, D. (1983). Studies on transformation of Escherichia coli with plasmids. *J Mol Biol* **166**, 557-580.

Harwood, Colin and Cutting (1990). Molecular biological methods for *Bacillus*. Chichester: Wiley.

Henriques, A. O., Glaser, P., Piggot, P. J. and Moran, C. P., Jr. (1998). Control of cell shape and elongation by the *rodA* gene in *Bacillus subtilis*. *Mol Microbiol* **28**, 235-247.

Hiraku, Y., Sugimoto, J., Yamaguchi, T. and Kawanishi, S. (1999). Oxidative DNA damage induced by aminoacetone, an amino acid metabolite. *Arch Biochem Biophys* **365**, 62-70.

Hopper, D. J. and Cooper, R. A. (1971). The regulation of *Escherichia coli* methylglyoxal synthase; a new control site in glycolysis? *FEBS Lett* **13**, 213-216.

Hopper, D. J. and Cooper, R. A. (1972). The purification and properties of *Escherichia coli* methylglyoxal synthase. *Biochem J* **128**, 321-329.

Huang, K., Rudolph, F. B. and Bennett, G. N. (1999). Characterization of methylglyoxal synthase from *Clostridium acetobutylicum* ATCC 824 and its use in the formation of 1, 2-propanediol. *Appl Environ Microbiol* **65**, 3244-3247.

Igarashi, K. and Kashiwagi, K. (2006). Polyamine Modulon in *Escherichia*

coli: genes involved in the stimulation of cell growth by polyamines. *J Biochem* **139**, 11-16.

Inoue, Y. and Kimura, A. (1995). Methylglyoxal and regulation of its metabolism in microorganisms. *Adv Microb Physiol* **37**, 177-227.

Ishikawa, S., Kawai, Y., Hiramatsu, K., Kuwano, M. and Ogasawara, N. (2006). A new FtsZ-interacting protein, YlmF, complements the activity of FtsA during progression of cell division in *Bacillus subtilis*. *Mol Microbiol* **60**, 1364-1380.

Jain, R. and Yan, Y. (2011). Dehydratase mediated 1-propanol production in metabolically engineered *Escherichia coli*. *Microb Cell Fact* **10**, 97.

Jerzykowski, T., Matuszewski, W., Otrzonsek, N. and Winter, R. (1970). Antineoplastic action of methylglyoxal. *Neoplasma* **17**, 25-35.

Jones, L. J., Carballido-López, R. and Errington, J. (2001). Control of cell shape in bacteria: helical, actin-like filaments in *Bacillus subtilis*. *Cell* **104**, 913-922.

Jung, I. L., Oh, T. J. and Kim, I. G. (2003). Abnormal growth of polyamine-deficient *Escherichia coli* mutant is partially caused by oxidative stress-induced damage. *Arch Biochem Biophys* **418**, 125-132.

Kalapos, M. P. (1999). Methylglyoxal in living organisms: chemistry, biochemistry, toxicology and biological implications. *Toxicol Lett* **110**, 145-175.

Kalapos, M. P., Mandl, J., Bánhegyi, G., Antoni, F. and Garzo, T. (1994). Net glucose production from acetone in isolated murine hepatocytes. The effect of different pretreatments of mice. *Int J Biochem* **26**, 1069-1079.

Kamio, Y. (1987). Structural specificity of diamines covalently linked to peptidoglycan for cell growth of *Veillonella alcalescens* and *Selenomonas ruminantium*. *J Bacteriol* **169**, 4837-4840.

Kamio, Y., Poso, H., Terawaki, Y. and Paulin, L. (1986). Cadaverine covalently linked to a peptidoglycan is an essential constituent of the peptidoglycan necessary for the normal growth in *Selenomonas ruminantium*. *J Biol Chem* **261**, 6585-6589.

Kang, Y., Edwards, L. G. and Thornalley, P. J. (1996). Effect of methylglyoxal on human leukaemia 60 cell growth: modification of DNA G1 growth arrest and induction of apoptosis. *Leuk Res* **20**, 397-405.

Karatan, E., Duncan, T. R. and Watnick, P. I. (2005). NspS, a predicted polyamine sensor, mediates activation of *Vibrio cholerae* biofilm formation by norspermidine. *J Bacteriol* **187**, 7434-7443.

Kawai, Y., Moriya, S. and Ogasawara, N. (2003). Identification of a protein, YneA, responsible for cell division suppression during the SOS response in *Bacillus subtilis*. *Mol Microbiol* **47**, 1113-1122.

Ko, J., Kim, I., Yoo, S., Min, B., Kim, K. and Park, C. (2005). Conversion of

methylglyoxal to acetol by *Escherichia coli* aldo-keto reductases. *J Bacteriol* **187**, 5782-5789.

Koski, P. and Vaara, M. (1991). Polyamines as constituents of the outer membranes of *Escherichia coli* and *Salmonella typhimurium*. *J Bacteriol* **173**, 3695-3699.

Kunst, F., Ogasawara, N., Moszer, I., Albertini, A. M., Alloni, G., Azevedo, V., Bertero, M. G., Bessieres, P., Bolotin, A., Borchert, S., Borriss, R., Boursier, L., Brans, A., Braun, M., Brignell, S. C., Bron, S., Brouillet, S., Bruschi, C. V., Caldwell, B., Capuano, V., Carter, N. M., Choi, S. K., Cordani, J. J., Connerton, I. F., Cummings, N. J., Daniel, R. A., Denziot, F., Devine, K. M., Dusterhoft, A., Ehrlich, S. D., Emmerson, P. T., Entian, K. D., Errington, J., Fabret, C., Ferrari, E., Foulger, D., Fritz, C., Fujita, M., Fujita, Y., Fuma, S., Galizzi, A., Galleron, N., Ghim, S. Y., Glaser, P., Goffeau, A., Golightly, E. J., Grandi, G., Guiseppi, G., Guy, B. J., Haga, K., Haiech, J., Harwood, C. R., Henaut, A., Hilbert, H., Holsappel, S., Hosono, S., Hullo, M. F., Itaya, M., Jones, L., Joris, B., Karamata, D., Kasahara, Y., Klaerr-Blanchard, M., Klein, C., Kobayashi, Y., Koetter, P., Koningstein, G., Krogh, S., Kumano, M., Kurita, K., Lapidus, A., Lardinois, S., Lauber, J., Lazarevic, V., Lee, S. M., Levine, A., Liu, H., Masuda, S., Mauel, C., Medigue, C., Medina, N., Mellado, R. P., Mizuno, M., Moestl, D., Nakai, S.,

Noback, M., Noone, D., O'Reilly, M., Ogawa, K., Ogiwara, A., Oudega, B., Park, S. H., Parro, V., Pohl, T. M., Portelle, D., Porwollik, S., Prescott, A. M., Presecan, E., Pujic, P., Purnelle, B., Rapoport, G., Rey, M., Reynolds, S., Rieger, M., Rivolta, C., Rocha, E., Roche, B., Rose, M., Sadaie, Y., Sato, T., Scanlan, E., Schleich, S., Schroeter, R., Scoffone, F., Sekiguchi, J., Sekowska, A., Seror, S. J., Serror, P., Shin, B. S., Soldo, B., Sorokin, A., Tacconi, E., Takagi, T., Takahashi, H., Takemaru, K., Takeuchi, M., Tamakoshi, A., Tanaka, T., Terpstra, P., Togoni, A., Tosato, V., Uchiyama, S., Vandebol, M., Vannier, F., Vassarotti, A., Viari, A., Wambutt, R., Wedler, H., Weitzenegger, T., Winters, P., Wipat, A., Yamamoto, H., Yamane, K., Yasumoto, K., Yata, K., Yoshida, K., Yoshikawa, H. F., Zumstein, E., Yoshikawa, H. and Danchin, A. (1997). The complete genome sequence of the gram-positive bacterium *Bacillus subtilis*. *Nature* **390**, 249-256.

Kunst, F. and Rapoport, G. (1995). Salt stress is an environmental signal affecting degradative enzyme synthesis in *Bacillus subtilis*. *J Bacteriol* **177**, 2403-2407.

Kwak, M. -K., Ku, M. and Kang, S. -O. (2014). NAD(+)-linked alcohol dehydrogenase 1 regulates methylglyoxal concentration in *Candida albicans*. *FEBS Lett* **588**, 1144-1153.

Leaver, M. and Errington, J. (2005). Roles for MreC and MreD proteins in

helical growth of the cylindrical cell wall in *Bacillus subtilis*. *Mol Microbiol* **57**, 1196-1209.

Lee, C., Yim, M. B., Chock, P. B., Yim, H.-S. and Kang, S.-O. (1998). Oxidation-reduction properties of methylglyoxal-modified protein in relation to free radical generation. *J Biol Chem* **273**, 25272-25278.

Leoncini, G. and Poggi, M. (1996). Effects of methylglyoxal on platelet hydrogen peroxide accumulation, aggregation and release reaction. *Cell Biochem Funct* **14**, 89-95.

Levin, P. A., Kurtser, I. G. and Grossman, A. D. (1999). Identification and characterization of a negative regulator of FtsZ ring formation in *Bacillus subtilis*. *Proc Natl Acad Sci U S A* **96**, 9642-9647.

Levin, P. A. and Losick, R. (1996). Transcription factor Spo0A switches the localization of the cell division protein FtsZ from a medial to a bipolar pattern in *Bacillus subtilis*. *Genes Dev* **10**, 478-488.

Litwin, C. M. and Calderwood, S. B. (1993). Role of iron in regulation of virulence genes. *Clin Microbiol Rev* **6**, 137-149.

Lowe, J. and Amos, L. A. (1998). Crystal structure of the bacterial cell-division protein FtsZ. *Nature* **391**, 203-206.

Lutkenhaus, J. (2007). Assembly dynamics of the bacterial MinCDE system and spatial regulation of the Z ring. *Annu Rev Biochem* **76**, 539-562.

MacLean, M. J., Ness, L. S., Ferguson, G. P. and Booth, I. R. (1998). The role of glyoxalase I in the detoxification of methylglyoxal and in the activation of the KefB K+ efflux system in *Escherichia coli*. *Mol Microbiol* **27**, 563-571.

Mannervik, B. and Ridderstrom, M. (1993). Catalytic and molecular properties of glyoxalase I. *Biochem Soc Trans* **21**, 515-517.

Marinari, U. M., Ferro, M., Sciaba, L., Finollo, R., Bassi, A. M. and Brambilla, G. (1984). DNA-damaging activity of biotic and xenobiotic aldehydes in Chinese hamster ovary cells. *Cell Biochem Funct* **2**, 243-248.

Marks, G. T., Susler, M. and Harrison, D. H. (2004). Mutagenic studies on histidine 98 of methylglyoxal synthase: effects on mechanism and conformational change. *Biochemistry* **43**, 3802-3813.

Marton, L. J. and Pegg, A. E. (1995). Polyamines as targets for therapeutic intervention. *Annu Rev Pharmacol Toxicol* **35**, 55-91.

McCann, P. P. and Pegg, A. E. (1992). Ornithine decarboxylase as an enzyme target for therapy. *Pharmacol Ther* **54**, 195-215.

Méndez, J. D. and Leal, L. I. (2004). Inhibition of in vitro pyrraline formation by L-arginine and polyamines. *Biomed Pharmacother* **58**, 598-604.

Misra, K., Banerjee, A. B., Ray, S. and Ray, M. (1995). Glyoxalase III from *Escherichia coli*: a single novel enzyme for the conversion of methylglyoxal into D-lactate without reduced glutathione. *Biochem J* **305 (Pt 3)**, 999-1003.

Miyamoto, S., Kashiwagi, K., Ito, K., Watanabe, S. and Igarashi, K. (1993). Estimation of polyamine distribution and polyamine stimulation of protein synthesis in *Escherichia coli*. *Arch Biochem Biophys* **300**, 63-68.

Moore, R. C. and Boyle, S. M. (1991). Cyclic AMP inhibits and putrescine represses expression of the *speA* gene encoding biosynthetic arginine decarboxylase in *Escherichia coli*. *J Bacteriol* **173**, 3615-3621.

Morgan, D. M. (1999). Polyamines. An overview. *Mol Biotechnol* **11**, 229-250.

Morgan, David M. L. (1998). Polyamine protocols. Totowa, N.J.: Humana.

Morris, D. R. and Fillingame, R. H. (1974). Regulation of amino acid decarboxylation. *Annu Rev Biochem* **43**, 303-325.

Mukherjee, A., Dai, K. and Lutkenhaus, J. (1993). *Escherichia coli* cell division protein FtsZ is a guanine nucleotide binding protein. *Proc Natl Acad Sci U S A* **90**, 1053-1057.

Nguyen, T. T., Eiamphungporn, W., Mader, U., Liebeke, M., Lalk, M., Hecker, M., Helmann, J. D. and Antelmann, H. (2009). Genome-wide responses to carbonyl electrophiles in *Bacillus subtilis*: control of the thiol-dependent formaldehyde dehydrogenase AdhA and cysteine proteinase YraA by the MerR-family regulator YraB (AdhR). *Mol Microbiol* **71**, 876-894.

Pastre, D., Pietrement, O., Landousy, F., Hamon, L., Sorel, I., David, M. O., Delain, E., Zozime, A. and Le Cam, E. (2006). A new approach to DNA

bending by polyamines and its implication in DNA condensation. *Eur Biophys J* **35**, 214-223.

Patel, C. N., Wortham, B. W., Lines, J. L., Fetherston, J. D., Perry, R. D. and Oliveira, M. A. (2006). Polyamines are essential for the formation of plague biofilm. *J Bacteriol* **188**, 2355-2363.

Pazhang, M., Khajeh, K., Asghari, S. M., Falahati, H. and Naderi-Manesh, H. (2010). Cloning, expression, and characterization of a novel methylglyoxal synthase from *Thermus* sp. strain GH5. *Appl Biochem Biotechnol* **162**, 1519-1528.

Pegg, A. E. and McCann, P. P. (1982). Polyamine metabolism and function. *Am J Physiol* **243**, C212-221.

Phillips, S. A. and Thornalley, P. J. (1993). The formation of methylglyoxal from triose phosphates. Investigation using a specific assay for methylglyoxal. *Eur J Biochem* **212**, 101-105.

Poli, G., Dianzani, M. U., Cheeseman, K. H., Slater, T. F., Lang, J. and Esterbauer, H. (1985). Separation and characterization of the aldehydic products of lipid peroxidation stimulated by carbon tetrachloride or ADP-iron in isolated rat hepatocytes and rat liver microsomal suspensions. *Biochem J* **227**, 629-638.

Popham, D. L. and Young, K. D. (2003). Role of penicillin-binding proteins

in bacterial cell morphogenesis. *Curr Opin Microbiol* **6**, 594-599.

Priyadarshini, R., de Pedro, M. A. and Young, K. D. (2007). Role of peptidoglycan amidases in the development and morphology of the division septum in *Escherichia coli*. *J Bacteriol* **189**, 5334-5347.

Ray, M., Halder, J., Dutta, S. K. and Ray, S. (1991). Inhibition of respiration of tumor cells by methylglyoxal and protection of inhibition by lactaldehyde. *Int J Cancer* **47**, 603-609.

Ray, M. and Ray, S. (1987). Aminoacetone oxidase from goat liver. Formation of methylglyoxal from aminoacetone. *J Biol Chem* **262**, 5974-5977.

Reiffen, K. A. and Schneider, F. (1984). A comparative study on proliferation, macromolecular synthesis and energy metabolism of in vitro-grown Ehrlich ascites tumor cells in the presence of glucosone, galactosone and methylglyoxal. *J Cancer Res Clin Oncol* **107**, 206-210.

Rose, I. A. and Nowick, J. S. (2002). Methylglyoxal synthetase, enol-pyruvaldehyde, glutathione and the glyoxalase system. *J Am Chem Soc* **124**, 13047-13052.

Rothfield, L., Justice, S. and Garcia-Lara, J. (1999). Bacterial cell division. *Annu Rev Genet* **33**, 423-448.

Ryu, H. -B., Shin, I., Yim, H. -S. and Kang, S. -O. (2006). YlaC is an extracytoplasmic function (ECF) sigma factor contributing to hydrogen

peroxide resistance in *Bacillus subtilis*. *J Microbiol* **44**, 206-216.

Saadat, D. and Harrison, D. H. (1998). Identification of catalytic bases in the active site of *Escherichia coli* methylglyoxal synthase: cloning, expression, and functional characterization of conserved aspartic acid residues. *Biochemistry* **37**, 10074-10086.

Saadat, D. and Harrison, D. H. (1999). The crystal structure of methylglyoxal synthase from *Escherichia coli*. *Structure* **7**, 309-317.

Sabo, D. L., Boeker, E. A., Byers, B., Waron, H. and Fischer, E. H. (1974). Purification and physical properties of inducible *Escherichia coli* lysine decarboxylase. *Biochemistry* **13**, 662-670.

Sabo, D. L. and Fischer, E. H. (1974). Chemical properties of *Escherichia coli* lysine decarboxylase including a segment of its pyridoxal 5'-phosphate binding site. *Biochemistry* **13**, 670-676.

Samartzidou, H., Mehrazin, M., Xu, Z., Benedik, M. J. and Delcour, A. H. (2003). Cadaverine inhibition of porin plays a role in cell survival at acidic pH. *J Bacteriol* **185**, 13-19.

Sambrook, Joseph and Russell, David W. (2001). Molecular cloning : a laboratory manual. Cold Spring Harbor, N.Y.: Cold Spring Harbor Laboratory Press.

Satishchandran, C. and Boyle, S. M. (1984). Antagonistic transcriptional

regulation of the putrescine biosynthetic enzyme agmatine ureohydrolase by cyclic AMP and agmatine in *Escherichia coli*. *J Bacteriol* **157**, 552-559.

Sekowska, A., Bertin, P. and Danchin, A. (1998). Characterization of polyamine synthesis pathway in *Bacillus subtilis* 168. *Mol Microbiol* **29**, 851-858.

Setlow, P. (1974). Polyamine levels during growth, sporulation, and spore germination of Bacillus megaterium. *J Bacteriol* **117**, 1171-1177.

Shah, P. and Swiatlo, E. (2008). A multifaceted role for polyamines in bacterial pathogens. *Mol Microbiol* **68**, 4-16.

Shumaev, K. B., Gubkina, S. A., Kumskova, E. M., Shepelkova, G. S., Ruuge, E. K. and Lankin, V. Z. (2009). Superoxide formation as a result of interaction of L-lysine with dicarbonyl compounds and its possible mechanism. *Biochemistry (Mosc)* **74**, 461-466.

Siefert, J. L. and Fox, G. E. (1998). Phylogenetic mapping of bacterial morphology. *Microbiology* **144 (Pt 10)**, 2803-2808.

Sousa Silva, M., Gomes, R. A., Ferreira, A. E., Ponces Freire, A. and Cordeiro, C. (2013). The glyoxalase pathway: the first hundred years... and beyond. *Biochem J* **453**, 1-15.

Souza, Wd (2012). Prokaryotic cells: structural organisation of the cytoskeleton and organelles. *Mem Inst Oswaldo Cruz* **107**, 283-293.

Souzu, H. (1986). Fluorescence polarization studies on Escherichia coli membrane stability and its relation to the resistance of the cell to freeze-thawing. II. Stabilization of the membranes by polyamines. *Biochim Biophys Acta* **861**, 361-367.

Stricker, J., Maddox, P., Salmon, E. D. and Erickson, H. P. (2002). Rapid assembly dynamics of the *Escherichia coli* FtsZ-ring demonstrated by fluorescence recovery after photobleaching. *Proc Natl Acad Sci U S A* **99**, 3171-3175.

Studier, F. W. (1991). Use of bacteriophage T7 lysozyme to improve an inducible T7 expression system. *J Mol Biol* **219**, 37-44.

Subedi, K. P., Choi, D., Kim, I., Min, B. and Park, C. (2011). Hsp31 of *Escherichia coli* K-12 is glyoxalase III. *Mol Microbiol* **81**, 926-936.

Szent-Györgyi, A., Együd, L. G. and McLaughlin, J. A. (1967). Keto-aldehydes and cell division. *Science* **155**, 539-541.

Tabor, C. W. and Tabor, H. (1984). Polyamines. *Annu Rev Biochem* **53**, 749-790.

Tabor, H., Hafner, E. W. and Tabor, C. W. (1980). Construction of an *Escherichia coli* strain unable to synthesize putrescine, spermidine, or cadaverine: characterization of two genes controlling lysine decarboxylase. *J Bacteriol* **144**, 952-956.

Takahashi, T. and Kakehi, J. (2010). Polyamines: ubiquitous polycations with unique roles in growth and stress responses. *Ann Bot* **105**, 1-6.

Takatsuka, Y. and Kamio, Y. (2004). Molecular dissection of the *Selenomonas ruminantium* cell envelope and lysine decarboxylase involved in the biosynthesis of a polyamine covalently linked to the cell wall peptidoglycan layer. *Biosci Biotechnol Biochem* **68**, 1-19.

Thomaides, H. B., Freeman, M., El Karoui, M. and Errington, J. (2001). Division site selection protein DivIVA of Bacillus subtilis has a second distinct function in chromosome segregation during sporulation. *Genes Dev* **15**, 1662-1673.

Thornalley, P. J. (1995). Advances in glyoxalase research. Glyoxalase expression in malignancy, anti-proliferative effects of methylglyoxal, glyoxalase I inhibitor diesters and S-D-lactoylglutathione, and methylglyoxal-modified protein binding and endocytosis by the advanced glycation endproduct receptor. *Crit Rev Oncol Hematol* **20**, 99-128.

Thornalley, P. J. (1996). Pharmacology of methylglyoxal: formation, modification of proteins and nucleic acids, and enzymatic detoxification--a role in pathogenesis and antiproliferative chemotherapy. *Gen Pharmacol* **27**, 565-573.

Tkachenko, A., Nesterova, L. and Pshenichnov, M. (2001). The role of the

natural polyamine putrescine in defense against oxidative stress in *Escherichia coli*. *Arch Microbiol* **176**, 155-157.

Totemeyer, S., Booth, N. A., Nichols, W. W., Dunbar, B. and Booth, I. R. (1998). From famine to feast: the role of methylglyoxal production in *Escherichia coli*. *Mol Microbiol* **27**, 553-562.

Tsai, P. K. and Gracy, R. W. (1976). Isolation and characterization of crystalline methylglyoxal synthetase from *Proteus vulgaris*. *J Biol Chem* **251**, 364-367.

Ulrich, P. and Cerami, A. (2001). Protein glycation, diabetes, and aging. *Recent Prog Horm Res* **56**, 1-21.

Vagner, V., Dervyn, E. and Ehrlich, S. D. (1998). A vector for systematic gene inactivation in *Bacillus subtilis*. *Microbiology* **144 (Pt 11)**, 3097-3104.

van den Ent, F., Leaver, M., Bendezu, F., Errington, J., de Boer, P. and Lowe, J. (2006). Dimeric structure of the cell shape protein MreC and its functional implications. *Mol Microbiol* **62**, 1631-1642.

Van Dessel, W., Van Mellaert, L., Geukens, N., Lammertyn, E. and Anne, J. (2004). Isolation of high quality RNA from *Streptomyces*. *J Microbiol Methods* **58**, 135-137.

Vander Jagt, D. L. (1993). Glyoxalase II: molecular characteristics, kinetics and mechanism. *Biochem Soc Trans* **21**, 522-527.

Vander Jagt, D. L. (2008). Methylglyoxal, diabetes mellitus and diabetic complications. *Drug Metabol Drug Interact* **23**, 93-124.

Wach, A. (1996). PCR-synthesis of marker cassettes with long flanking homology regions for gene disruptions in *S. cerevisiae*. *Yeast* **12**, 259-265.

Wallace, H. M., Fraser, A. V. and Hughes, A. (2003). A perspective of polyamine metabolism. *Biochem J* **376**, 1-14.

Ware, D., Jiang, Y., Lin, W. and Swiatlo, E. (2006). Involvement of *potD* in *Streptococcus pneumoniae* polyamine transport and pathogenesis. *Infect Immun* **74**, 352-361.

Watson, N., Dunyak, D. S., Rosey, E. L., Slonczewski, J. L. and Olson, E. R. (1992). Identification of elements involved in transcriptional regulation of the *Escherichia coli cad* operon by external pH. *J Bacteriol* **174**, 530-540.

Weart, R. B., Lee, A. H., Chien, A. C., Haeusser, D. P., Hill, N. S. and Levin, P. A. (2007). A metabolic sensor governing cell size in bacteria. *Cell* **130**, 335-347.

Weart, R. B., Nakano, S., Lane, B. E., Zuber, P. and Levin, P. A. (2005). The ClpX chaperone modulates assembly of the tubulin-like protein FtsZ. *Mol Microbiol* **57**, 238-249.

Westwood, M. E., McLellan, A. C. and Thornalley, P. J. (1994). Receptor-mediated endocytic uptake of methylglyoxal-modified serum albumin.

Competition with advanced glycation end product-modified serum albumin at the advanced glycation end product receptor. *J Biol Chem* **269**, 32293-32298.

White, J. S. and Rees, K. R. (1982). Inhibitory effects of methyl glyoxal on DNA, RNA and protein synthesis in cultured guinea pig keratocytes. *Chem Biol Interact* **38**, 339-347.

Wu, L. J. and Errington, J. (2004). Coordination of cell division and chromosome segregation by a nucleoid occlusion protein in *Bacillus subtilis*. *Cell* **117**, 915-925.

Xu, D., Liu, X., Guo, C. and Zhao, J. (2006). Methylglyoxal detoxification by an aldo-keto reductase in the cyanobacterium *Synechococcus* sp. PCC 7002. *Microbiology* **152**, 2013-2021.

Yamamoto, Y., Miwa, Y., Miyoshi, K., Furuyama, J. and Ohmori, H. (1997). The *Escherichia coli ldcC* gene encodes another lysine decarboxylase, probably a constitutive enzyme. *Genes Genet Syst* **72**, 167-172.

Yanisch-Perron, C., Vieira, J. and Messing, J. (1985). Improved M13 phage cloning vectors and host strains: nucleotide sequences of the M13mp18 and pUC19 vectors. *Gene* **33**, 103-119.

Yim, H. -S., Kang, S. -O., Hah, Y. -C., Chock, P. B. and Yim, M. B. (1995). Free radicals generated during the glycation reaction of amino acids by methylglyoxal. A model study of protein-cross-linked free radicals. *J Biol*

Chem **270**, 28228-28233.

국문 초록

세포내 대사 중간물질인 methylglyoxal 은 세포 생장 또는 분열의 저해 요소로 작용하는 것으로 알려져 있다. 이러한 α-ketoaldehyde 중 glyoxal, methylglyoxal, deoxyglycosone 는 advanced glycation end product 를 야기하는 것으로 알려져 있으며 세포 내 혹은 세포 외의 polyamine 에 의해 조절됨이 보고되었다. 세포 내 다량 존재하는 polyamines 의 경우 박테리아부터 동물세포에 이르기 까지 세포 성장과 세포 분열 또한 세포 분화에 관여한다고 알려져 있다.

본 연구에서는 전자상자기공명을 이용하여 methylglyoxal 과 몇 종류의 polyamines 이 서로 반응하여 라디칼을 형성함을 관찰하였다. Methylglyoxal 과 polyamine 의 관계를 고초균에서 조사하기 위해 polyamines 를 생합성하는 유전자, *speA*, *speB* 그리고 *ΔyaaO* 에 의해 부호화 되는 arginine decarboxylase, agmatinase, 그리고 lysine decarboxylase 의 결손 균주와 과량발현 균주을 제작하였다. Polyamines 이 결손된 균주에서는 야생균주에 비해 세포의 성장이 저해되었다. 그러나, $speA^{OE}$ 균주를 제외한 $speB^{OE}$, $yaaO^{OE}$ 균주에서는 오히려 세포의 성장이 대조균주에 비해 현저하게 저해됨을 관찰하였다. 세포 내 methylglyoxal 이 대조균주에 비해 2.5-3 배 정도 증가된 것을 $speB^{OE}$, $yaaO^{OE}$ 균주에서 관찰하였다. 또한 고초균의 유전자 정보를 바탕으로 methylglyoxal 를 합성할 것이라 예측되는 *mgsA* 의 유전자 발현이 $speB^{OE}$ 와 $yaaO^{OE}$ 에서 뚜렷이 증가되었다. 이들 균주에서 보이는 세포의 생리적 변화를 바탕으로 methylglyoxal

과 polyamines 의 증가가 세포의 형태에 영향을 주는지 현미경으로 관찰하였다. 대조균주에 비해 60% 이상 길어진 세포가 *speB*^{OE} 과 *yaaO*^{OE} 균주에서 관찰되었다. 원핵생물에서 세포 신장 혹은 형태에 관련된 중요 조절인자로 알려진 액틴 단백질인 *mreB* 의 발현양이 *speB*^{OE} 과 *yaaO*^{OE} 균주에서 증가되었다. 이러한 결과로 *speB*^{OE} 과 *yaaO*^{OE} 균주에서 *mgsA* 의 발현량의 증가에 의한 methylglyoxal 의 축적이 세포 생장 저해와 *mreB* 발현을 개시하여 세포 형태에 영향을 미침을 관찰하였다.

다른 실험 조건 하에서 세포내 methylglyoxal 과 세포 형태의 관계를 살펴보기 위해 pET3a 벡터를 이용한 고초균의 methylglyoxal 합성효소를 대장균에서 분리하였다. dihydroxyacetone phosphate 를 주요 기질로 이용한 고초균의 methylglyoxal 합성효소 활성의 K_m 은 3.17 mM 이었고은 0.009 (s^{-1})로 측정되었다. 고초균의 methylglyoxal 합성효소는 40°C 와 pH 5.5 에서 최대의 활성을 보였으며 원래의 분자량은 이량체 형태로 계산되었다. 고초균의 methylglyoxal 합성효소의 활성은 농도 의존적으로 외부에서 처리한 인산화합물에 의해 저해되었다. 이러한 결과로 보아 methylglyoxal 합성 유전자에 의해 암호화된 고초균의 methylglyoxal 합성효소는 dihydroxyacetone phosphate 를 methylglyoxal 로 전환시키는 활성를 보이며 다른 미생물의 단백질과는 다른 생화학적 특성을 보였다.

흥미롭게도, *mgsA*^{OE} 균주에서 세포내 methylglyoxal 이 대조균주에 비해 2.5-3.5 배 증가됨을 관찰하였다. 세포 생장과 생균수 역시 *mgsA*^{OE} 균주에서 확연히 저해 됨을 관찰하였다. *mgsA*^{OE}

균주에서 세포의 신장 역시 *speB*^{OE} *or yaaO*^{OE} 과량발현 균주와 마찬가지로 대조 균주에 비해 2.5-3.5 배 길어짐을 관찰하였다. 또한 *mgsA*^{OE} 균주에서도 *speB*^{OE} *or yaaO*^{OE} 과량발현 균주처럼 세포 신장 인자인 *mre*B 의 발현량이 증가하였다.

이 결과를 통하여 고초균에서 세포내 methylglyoxal 과 polyamines 이 고초균의 세포 생장동안 세포 신장에 관여하는 중요한 요인이라고 생각된다.

주요어 : Methylglyxoal, Methylglyoxal 합성효소, Polyamine, 세포 신장, *Bacillus subtilis*